NORRÆNA ELDFJALLASTÖDIN

A DYNAMIC MODEL OF RIFT ZONE PETROGENESIS

AND THE REGIONAL PETROLOGY OF ICELAND

by

Níels Óskarsson,
Gudmundur E. Sigvaldason,
Nordic Volcanological Institute,
University of Iceland

and

Sigurdur Steinthórsson
Science Institute,
University of Iceland

December 1979

A DYNAMIC MODEL OF RIFT ZONE PETROGENESIS

AND THE REGIONAL PETROLOGY OF ICELAND

by

Níels Óskarsson,
Gudmundur E. Sigvaldason,
Nordic Volcanological Institute,
University of Iceland

and

Sigurdur Steinthórsson
Science Institute,
University of Iceland

December 1979

Even if the mineralogy and major element concentration of the mantle
were well understood, it is doubtful that this knowledge would lead
to a detailed understanding of the abundance of dispersed elements
in the upper mantle.

Paul W. Gast (1968)

C O N T E N T

ABSTRACT

      The present model of rift zone petrogenesis relates the diffe-
rent suites of oceanic rocks to dynamic processes within the rift
zone crust. The compositional variation along the ocean ridges is
related to different production rate of otherwise similar mantle
derived magma. The composition of mantle derived ol-tholeiite added
to the accreating plate margins is modified by mixing with crustal
derived magmas and to a lesser extent fractional crystallization.
The movement of mass elements of the rift zone crust is defined by
the velocities of horizontal drift and isostatic subsidence in re-
sponse to volcanic load. The geothermal gradient across a rift zone
reaches maximum at the rift center and falls off towards its margins
Rocks deposited on the rift surface subsides towards higher tempera-
tures and are brought outwards towards lower temperatures. During
subsidence the rocks deposited at the rift center assume the highest
metamorphic grade (greatest depth) while rocks deposited at the rift
margins reach the lowest metamorphic grade before they are expelled
towards lower temperatures in the accreating plate. The resulting
metamorphic stratification outside the rift zone is known as the
layering of the oceanic crust. Extensive geothermal alteration in
the upper sections of the rift results in the formation of hydrated
mineral assemblages at depth. As the hydrated subsiding rocks cross
their solidus isotherm, crustal derived magmas are formed by partial
melting. These anatectic melts form in the depth interval of the
high grade amphibolite facies. Rocks crossing the boundary between
the amphibolite and granulite facies are dehydrated by melting of
amphibole and retention of that magma at the site of formation. The
locus of this reaction boundary defines the surface of crustal layer
4 i.e. the upper mantle. The segregation and retention of crustal
derived magmas within the rift zone result in a chemical fractiona-
tion of the oceanic crust, since its lower sections are depleted in
elements entering the crustal melt fractions. The earliest crustal
derived magmas are silicic and enriched in the dispersed elements.
The last magmas melted from the same subsiding pile at the mantle
crust boundary are ne-normative basalts.
      A dynamic model of rift zone petrogenesis is based on mixing
between mantle derived homogeneous ol-tholeiite and minor amounts of
crustal derived magmas ranging from silicic liquids to ne-normative
basaltic liquids. The mixtures equilibrate at three different major
element compositions by mineralogical evolution towards invariant
points in the basalt system resembling ol-tholeiite, qz-tholeiite
and alkali olivine basalt. Volcanism outside the rift zone is domi-
nated by the crustal derived magmas in contrast to the rift zone,
where the mantle derived ol-tholeiite dominate. The dispersed element
geochemistry of the oceanic rocks reflect the mixing ratios of
ol-tholeiite and crustal derived magmas and the composition of the
crustal derived magmas involved. Dispersed element concentrations
are only slightly modified by crystal fractionation. The geochemistry
of radiogenic isotopes of the crustal derived magmas is controlled by
long standing fractionation processes separating mother and daughter
elements. Stable isotopes of the upper crustal layers are fractionated
in hydrothermal processes where isotope exchange with the hydrosphere
also takes place.

The present model reveals the petrogenetic relation between the tholeiitic rift zone volcanism and the alkaline off rift volcanism in Iceland and, by inference, other oceanic rifts. The alkaline rocks are derived from tholeiites depleted in silica by crustal fractionation. The only material added to the oceanic crust is therefore primitive ol-tholeiite formed by partial melting in a homogeneous mantle.

INTRODUCTION

The invention of plate tectonics created a need for a global model of oceanic petrogenesis. The narrow compositional range and world wide occurrence of the abyssal tholeiites favoured their desired mantle origin (Engel & Engel, 1964). During the sixties the evolution of ideas on the subject encircled the observed compositional variation across an oceanic rift (McBirney & Gass, 1967) and the inferred magma generation in a homogeneous mantle. The petrological incompatibility of silica undersaturated basalts of the rift flanks and the ol-tholeiites of the rift valleys was circumvented by the experimental evidence that the two magma suites are generated by different degrees of partial melting in the mantle (Green & Ringwood, 1967). This supplied the basalt petrology with the primary liquids needed to explain observed petrochemical trends. Models of convective cells of the rift zones (Oxburgh & Turcotte, 1968) solved the volume relations and spatial distribution of the two magma suites. Gast (1968) interpretated the dispersed element chemistry of the oceanic rocks as the result of different degree of partial melting in different thermal regimes of the oceanic mantle.

The simple petrogenetic models came to an end when the source regions of the oceanic rocks were shown to be unrelated in time as manifested by classical interpretation of Sr-isotope ratios (Hart, 1969; Hedge & Peterman, 1970).

The mantle plume theory (Morgan, 1972), however, explained the anomalous production at elevated rift segments (Iceland) as well as productive areas outside the rifts (Hawaii).

The present state of the art can be illustrated by mentioning two rival theories.

The first theory assumes that there is a systematic variation in dispersed element chemistry and isotopic composition along the oceanic ridges adjoining the most productive areas (hot spots), whereas the variability within the hot spot itself is insignificant. This is explained in terms of two types of mantle, i.e. mantle plumes and "a common mantle", and the mixing of their derived melts at the juncture of the two (Schilling, 1974). The basic premise of this hypothesis - that the variability within the hot spot is insignificant or random - has been dispersed by later research (Sigvaldason et al., 1974), and further that the observed isotope patterns unlikely results from binary mixing (O´Nions et al., 1974; Tatsumoto, 1978).

The second theory assumes the immutability of isotopes in relatively short-term mantle or crustal processes. Recent investigations have brought out considerable heterogeneities in the isotopic compositions of oceanic lavas which, according to this theory, are to be explained in terms of mantle heterogeneities on every scale (O´Nions et al., 1974; Sun & Gilbert, 1975; Hart, 1976). According to this theory the regional distribution of the alkaline and tholeiitic magma suites have no other deeper meaning than hypothetical depletion events of their source regions in the past.

At the present time some confusion arises from the different frames of observation of scientists working in the fields of experimental and classical petrology, geochemistry, field geology and geophysics. Our tendency to believe what we see in our own data and see what we believe in other data inevitably results in large scale models based on specialized research. Therefore the search of a unifying theory of ocean petrogenesis have to test a multitude of inferred processes against field observations and put them to work within the frame of geophysical restriction.

The Icelandic rift system is a unique workshop in oceanic petrogenesis, where most of the features relevant to the discussion appears. The present paper reports the results of five years of research in basalt petrology in Iceland and a systematic review of rift zone geology and petrology taking account of the following main subjects:

(1)   Geophysical evidence for the crustal structures and thermal
       regime.

(2)   Mineralogical constitution of the crust with reference to deep
       drilling data from the rift zone and regional metamorphism of
       the tertiary formation outside the rifts.

(3)   The distribution and evolution history of volcanic centers in
       and outside the rift zone.

(4)   Regional distribution, tectonic environment and mineralogical
       evolution of the tholeiitic and alkaline magma types.

(5)   Distribution of dispersed elements within the Icelandic rift
       system.

(6)   Isotope geochemistry of the Icelandic rift system.

       Our conclusion is that the observed regional petrology, chemical
variations, isotope evolution and volume relations of the oceanic magma
types are controlled by the dynamic processes within a rift zone crust
which is fed by a single mantle derived magma type of ol-tholeiite com-
position.

       In order to manage the multitude of available data the represen-
tation of the above conclusion is paraphrased in a model of oceanic
petrogenesis appearing in the first sections of the paper. The later
sections contain an introduction to the Icelandic rift system written in
the form of supporting evidence for the model where also alternative
models are discussed with references to other areas.

THE CRUSTAL ACCRETION

A kinematic model of crustal accretion

       The kinematic processes at accreting plate margins were modelled
by Pálmason (1973). The parameters of the model are drift and subsidence
velocities, and rift zone width. Subsidence velocity is taken as equi-
valent to accumulation of volcanic material at the surface, assuming
local isostatic equilibrium. Drift velocity is estimated from field

observation. Rift zone half-width is defined as the distance from the
rift zone axis to the rift zone margin, where subsidence due to accumu-
lation becomes zero (the farthest distance which lavas flow to either side
of the axis). A numerical calculation of the model based on best avail-
able values for drift and subsidence in Iceland (drift: 2 cm/year; sub-
sidence: $4/3 \times 10^{-4}$ km/year) is shown in Fig. 1. The paths of mass-element
trajectories are shown with broken lines, while solid lines indicate
isochrones

    The parting of the lithospheric plates is compensated for by the
injection of magma from the upper mantle. Model calculations of the
thermal regime across the rift zone and the adjoining plate margins show
good correspondence to extrapolated geothermal gradients measured in
Iceland (Pálmason, 1973).

    Several relevant deductions can be made on the basis of Fig. 1.

(1)   By definition all surface rocks are of zero age from rift axis
      to the rift margin.

(2)   As shown by the 1 m.y. isochrone the surface rocks of this age
      occur 10 km away from the rift margin and at a depth of 7 to
      10 km within the rift zone. Higher rates of subsidence or slower
      rates of drift result in steeper isochrones.

(3)   Only those rocks, which accumulate near the rift margin, remain
      visible at the surface of the oceanic plate. Deep (2 km)
      erosion or drilling, will only expose rocks, which accumulated
      at the marginal zones of the rift. The central part of the rift
      zone subsides below reach.

(4)   Numerical evaluation of the model and available evidence on
      temperature distribution in the rift zone show that the solidus
      temperature of amphibolite is reached at shallow depth (5-7 km).

(5)   Assuming steady state of production and drift the isotherms
      stay at a constant depth. Subsidence and drift move the rift
      zone material relative to the isotherms. A mass element depo-
      sited at a short distance from the rift zone axis is carried
      down through a steep thermal gradient towards a maximum tempera-
      ture and then laterally through a decreasing temperature gradient.
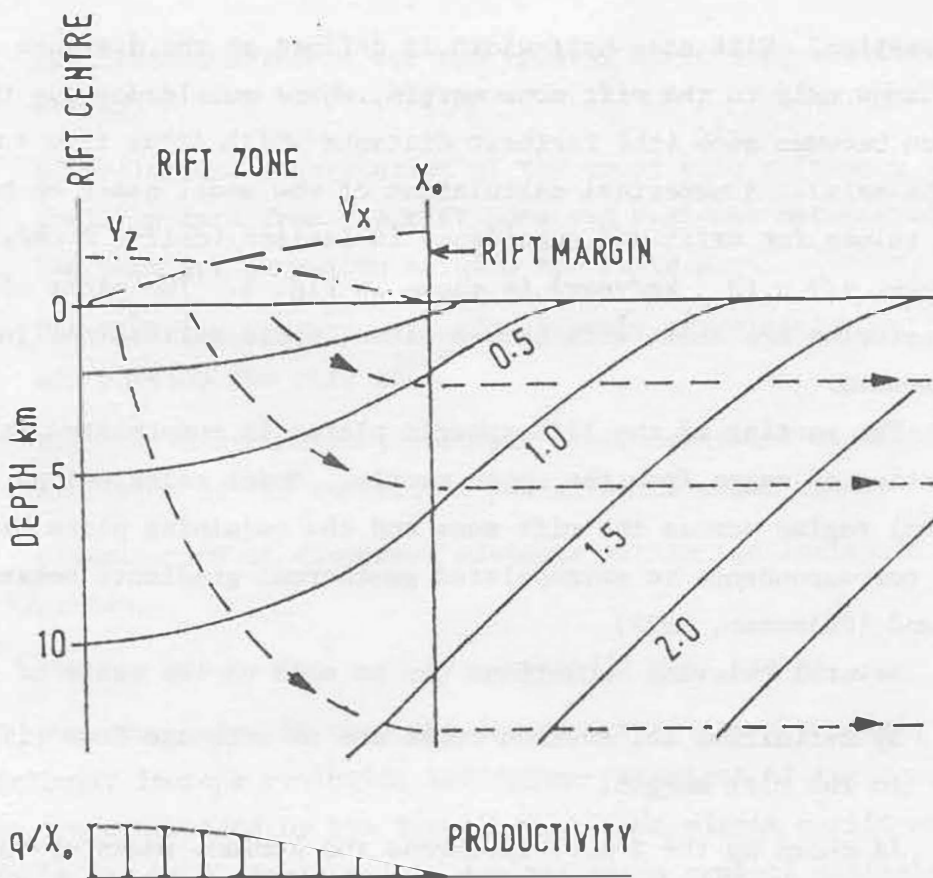
Fig. 1. The parameters of the kinematic model of crustal accretion (Pálmason, 1973). The extruded material at the rift surface is represented by the productivity function q/Xo, where Xo is the distance from rift center. The rift margin is at a point, where the time integrated productivity of the rift zone approaches zero. The velocity vectors of a mass element within the rift are termed Vx (drift) and Vz (subsidence). At the rift margin Vx reaches a constant value as Vz reaches zero. Across the rift the subsidence vector Vz varies as the productivity function q/Xo. The variable magnitude of Vz across the rift results in mass trajectories (dashed lines) producing the isochrone pattern (0.5-2 m.y.) shown by even lines in the figure. It is evident, that (a) the material retention time within the rift depends on the kinematic parameters and (b) that the accreting plate surface is almost exclusively composed of material erupted at the rift margin (off rift rocks). The kinematic model is applied to the rift zone as a whole or its subunits (fissure swarms).

Metamorphism and chemical fractionation in the rift zone and layering of the oceanic crust

The metamorphic zonation of the Icelandic crust (Fig. 2) and, by inference, the oceanic crust in general, can be deduced from geophysical measurements, extrapolation of data from geothermal wells and the denuded Tertiary formation, as well as by comparison to other areas.

Pálmason (1971) made a detailed seismic refraction survey of the Icelandic crust. According to his interpretation, a surface layer with P-wave velocities ranging from 2.0-3.3 km/s is followed downwards by "layer 3" of V_p = 6.5 km/s, which is considered to correspond to the oceanic layer. Finally, the surface of the upper mantle represents "layer 4" of V_p = 7.2 km/s, an anomalously low P-wave velocity thought to indicate a liquid fraction.

The temperature regime of the Icelandic crust (Pálmason, 1971 & 1973; Hermance & Grillot, 1974) is consistent with the contention of a liquid fraction at the top of "layer 4" and amphibolite-facies metamorphism in "layer 3", which consists of "metabasite" (Mevel et al., 1978). Björnsson (1977), using in situ resistivity measurements, compared to experimental results, concluded that the upper part of "layer 3" consists of water saturated rocks with 1-3% pore space.

In geothermal areas, associated with magmatic activity, mineral assemblages corresponding to the lower greenschist facies, are reached at about 800 m depth and 280°C (plagioclase + actinolite + epidote + quartz + calcite + pyrite). This assemblage persists down to about 2500 m (Pálmason et al., 1979).

The highest metamorphic grade found in Iceland is distinguished by the appearance of garnet in the aureoles of intrusions (e.g. Sigurdsson, 1970; Annels, 1968) and in geothermal wells (Kristmannsdóttir et al., 1976) at about 700 m depth, attributed to contact metamorphism at 500-600°C. In the Troodos ophiolite complex of Cyprus (Moores & Vine, 1971), the metamorphic grade of the sheeted dike complex ranges from a plagioclase-actinolite-chlorite-quartz-magnetite assemblage, to one in which the actinolite + chlorite is replaced by hornblende + diopside (Gass & Smewing, 1973).

The heat source of an accreting oceanic plate is the magma injected into the rift zone. The temperature regime for an oceanic crust shows that all prograde metamorphic reactions take place within

Fig. 2.

LAYER 1
Zeolite facies
200°
Chlorite-epidote facies
LAYER 2
Greensch.
Amphibolite
Greenschist
400°
ANATEXIS
Low grade amphibolite
600°
High grade amphibolite
LAYER 3
DEHYDRATION of AMPHIBOLITE
800°
1000°
Granulite facies
1200°
LAYER 4

RIFT
RIFT

① ② ③ ④

X_o

DEPTH km
0
5
10
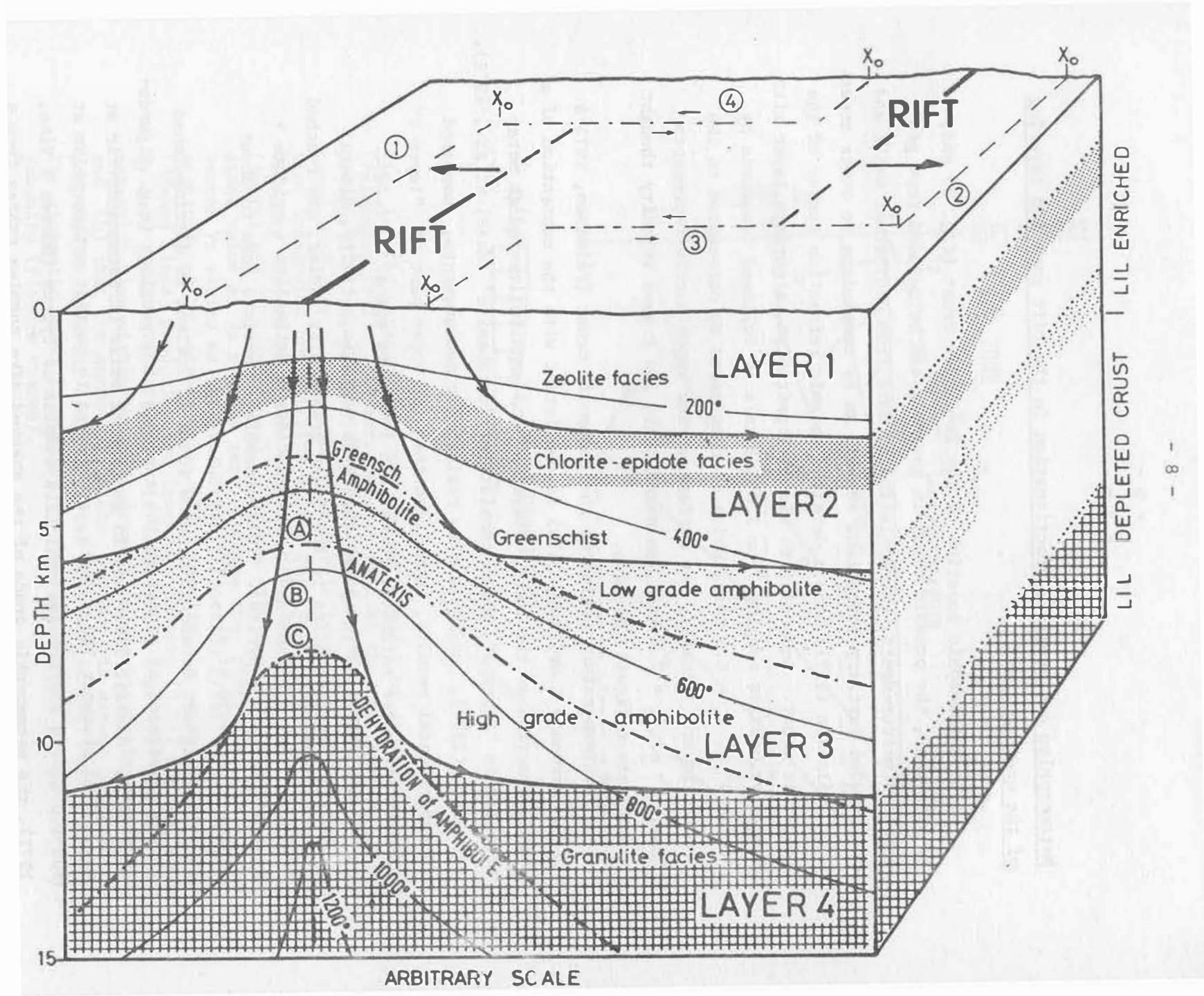15

ARBITRARY SCALE

LIL ENRICHED | LIL DEPLETED CRUST

- 8 -

Fig. 2. The isotherms and layering of the oceanic crust is shown on
the front of the diagram. Where the temperature maxima of mass tra-
jectories coincide with the PT conditions of a metamorphic reaction
a layering of the crust is established. In the uppermost crustal
layers (1 and 2) the reactions are isochemical. The shallowest mass
trajectory shown in the figure touches the zeolite chlorite/epidote
facies boundary. The second mass trajectory shown in the figure
touches the greenschist/amphibolite facies boundary. A mass element
reaching its solidus temperature suffers partial melting (anatexis).
The mass element reaching its max. temperature at the anatectic
boundary marks the surface of the high grade amphibolite which is
silica and dispersed element depleted (point A).   Here
the transport of crustal derived magma to the upper crustal layers is
equivalent to material recycling within the rift zone since that magma
subsides down a new (younger) material path. In the interval between
the anatexis boundary and dehydration of amphibolite a continuous
equilibration involving magma formation takes place (point B in the
figure). At point C dehydration of amphibole is finished. The mate-
rial subsiding below this point assumes granulite facies, and a mass
trajectory touching the dehydration line defines the boundary between
crustal layers 3 and 4. The thickness of the oceanic crust is con-
trolled by the thermal gradient across the rift fixing the depth of
granulitization.

The surface of the block diagram shows the relation between the kine-
matic parameters in a rift, offset by a fracture zone. The regional
drift velocity is indicated by arrows on the surface and the rift
margins are marked by Xo. Since the two rift zones are overlapping,
a variable width and material retention time will be observed along
the rift. A rift zone is composed of discrete spreading centers
(fissure swarms). The spreading is randomly distributed among these
subunits. An extensive rifting on the western flank of the join
(point 1 in the figure) results in active fracturing along the northern
margin of the fracture zone (point 4). A volcanic center at the south
termination of the eastern rift will be trapped in the eastern plate
margin (point 2). Similarily an extensive rifting on the eastern zone
(point 2) results in fracturing along the southern fracture zone
(point 3) and plate trapping of volcanic centers at the western rift
margin (point 1). The right face of the block diagram shows the dis-
continuity in crustal layering aside the fractured rift system. At
the south termination of the eastern rift the older plate, formed on
the western rift, is exposed to high thermal regime. Here the chemi-
cally fractionated volcanic centers of the older plate are reactivated
by thermal impact. The figure is a simplified model of the Icelandic
rift system. Volcanism outside the rift zone is observed at the rift
terminations and on the flanks of the fractured section of the rift
(point 1 and 2).

the zone of rifting. Thus, for the purpose of estimating the tempera-
ture regime of metamorphic zonation in the crust, the highest gradients
should be used.

In view of the above, a static picture of the crustal layering in
Iceland can be constructed. We follow an element of basaltic rock
along its kinematic path (Fig. 2).

The uppermost kilometers of water permeable crust are subjected
to extensive hydrothermal alteration. The rock is converted into a
hydrated mineral assemblage in the zeolite facies. With increasing depth
and temperature dehydration sets in, zeolites break down, and the
phyllosilicates are replaced by amphiboles. The rock is now in the
greenschist facies.

As the rocks assume lower amphibolite facies, actinolite is re-
placed by hornblende, containing still less structural water. The
alteration, patchy at first, becomes ever more pervasive; the water
given off by the dehydration of the hydrous minerals goes to hydrate
the still-remaining igneous minerals; clinopyroxene and plagioclase are
replaced by amphibole, biotite, sericite and calcic plagioclase.

The boundary between the low and high grade amphibolite facies
is set at 650-700°C. This is the beginning of incongruous melting of a
hydrated basalt at 5 kb in Helz´s (1973, 1975) experiments. Silicic
minimum melt fractions are produced initially, while a continuous com-
positional readjustment of the residual minerals takes place: the
amphibole changes from green hornblende at 700°C to kaersutite at
1000°C, plagioclase diminishes in amount, to disappear at about 850°C,
when augite starts replacing it. Therefore, at about 700°C anatexis
sets in, separating decreasingly silicic magma fractions physically
from a refractory crystal assemblage, which is carried further down.

At about 1000°C the kaersutite amphibole melts incongruently,
yielding a ne-normative melt increment   the remaining refractory
part has upper mantle mineralogy of olivine and pyroxene   this is
the boundary between seismic layers 3 and 4. Accordingly the upper
mantle contains peridotite domains isotopically equilibrated with the
rift zone crust.

During subsidence through the zeolite-greenschist and lower grade
amphibolite facies the continuous equilibration of the hydrated crust
is essentially an isochemical process.

The passage of material into the high grade amphibolite facies marks the beginning of chemical fractionation by anatexis, resulting in a chemical gradient in the lower part of crustal layer 3 (Fig. 2).

The fractionation processes as inferred form experimental data (Helz, 1973 & 1975; Holloway & Burnham, 1972; Yoder & Tilley, 1962; Luth, 1976) can be resolved into three steps, each resulting in a characteristic change in major and trace elements of the respective crustal derived magmas.

A magma formed below 750-800°C contains all the phlogopite and alkali feldspar of the amphibolite. It is of rhyolite composition in equili-brium with residual plagioclase and amphibole;

(a)   The K/Na ratio of the magma is high compared to that of the residue, since practically all the normative orthoclase com-ponent of the bulk enters the magma.

(b)   The K/Rb ratio of the magma is low, since the residual amphibole controls the ratio as the sole K-host after the alkali feldspar and phlogopite (K/Rb = 200-300) disappear. In contrast, the K/Rb ratio of the residue (amphibolite) is about 1000 (Philpotts & Schnetzler, 1970; Hart & Aldrich, 1967; Shimuzu, 1974).

(c)   The plagioclase persisting through the incipient melting stage controls a low Sr content and a strong negative Eu anomaly in the liquid magma. The residue is Sr rich with a weak positive Eu anomaly. The REE pattern of the magma is strongly enriched in the light REE, with a high Nd/Sm ratio (Drake, 1972).

(d)   The volatile chemistry of the magma is characterized by increased HCl/HF ratio relative to the bulk composition since the residual apatite and amphiboles favour HF over H_2O and HCl (Burnham, 1967; Stormer & Carmichael, 1971).

The second step of predictable chemical fractionation occurs during the formation of silicic to intermediate magmas in the tempera-ture interval 750-900°C. The end of this stage is marked by the appearance of augite in the magma produced in this residual assemblage. The melt interval is characterized by

(a)   an increasing Na/K ratio, high Sr content, and a positive Eu anomaly, due to melting of plagioclase,

(b)   light RE element enrichment resulting from the presence of
      residual clinopyroxene,

(c)   intermediate to high K/Rb ratio due to earlier depletion of
      Rb and low Rb/Sr ratio.

     In the third fractionation step kaersutitic amphibole and apatite
are consumed yielding a ne-normative magma. The magma is high in
titanium, iron, phosphorus, zirconium and fluorine, since the residual
olivine and clinopyroxene incorporate none of them. The REE pattern of
the ne-normative magma is light element enriched due to incorporation
of the heavy RE elements in clinopyroxene. The Na/K ratio of the magma
decreases due to increased jadeite solid solution in clinopyroxene.
     The layering of the oceanic crust is established in the rift zone
by the different travel paths of the plate forming material. The most
important processes taking place are:

(a)   The retention of crustal derived magma within the rift zone crust
      crust

(b)   The silica and dispersed element depletion of the lower part of
      crustal layer 3 and

(c)   The passage of material through the amphibolite/granulite
      boundary returning a significant amount of crustal derived
      material to the upper mantle.

     An important factor implicit in the crustal accretion process
is the production rate of mantle derived magma, which can be illustrated
by comparison of two rift segments with the same drift velocity but
different injection rate of otherwise similar material.

(a)   In both cases the only heat and potential energy added to the
      rift zone is that of the mantle derived magma.

(b)   The more productive segment maintains a thermal structure with
      flat isotherms as compared with steep gradient across the axis
      of the less productive rift.

(c)   Since the minimum depth of reaction boundaries in the rift zone
      crust stays almost constant in the PT space above the thermal
      maxima the more productive rift passes more material through
      these boundaries and thus returns more refractory material to

the upper mantle. The thickness of the upper crustal layers
is, however, comparable in both cases resulting in higher
enrichment of dispersed elements in the crust of the more
productive rift.

(d)   Since the width of a rift zone is defined as the farthest reaches
of lavas aside the rift axis, the higher potential energy of the
productive rift results in a wider rift zone as compared to the
less productive and thus narrower rift.

(e)   The average retention time of material within a rift zone is its
volume divided by the annual output as given by the drift velocity.
The more productive, wider rift retains its crustal derived
material longer than the narrow rift.

(f)   All mantle derived melts entering the surface ascend through a
column of fractionated subsiding material in a counter current
fashion. The inevitable reactions of the mantle derived magma
with the different layers at the rift zone crust is more extensive
the more productive the rift.

The surface manifest of a productive rift segment is therefore a
wide rift zone and high average content of dispersed elements. Geo-
physically the productive rift appears as a wide zone of high heat flow
and increased thickness of the lower crustal layers. We therefore
identify the most productive segments of the world´s rift systems as
hot spots.

A DYNAMIC MODEL OF RIFT ZONE PETROGENESIS

The equilibration of a mantle derived ol-tholeiite with the
fractionated crust alters its subsequent chemical and minera-
logical evolution. The most important process in basalt genesis is
mixing of the primitive ol-tholeiite with subordinate amounts of
(a) alkali olivine basalt at the mantle crust boundary and (b) silicic
magma in the amphibolite facies. The observed rock suites of the rift
zone and its margins represent mixtures of the three magma types in

different proportions or the end members. The mixtures are modified
to various extent by crystal fractionation towards invariant composi-
tions.

The basaltic magma types of the oceanic environment can be re-
solved into divisions resembling mineralogical equilibration at
quaternary invariant points. In the "basalt tetrahedron" (Yoder &
Tilley, 1962) there are three such invariant points, termed olivine
tholeiite, tholeiite and nepheline basanite (Schairer & Yoder, 1964).
A fourth invariant point relevant to this discussion is the minimum
melt in the granitic system (Luth, 1976).

In Fig. 3a (right) the mineralogical evolution path of ol-tholeiite
is illustrated by an arrow within the tetrahedron Di-An-Fo-SiO$_2$, and a
dashed arrow on its bottom plane SiO$_2$-An-Fo. The idealized path goes
by precipitation of olivine and plagioclase until the magma reaches an
univariant mineralogical composition when clinopyroxene enters the
assemblage at a point inside the tetrahedron (Presnall, 1978). Towards
the end of crystallization orthopyroxene joins the assemblage as the
system reaches the ol-tholeiite invariant.   Ol-tholeiite dominates
all oceanic rift zones but appears at widely different degrees of mine-
ralogical evolution.

Mixing of a silicic liquid, formed at the invariant of the
granite system, with olivine tholeiite establishes a reaction between
forsterite and silica. The consumption of forsterite drives the liquid
across the enstatite field in the system SiO$_2$-An-Fo towards the
tholeiite invariant (an, cpx, opx, tr.) in the basalt system as indi-
cated by the dashed arrow in Fig. 3a (right). In the rift zone this
magma type occurs only in the evolved volcanic centers and is identical
with so called "oceanic island tholeiites" and qz-tholeiites.

The alkali olivine basalts are formed by partial melting of silica
depleted amphibolite in the system Fo-Di-An-Ne (Fig. 3a, left). The
liquid evolves along the phase boundary Di-An-Fo towards the plane of
silica undersaturation representing the third invariant (an, fo, cpx,
ne) of the basalt system, i.e. nepheline basanite. If olivine is
assumed to be the last phase to disappear during extensive melting,
two evolution paths are possible depending on which phase Di or An is
consumed first (indicated in Fig.3a). The majority of the ne-normative
basalts are, however, near equilibrium with all three phases (alkali
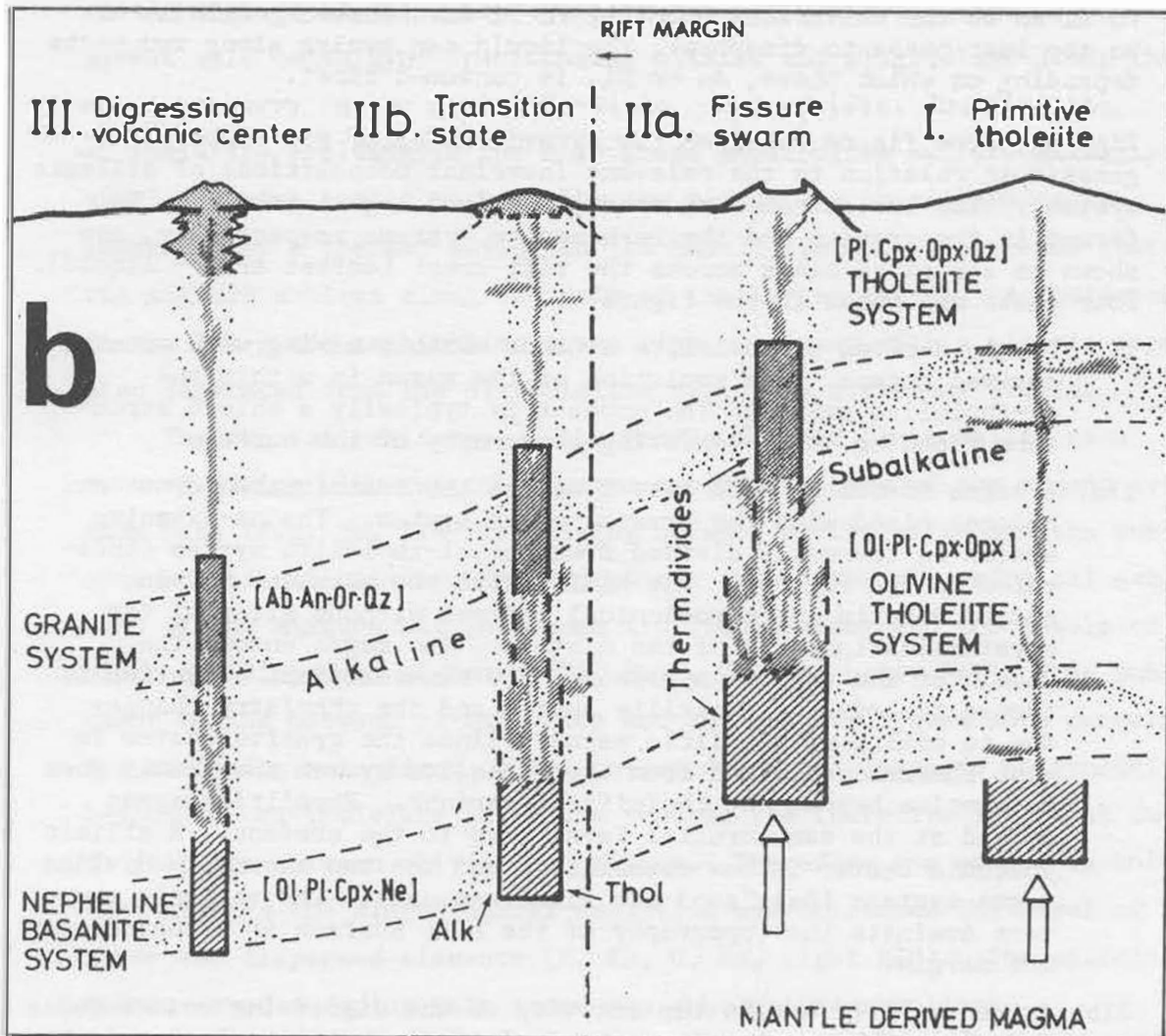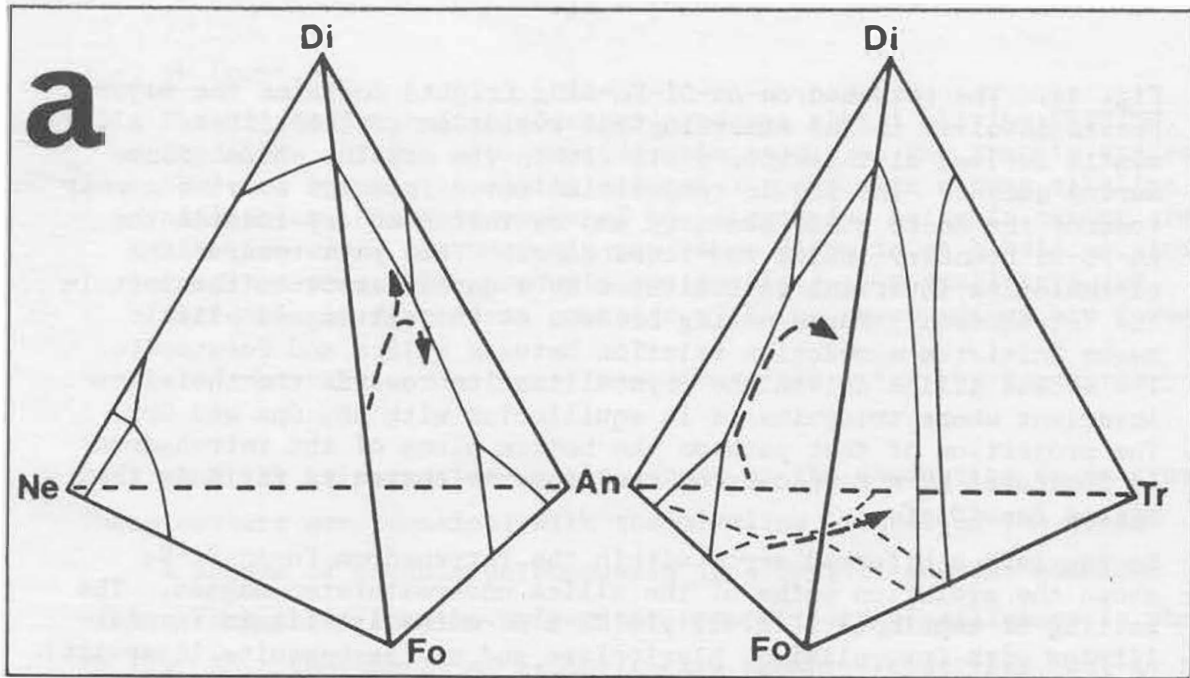olivine basalts). In active volcanic centers digressing away from the

Fig. 3.

Fig. 3a. The tetrahedron An-Di-Fo-SiO$_2$ (right) contains the major phases involved in the mineralogical evolution of tholeiites. A mantle derived ol-tholeiite plots within the olivine phase volume during ascent. The liquid composition moves from the olivine corner towards the An-Fo phase boundary and on that boundary towards the An-Fo-Di boundary inside the tetrahedron. This path towards the ol-tholeiite invariant is indicated by a dashed arrow to the left in the tetrahedron. Magma mixing between ol-tholeiites and silicic magma initiates a reaction relation between silica and forsterite. The excess silica drives the crystallization towards the tholeiite invariant where tridymite is in equilibrium with An, Cpx and Opx. The projection of that path on the bottom plane of the tetrahedron is indicated by a dashed arrow crossing the enstatite field in the system An-SiO$_2$-Fo.

To the left a biforced arrow within the tetrahedron Fo-An-Di-Ne shows the evolution paths of the silica undersaturated magmas. The melting of amphibole (Fig. 2) yields a ne-normative liquid in equilibrium with Cpx, olivine, plagioclase and ne (ne-basanite invariant). Increased melting drives the liquid composition towards the plane Fo-Di-An on the univariant boundary Fo-Di-An. Assuming olivine to be the last phase to disappear, the liquid can evolve along two paths depending on which phase, An or Di, is consumed first.

Fig. 3b. The figure outlines the dynamic model of rift zone petrogenesis in relation to the relevant invariant compositions of silicate systems. The two extremes of crustal derived magmas (see Fig. 2) formed in the granite and the re-basanite systems respectively, are shown as separated bands across the rift crest (dottet area = liquid). Four cases are shown in the figure:

I. Mantle derived ol-tholeiite ascends without mixing with crustal derived magmas. The evolution of the magma is within the ol-tholeiite system. The product is typically a shield structure flooding the preexisting topography of the surface.

IIa. A magma identical with case I enters the fractionated crust and becomes mixed with the crustal magma system. The ne-basanite system is thermally divided from the ol-tholeiite system (indicated in the figure). The mixing with the alkaline olivine basalt results in petrochemical changes without altering the crystallization path of the mixture. The magma enters the domain of the granite system and the mineralogical evolution is turned towards the tholeiite system and the chemistry changes due to mixing with silicic magma. Since the granite system is also thermally divided from the tholeiite system the basalt does not evolve beyond the tholeiite invariant. Rhyolitic magmas formed at the same crustal level rise to the surface. A silicic volcanic center is now established and the two thermally divided magma systems (Daly gap) act simultaneously. The volcanic centers dominate the topography of the rift surface if situated near its margin.

IIb. Aside the rift margin the activity of the digressing center fades out since the supply of mantle derived ol-tholeiite is terminated. When the ne-basanite magma exceeds the remnant ol-tholeiite the evolution goes along the path of silica undersaturated rocks (right to left in the figure).

Fig. 3b (cont.).

III. The digressive volcanic center produces alkali olivine basalts
at depth. Mixing with considerable amount of the granite system,
however, results in silica saturated rocks with strong alkaline
affinities. Silicic rocks of the digressive volcanic center are
alkaline since the anatexis now takes place in an alkali olivine
basalt matrix. The products are confined to a small area and
increasingly discordant contacts with the surroundings are formed.

rift zone the ne-normative basalts occur as the dominating magma type.
These centers are identical with the alkaline islands of the ocean.

A scheme of oceanic petrogenesis in a crustal section combined
with a flow sheet for the univariant compositions of silicates is shown
in Fig. 3b. Four paths of evolution are shown: First (Fig. 3b, I) a
mantle derived ol-tholeiite equilibrates below crustal layer 3. During
ascent this magma type fractionates olivine and plagioclase along the
An-Ol boundary in the system Fo-Di-An. Second (Fig. 3b, IIa) the
ol-tholeiite residing in the high grade amphibolite suffers mixing with
alkali olivine basalt magma. The two magmas are physiochemically
separated by a thermal divide in the basalt system, which means that
the mixture evolves along the path of the larger system. A residence
in the low grade amphibolite gives rise to mixing with a silicic magma
also separated from the ol-tholeiite system by a thermal divide.

The crustal residence of the mantle derived ol-tholeiite thus
favours mixing with two other magma types. In case of the second evolu-
tion path (Fig. 3b, IIa) the mixing between ol-tholeiite and the sub-
ordinate alkali olivine basalt does not affect the mineralogical evolu-
tion of the mixture but increases its iron content and the levels of
minor and dispersed elements (Ti, P, F, Zr, Sr, heavy REE). The subse-
quent mixing between ol-tholeiite and the granite system both cancels
the mineralogical effect of the ne-component and leads to an evolution
beyond the ol-tholeiite invariant towards the tholeiite invariant due
to reaction between olivine and silica. Therefore the mixing in this
case affects the mineralogical evolution and increases the level of
minor and dispersed elements (K, Rb, U, Ba, light REE). The silicic
magmas erupted during this stage are subalkaline rhyolites.

The transition from tholeiitic to alkaline volcanism is outlined
in Fig. 3b, IIb, showing the continued evolution of an active volcanic
center digressing away from the rift zone. The center is detached from

its supply of ol-tholeiite and the only remaining kinematic parameter
is subsidence. Consequently the crustal derived magmas dominate the
petrology and the volume produced decreases. The basalts change from
a tholeiitic type with strong alkaline affinities (transitional basalts)
to ne-normative basalts with almost tholeiitic mineralogy. The petro-
logical classification of these rocks is only possible by examination
of the latest phases formed during crystallization, since the major
phases in both cases are Ol, An and Cpx. The fourth phase is Opx,
where the ol-tholeiite system still dominates but Ne where the ne-basanite
takes over. The silicic magmas formed during the transition stage are
mildly alkaline.

The purely alkaline digressive volcanic centers produce crustal
derived magmas (Fig. 3b, III). The total production is small as com-
pared to the tholeiitic centers of the rift zone. The basalts are
ne-normative and give rise to alkaline silicic rocks during anatexis in
the amphibolite facies. Since the activity continues until the magmatic
energy stored in the center is exhausted, the subsiding core can reach
a great depth. The thermal structure of the crust requires greater
depth of magma formation the longer the distance from the rift zone.
In extreme cases of evolution the roots of the digressive center may
reach well into the granulite facies. In this sence the extreme
alkaline basalts are mantle derived but their material is of crustal
origin. Therefore no mantle source can be defined for the alkaline rock
but instead the petrochemical character of these rocks reflects the
state of their parental crust.

Before the above model will be compared to the regional petrology
and chemistry of the Icelandic rocks, the compositional variability
of the oceanic rocks will be compared to the evolution stages of the
model. In Fig. 4 the Mg/Mg+Fe ratio of rocks from the Icelandic rift
system is plotted against their TiO_2 content. The filled circles
represent the rocks from the rift zone. The primitive ol-tholeiites
(case I in Fig. 3b) occupy the upper left of the figure at TiO_2 below
1.2%. The filled circles at TiO_2 between 1.2% and 2.5% represent vol-
canic centers of the rift zone (case IIa in Fig. 3b). The crosses in
the figure represent transition state of the rift margin volcanism
(case IIb in Fig. 3b) and the digressive volcanism (case III in Fig. 3b).
The trends to the right in the figure show evolution of a digressive
volcanic center (marked Snaefellsnes) within the Icelandic rift system
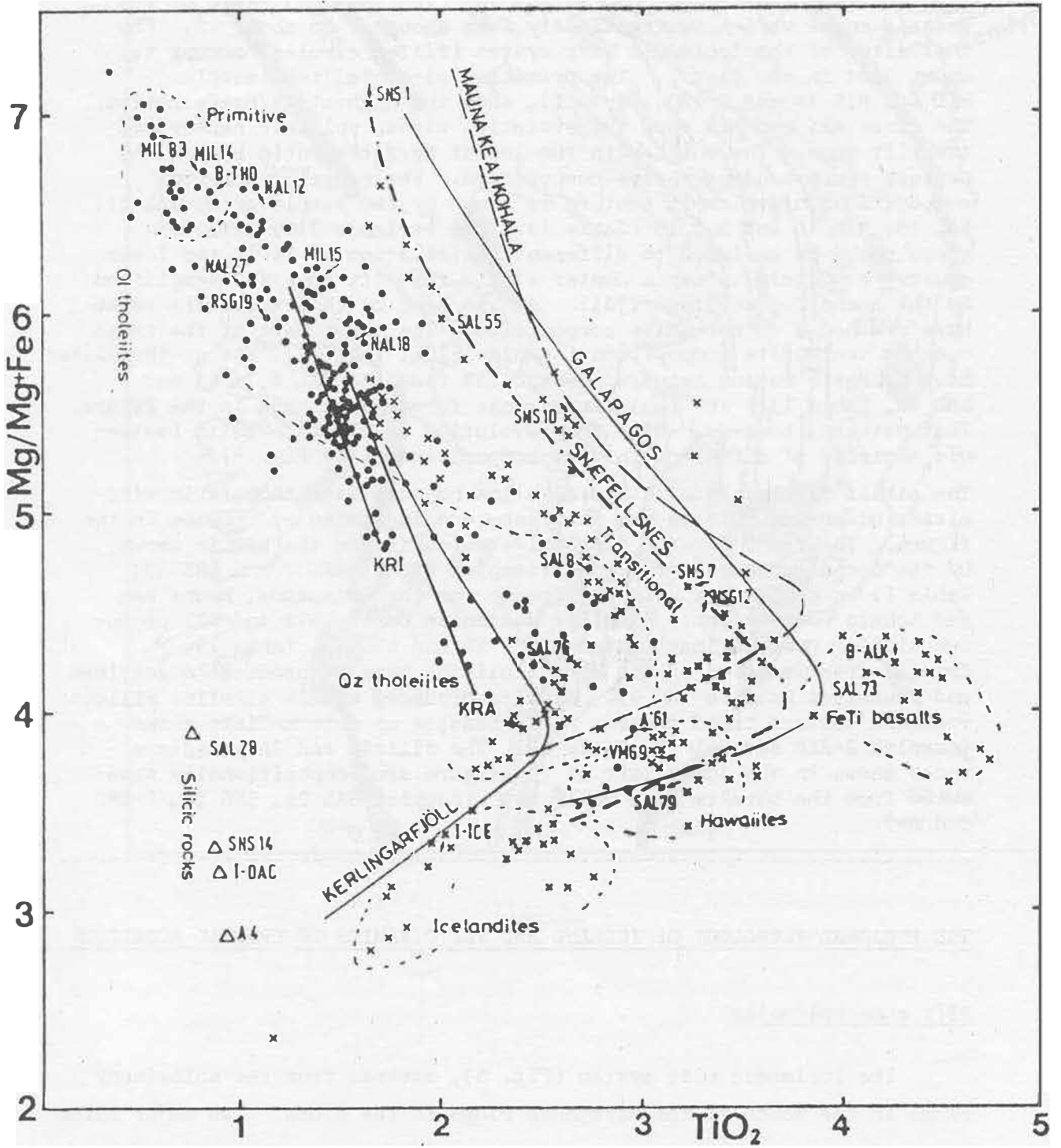in comparison to evolution of alkaline rocks from other areas.

Fig. 4.

Fig. 4. The Mg/Mg+Fe (atomic ratio, Fe^{III}/Fe^{II} = o.1) ratio of the oceanic rocks varies systematically from about .7 to about .3. The tholeiites of the Icelandic rift system (filled circles) occupy the upper left in the figure. The primitive ol-tholeiites (samples MIL 83, MIL 14 and B-THO, Table I), show the highest Mg/Mg+Fe ratios. The lines KRI and KRA show the evolution within volcanic centers of the rift zone. The rocks with the lowest Mg/Mg+Fe ratio within the centers reach a qz-normative composition. The range of parental compositions of volcanic centers is shown by the sample group NAL 27, NAL 18, MIL 15 and RST 19 (Table I). The variable TiO_2 level of these rocks is assigned to different assimilation of Ti in the lower crust. A silicic volcanic center within the rift zone is exemplified by the trend for Kerlingarfjöll. At the bend of this trend the rocks have reached a qz-normative composition. The lower part of the trend reaches icelandite composition (sample I-ICE, Table I). The qz-tholeiites have Mg/Mg+Fe ratios between .35 and .55 (samples SAL 8, A´61 and SAL 79, Table I). The tholeiitic rocks form a continuum in the figure. That pattern, however, arise from evolution of discrete units (volcanic centers) of different initial compositions (see Fig. 5).

The alkali olivine basalts and alkaline basalts with tholeiitic affinities occurring outside the rift zone are indicated by crosses in the figure. The trend for the digressive volcanism on the WDV is shown by the trend marked Snaefellsnes (samples SNS 1, SNS 7 and SNS 10, Table I) in comparison with the trends for the Galapagos, Mauna Kea and Kohala rock suites. Alkaline volcanism on the STZ and NTZ produces similar compositions (samples SAL 55 and NSG 12, Table I). Crystal fractionation of the alkali olivine basalts produces mugearites and hawaiites (sample VMG 9). Basalts produced within alkaline silicic volcanic centers trend towards Fe-Ti basalts or intermediate rocks (samples B-ALK and SAL 73, Table I). The silicic and intermediate rocks shown in the lower left of the figure are compositionally separated from the basalts by a "Daly gap" (samples SAL 28, SNS 14, I-DAC and A4).

THE REGIONAL PETROLOGY OF ICELAND AND THE DYNAMICS OF CRUSTAL ACCRETION

Rift zone volcanism

The Icelandic rift system (Fig. 5), extends from the Kolbeinsey ridge in the north to the Reykjanes ridge in the south. Two major rifts are active across the system; the western rift zone (WRZ),which joins the Reykjanes ridge,and the eastern rift zone (ERZ) joining the Kolbeinsey ridge in the Tjörnes fracture zone (TFZ). The two rifts join in central Iceland (MIL) which is the widest section of the entire rift. The volcanic productivity, crustal thickness and the rift zone width decrease away from Central Iceland towards the north and south (Tryggvason, 1973; Pálmason, 1971; Saemundsson, 1978). The relatively uniform distance from the rift margins to reliable isochrones aside the rift indicate that
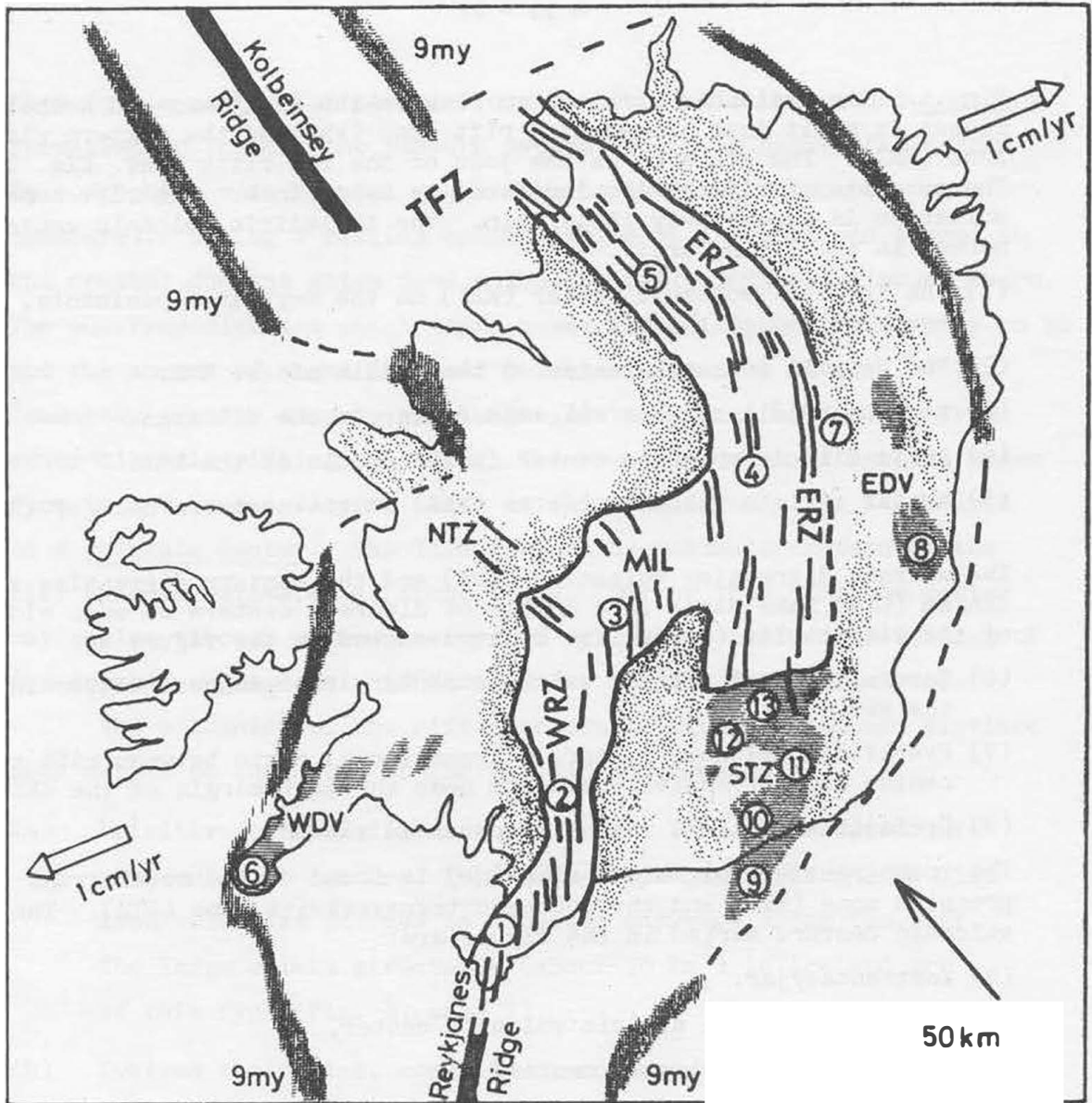
Fig. 5.

Fig. 5. The Icelandic rift system between the Reykjanes and Kolbeinsey ridges is split into the western rift zone (WRZ)and the eastern rift zone (ERZ). The MIL area is the join of the two rifts (ref. Fig. 2). The subunits of rifting are indicated by even lines. The rift zone volcanism is exclusively tholeiitic. The tholeiitic volcanic centers marked in the figure are:

(1) The Krísuvík volcanic center (KRI) on the Reykjanes peninsula, southern end of the WRZ.

(2) The Hengill volcanic center on the middle of the WRZ.

(3) Kerlingarfjöll silicic volcanic center in the MIL area.

(4) Askja silicic volcanic center in the middle of the ERZ.

(5) Krafla silicic volcanic center (KRA) in the northern half of the ERZ.

The western digressive volcanism (WDV) and the eastern digressive volcanism (EDV) take place in a number of discrete centers on each side of the widest rift (MIL). The centers marked in the figure are:

(6) Snaefellsjökull silicic volcanic center, the youngest center in the WDV.

(7) Kverkfjöll volcanic center, a transitional state between rift volcanism and digressive volcanism near the east margin of the ERZ.

(8) Öræfajökull silicic volcanic center in the EDV.

The transgressive volcanism (alkaline) is found on the north transgressive zone (NTZ) and the southern transgressive zone (STZ). The volcanic centers marked in the figure are:

(9) Vestmannaeyjar.

(10) Eyjafjallajökull silicic volcanic center.

(11) Katla silicic volcanic center.

(12) Hekla silicic volcanic center.

(13) Torfajökull silicic volcanic center.

The approximate extent of the alkaline rocks is shaded in the figure. The dotted rims in the figure outside the rift zone shows the approximate exposures of quaternary rocks. The approximate position of the 9 m.y. isochrone is shown by a hatched band aside the rift zones and inferred by a dashed line, where data are lacking. Towards the northern end of the ERZ, the Tjörnes fracture zone (TFZ) joins the Icelandic rift system and the Kolbeinsey ridge. To the left and right in the figure the approximate regional drift vectors (1 cm/yr) are shown.

the present geometric arrangement and variable width of the rift zone have been stable at least 9 m.y. and probably much longer (Saemundsson, 1978). The Icelandic rift is composed of a number of subparallel fissure swarms. A fissure swarm is a set of fissures formed in response to crustal dilation. At the surface the fissures are open or

they form a pattern of parallel dislocations. In the eroded tertiary
formation in Iceland the fissure swarms appear as dense dike swarms
in connection with crustal magma domains (holding chambers, magma
chambers). During a rifting episode magma is intruded and stored in
the crustal domains which feed magma laterally into the fissure swarm.
The observed distance which magma moves in one such episode is up to 50 km
and the amount of magma is about 0.5 km^3 (Björnsson et al., 1977).
Immensely greater amounts and longer distances can be implied from
other historic rifting episodes. The observed depth of lateral magma
flow is 3-7 km. A fissure swarm at this evolution stage is defined
as a <u>volcanic center</u>. The lifetime of the volcanic centers of the
rift zone is estimated at about 1 m.y. During that time the center
may evolve through numerous eruptive cycles and periodic refilling of
its crustal magma domain (O´Hara, 1974; Dungan & Rhodes, 1978).

The volcanism of the rift zone can be divided into two distinct
rock suites on the basis of their field occurrence.

(a)   Primitive ol-tholeiites (samples 1-8, Table I) erupted out-
      side volcanic centers. This magma type dominates in the rift
      zone volcanism and can be expected anywhere along the rift.
      The large shield structures (about 10 km^3) in Iceland are
      of this type (Fig. 3, case I).

(b)   Evolved tholeiites, commonly qz-normative (samples 9-11,
      Table I) produced in numerous eruptions within volcanic
      centers. These eruptions are small (about 1 km^3) fissure
      eruptions.

The volcanic centers show increased petrological evolution and
dispersed element enrichment towards central Iceland (Sigvaldason et
al., 1974). The most highly evolved are the <u>silicic volcanic centers</u>
(Fig. 3, case IIa), where subalkaline silicic rocks (samples 12-15,
Table I) are produced in addition to the qz-tholeiites. The silicic
volcanic centers develop caldera structures and high temperature geo-
thermal areas and occur in the widest section of the rift but are not
observed on the narrowest rifts towards the north and south.
Since the magma injected into the crustal magma domains is iden-
tical with the primitive ol-tholeiite which dominates the rift zone
(Wood, 1978), their different evolution possibilities have
to be sought within the rift zone crust.   Where two or

more rifting fissure swarms act in parallel arrangement, only the
marginal swarms will contribute to the plate surface. The enclosed
central section (central graben, rift valley) will subside more or
less vertically. The average residence time of material within a
50 km wide rift, where plate accretion amounts to 2 cm/yr, is 2.5 m.y.
A volcanic center in the widest section of the Icelandic rift which
is composed of at least six fissure swarms, can thus be enclosed
within the rift during its entire lifetime (1 m.y.). These centers,
when extinct, are flooded by the ol-tholeiites and products from
adjoining volcanic centers. The subsidence of volcanic centers favours
material recycling within the rift zone crust. It is evident that the
geothermally altered (hydrated) rocks of the silicic volcanic centers
provide reactive surroundings for randomly intruded mantle derived
ol-tholeiite. The sialic material of the centers can thus recycle
for millions of years within the crust of a wide rift zone and provide
silicic magma with ever increasing dispersed element abundance for
repeated mixing with ol-tholeiite.

In Fig. 4 the Mg/Mg+Fe vs. TiO_2 for the rift zone tholeiites is
shown by filled circles. The primitive ol-tholeiites plot in the
upper left. The moderately evolved volcanic centers show linear trends
from ol-tholeiites to qz-tholeiites (centers 1 and 5, Fig. 5). A com-
plete trend for a silicic volcanic center (center 3, Fig. 5), shows
evolution towards icelandite but the silicic rocks are compositionally
separated from the basalts by a "Daly gap".

Digressive volcanism

Extensive rifting activity during the lifetime of a fissure swarm
(1 m.y.) expells a less active parallel marginal swarm out of the rift
zone (10 km) (Fig. 3, case IIb). Subsequently that plate trapped volca-
nic center digresses away form the rift zone and its supply of primitive
ol-tholeiite is terminated. Depending on the stored magmatic energy
the digressing center can sustain volcanic activity over extended time
periods (Fig. 3, case III). Aside the widest section of the Icelandic
rift zone there are two areas of digressive volcanism. The western
digressive volcanism (WDV), indicated by shaded areas in Fig. 5, consists

of several short swarms around volcanic centers (center 6, Fig. 5)
and the eastern digressive volcanism (EDV) also shown in Fig. 5 con-
sists of few discrete volcanic centers (centers 7 and 8, Fig. 5).
Although the plate surface aside the rift zones is to a large extent
covered by products of marginal volcanic centers (evolved rocks, off
rift volcanism), only the largest digressing centers have been active
for millions of years[x), and their production rate decreases with time
(distance from rift margin).

Transgressive volcanism

At locations where a rift zone is directionally offset or
"terminated" fissure systems do not end abruptly. While the locus of
injection from the mantle is within the rift zone, the fissure system
can extend far into the adjoining crust. Accordingly we define the
termination of a rift zone as the boundary where the crust no longer
is formed exclusively by the rift zone itself.

Fissure swarms transfer material and energy beyond this boundary.
In Iceland the intruded older crust was formed in another rift zone.
The amount of energy needed to reactivate magma generation (transgressive
volcanism) in the older crust and the type of magma formed, depends on
the degree of its previous chemical fractionation. That again depends
on the productivity of the rift where the older crust was formed.

The geometry of the Icelandic rift system results in two major
zones of transgressive volcanism. The northern transgressive zone
(NTZ) at the termination of the WRZ and the southern transgressive zone
at the termination of the ERZ. A minor zone of transgressive volcanism'
is also observed in the TFZ of the north termination of the ERZ. In
Fig. 2 (right side of the block diagram) the interface between a rift
zone crust and an older crust is outlined. The hot crust of the rift
zone is in contact with mineral assemblages of lower metamorphic grade
giving rise to extensive reequilibration within the older crust. Ana-
texis in the amphibolite facies of the older crust is therefore initiated,
where its composition permits i.e. in its extinct volcanic centers.
The regional petrology of the STZ which shows the distance dependant
evolution of the transgressive volcanism, will be discussed below.

[x)] This fact has resulted in very misleading conclusions about the
proportions of primitive ol-tholeiite and evolved tholeiites in
the plate forming material (Wood et al., 1979).

The rocks produced in the digressive and transgressive volcanism
are alkaline (samples 16-31, TAble I). In the least evolved alkaline
centers the rocks are, however, transitional between tholeiitic and
alkaline rocks. Rocks of the highly evolved alkaline centers on the
ohter hand show petrochemical trends indistinguishable from trends for
alkaline oceanic islands in general (Fig. 4). Another common feature
of the digressive and transgressive volcanism is that the tectonics
surrounding the centers can be of twofold origin. Generally there
exists a tectonical pattern remnant from the parental rift margin of
the centers in addition to the superimposed pattern, active at the
present time, due to changing stress fields and the local subsidence
characteristic for this volcanism.

The regional petrology of the transgressive volcanism on the STZ
shows a fairly regular variation away from the rift termination. In
Fig. 6a the field relations of these rocks are outlined on a sketch map
of the STZ. North of the termination of the ERZ (dashed line) the
regional fissure direction is indicated by the Laki 1783 eruptive
fissure and the Vatnaöldur fissure (Larsen, 1979). In the upper left
of Fig. 6 the regional fissure direction of the WRZ is indicated by a
dashed line. South of the rift termination the six large volcanic
centers of the STZ are shown. The Torfajökull center produces silicic
rocks of potassic composition (samples 30 and 31, Table I). The Hekla
center (Sigvaldason, 1974) produces alkaline (sodic) intermediate to
silicic rocks with tholeiitic affinites (samples 28 and 29, Table I).
The Katla volcanic center and the Tindfjöll center produce small amounts
of sodic silicic rocks but are dominated by alkaline basalts. In the
Katla center the basalts are rich in Fe and Ti, occasionally with few
per cent Qz in the norm. The Eyjafjallajökull center produces subordi-
nate amounts of sodic silicic rocks but is dominated by extensive pro-
duction of alkali olivine basalts. Few exposures of hawaiites and
mugearites are known. The basalts on the plateau between the volcanic
centers in the northern STZ are typically Fe-Ti basalts, issuing from
eruptive fissures. The fissures extend into the STZ from the rift
termination but are offset in direction of the tectonics of the
older plate as exemplified by the Eldgjá fissure marked in the figure.
The off shore volcanism at the south end of the STZ (Vestmannaeyjar)
forms a line from Surtsey towards the western flank of the Eyjafjalla-
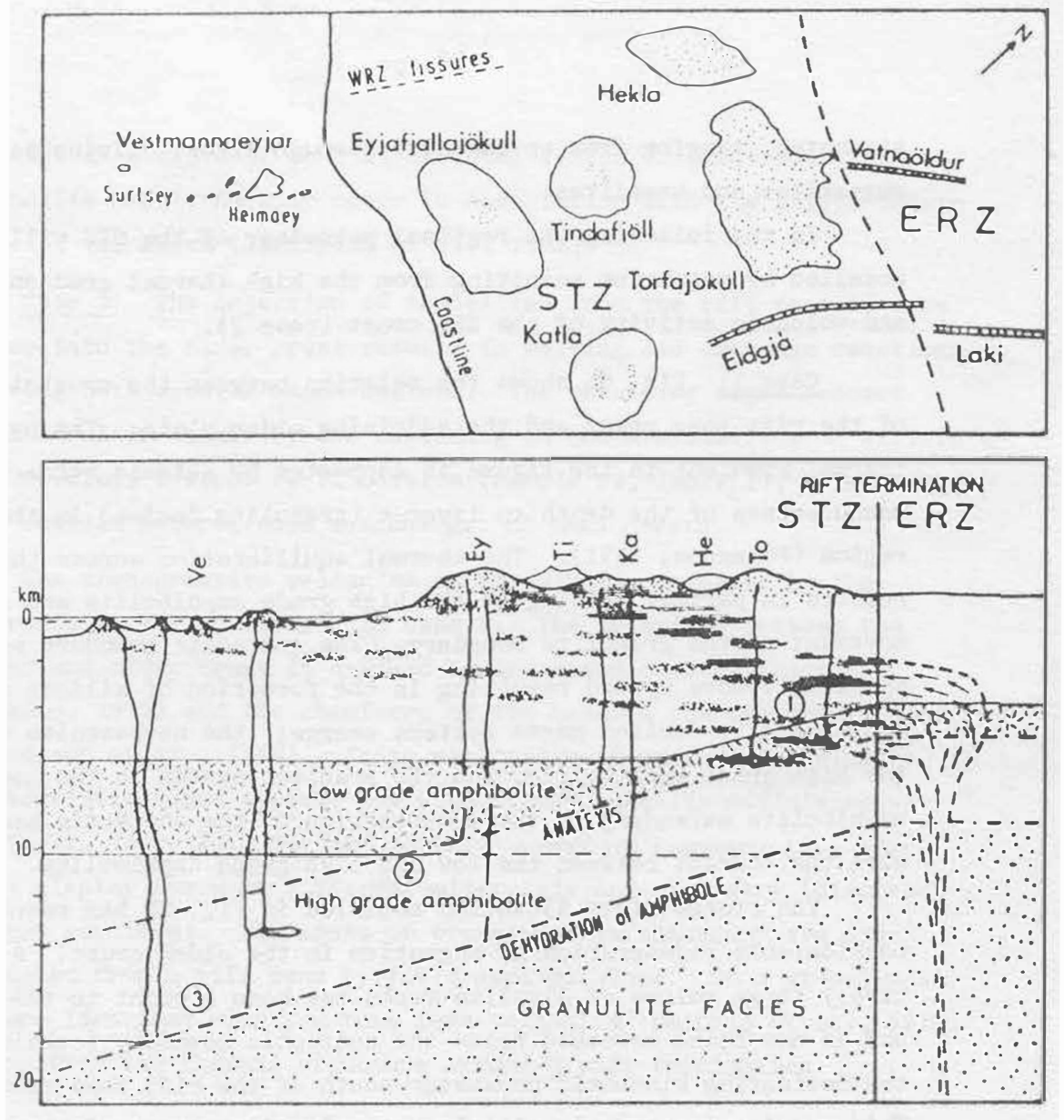jökull center. The Vestmannaeyjar rocks are exclusively silica under-

Fig. 6.

(A) A schematic map of the STZ. The ERZ termination is shown by a dashed line to the right in the figure. The regional fissure direction in the ERZ is indicated by the Laki (1783) and Vatnaöldur eruptive fissures. For comparison the direction of the fissures on WRZ is shown. The volcanic centers produce decreasingly alka-line silicic rocks (dotted areas) away from the rift termination (see Fig. 7).

(B) A hypothetical section through the STZ crust. The figure shows the migration of the high thermal gradient of the ERZ into the older crust. The associated crustal magma generation is indicated in the figure. The alkali olivine basalt formed at the amphibole dehydration line is indicated by dark shaded areas in the upper crust and the Fe-Ti basalt (above) by dashed areas. The production of alkaline basalts increases towards the rift termination. The silicic magmas formed at the anatexis boundary are indicated by dotted areas in the mountain summits. In the Torfajökull area the anatexis (peralkaline, potassic) is taking place in a crust con-taining alkali olivine basalt (point 1 in the figure). In the sec-tion between point 1 and 2 magma mixing is most favoured. South of point 2 the magma formation is exclusively taking place below the silica enriched low grade amphibolite, where differentiation of silica undersaturated rocks of the sodic series is favoured (point 3 in the figure). To the right in the figure a dike injection from the ERZ is indicated. The intruded magma equilibrates with a crust containing substantial amounts of alkaline rocks (Eldgiá).

saturated, ranging from ne-basanite through alkali olivine basalts to mugearites and hawaiites.

In the following the regional petrology of the STZ will be modelled by magmatism resulting from the high thermal gradient (case 1) and volcanic activity of the ERZ crest (case 2).

Case 1: Fig. 6b shows the relation between the crustal layers of the rift zone crest and the adjoining older plate. The hypothetical thermal gradient in the figure is supported by seismic refractive measurements of the depth to layer 4 (granulite facies) in the Katla region (Pálmason, 1971). The thermal equilibration across the interface results in partial melting of the high grade amphibolite and upward movement of the granulite boundary. The anatectic boundary will correspondingly move upward resulting in the formation of silicic magmas. Two crustally derived magma systems emerge; the ne-basanite system in the high grade amphibolite, and the granitic system in the low grade amphibolite extending to the intersection of the anatectic boundary with the contact between the low and high grade amphibolite.

The steady state situation modelled in Fig. 6b has resulted in considerable regeneration of magmatism in the older crust. A comparatively large volume of alkaline rocks has been brought to the surface and is now being reworked below the anatectic boundary (subsidence is the dominating kinematic parameter south of the rift zone termination). This results in potassic silicic volcanism just south of the rift zone termination. Further along the inclining gradient the proportion of the now sodic silicic rocks diminishes and is nonexistent beyond a point where the anatectic isotherm dips below the low grade amphibolite.

The basalts produced along the transgressive volcanic zone reflect the position of isotherms relative to the crustal layering. Close to the rift zone termination the alkali olivine basalts formed in the high grade amphibolite react with silicic liquid at the anatectic boundary in the low grade amphibolite. Mixing of the two magmas results in crystal fractionation (mainly feldspar) which drives the resulting basalts towards high Fe and Ti contents (Fe-Ti basalts, icelandites, Katla, Hekla). Beyond the point where the anatectic boundary dips below the low grade amphibolite no silicic liquid is available and the basalt retains its silica undersaturated character (Heimaey, Surtsey). The only signs of traversing the low grade amphibolite are silicic

xenoliths in a state of partial or total fusion (Sigurdsson, 1968). Amphibolite xenoliths also occur in association with the silica under- saturated volcanism (Jakobsson et al., 1973).

Case 2: The injection of tholeiites from the rift zone fissure systems into the older crust results in melting and exchange reactions involving both crustal magma systems. The resulting magma becomes transitional in chemistry and depending on the availability of silicic magma develops towards Fe-Ti basalts (sample 23, Table I), which typi- cally contain heterogenous assemblages of phenocrysts.

The transgressive volcanism on the NTZ is dominated by the occurrence pattern described in case 2. The interface between the younger and older crust is defined by increased crustal thickness (Pálmason, 1971) and the chemistry of the basalts changes drastically (Sigurdsson et al., 1978). These magmas are in general evolving in the tholeiitic magma system, but with strong alkaline affinities (sample 24, Table I). The two genetic types of transgressive vol- canism display somewhat different mineralogy and chemistry (discussed in later sections). The areas of transgressive volcanism are dis- tinguished from a rift zone by field geology alone. On a global scale they are identical with fracture zone volcanism (Shibata et al., 1979) arising from the thermal structure across a rift termination.

THE ORIGIN AND CHEMICAL DISTINCTIONS OF END MEMBERS AND HYBRIDS IN MAGMA MIXING

Primitive ol-tholeiites   the mantle derived end member

The term "primitive ol-tholeiites" is used to describe rocks (samples 1-4, Table I) with high MgO, Ni and Cr and low TiO_2, K_2O, P_2O_5 and dispersed elements in general with light depleted REE pattern and high K/Rb ratio (Engel et al., 1965; Gast, 1965, 1968; Key et al., 1970). In Fig. 7 the K_2O-P_2O_5 trend for the primitive ol-tholeiite (lower left corner) forms the low potassium margin of the scatter, which extrapolates roughly through zero. The range .02 - .05 for
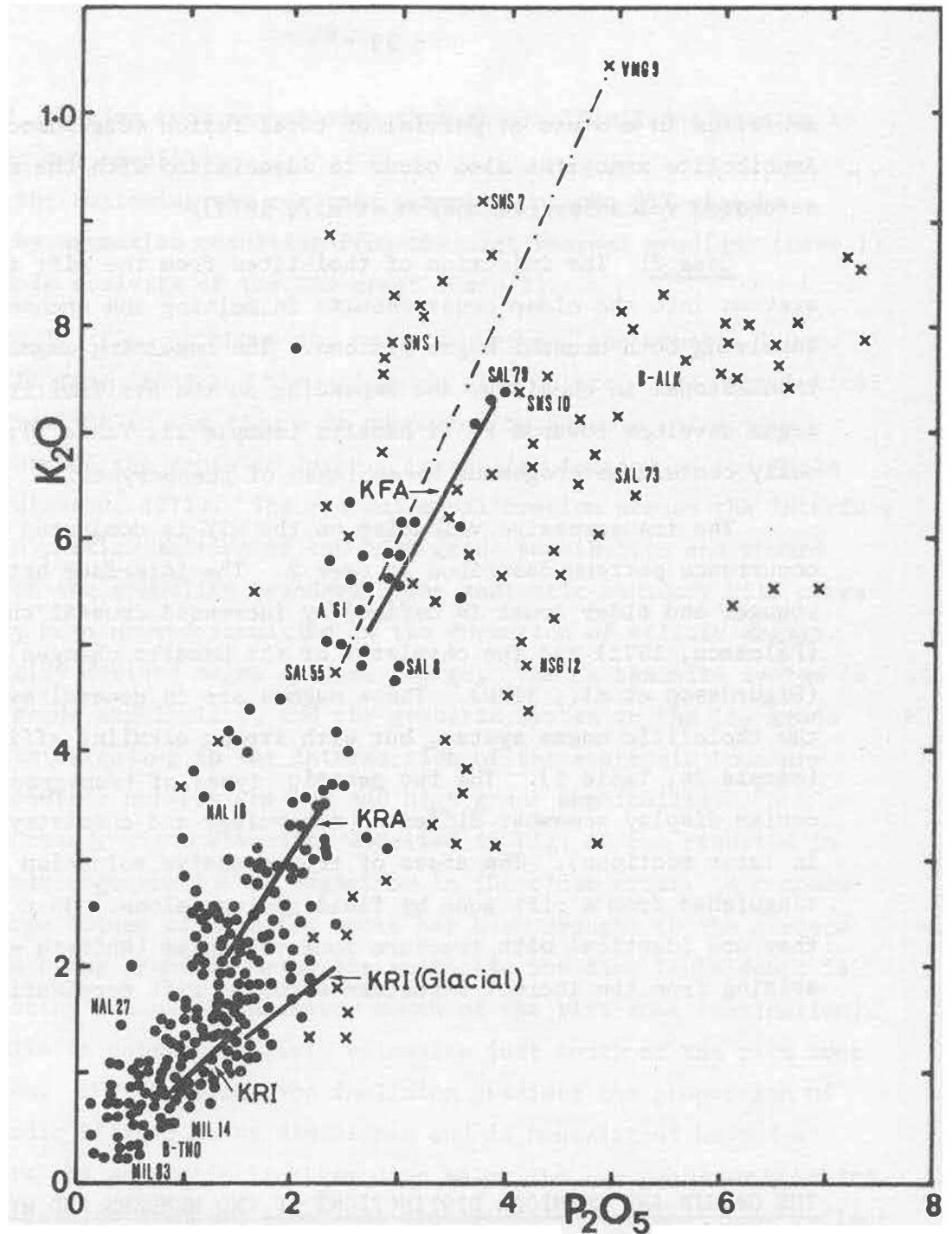
Fig. 7. The figure shows K₂O vs P₂O₅ for the Icelandic basalts. Filled circles show the tholeiitic and crosses the alkaline rocks, respectively. The primitive ol-tholeiites are shown in the lower left of the figure. The evolution trends for the KRI, KRA (Fig. 5) are shown by straight lines. In addition to the KRI trend referred to in the text, the trend for a glacial eruptive cycle (older than 10.000 yrs) of the center is shown. The KFA center, here shown among the tholeiitic rocks, is on the ERZ rift margin. The close resemblance of this center to the remnant centers of the WDZ (samples SNS 1, SNS 7 and SNS 10) is shown. As compared to the highly evolved tholeiites A´61 and SAL 8, the KFA trend belongs to the off rift volcanism, although its mineralogy retains strong tholeiitic affinities. The transgressive volcanism (silica undersaturated) shows extensive crystal fractionation (samples SAL 55 and VMG 9, dashed line). The hybrid transgressive volcanism of the NTZ plots below the purely alkaline suites (sample NSG 12) as do the Fe-Ti basalts of the STZ (sample B-ALK).

potassium reflects (a) a different degree of melting during formation
and to a lesser extent (b) fractionation of olivine and spinel during
ascent as indicated by the high and somewhat scattered values for Ni
and Cr. The limited early fractionation of ol drives the Mg/Mg+Fe
ratio from .7 - .65 (Fig. 4, upper left). Experimental evidence
suggests that these rocks are equilibrated below the oceanic crust
(Kushiro & Thompson, 1972; Fisk, 1978) at pressures between 2 and 10 kb
and are thus derived from the oceanic mantle.

Alkaline basalts   the ne-basanite end member

The chemistry of the alkaline basalts calls attention to their
worldwide occurrence in association with the tholeiitic rocks (Carmichael,
Turner, Verhogen, 1976) and the close petrochemical resemblance of the
various rock suites. In Fig. 4 the compositional trends for Hawaii,
Galapagos and Iceland are compared to demonstrate the strong mineralogi-
cal control of their major element evolution.

The observed transition from tholeiitic to alkaline volcanism in
the off rift centers of Iceland in terms of the dynamic model, is brought
about by continuous silica depletion of the amphibolite of these centers.
Although strongly undersaturated rock suites are not represented in
Iceland, with the exception of few ankaramites (Steinthórsson, 1964),
the present discussion applies to other areas as well. We cite McDonald
(1968) introducing Hawaiian volcanism: "The three major rock suites,
tholeiitic, alkalic and nephelinic, are chemically intergradational.
The main mass of the volcanoes is tholeiitic, followed by a relatively
small volume (generally less than 1 per cent) of alkalic lavas; the
two types of lavas are interbedded in a thin transitional zone. The
nephelinic lavas are separated from the others by a long time interval
that is marked by a profound erosional unconformity". And Powers (1955)
claims: "Most of the data of Hawaiian volcanism and petrology can be
explained by a hypothesis that batches of magma are melted from crystal-
line peridotite by a recurrent process .... that accomplishes the
melting only of the plagioclase and pyroxene component but not the
excess olivine and more refractory components within a zone of fixed
and limited depth. Eruption exhausts the supply of meltable magma under
a given locality and, in the absence of more violent melting processes,
leaves a stratum of crystalline refractory components".

It was stated earlier that no "parental" magma exists for the alkali olivine basalts. Instead we introduced the term parental crust. The composition of the residual amphibole sets the initial limits to the dispersed elements of the alkaline basalts (Kesson & Price, 1972; Mason & Allen, 1973; Basu & Murthy, 1977). The abundancies are varied by different degree of partial melting and the degree of previous fractionation of the parental crust controlles element ratios and silica undersaturation of the product. The extent of hydration on the other hand controls the amount of magma which can form.

Each alkaline center in the digressive and transgressive volcanism therefore displays its characteristic dispersed element enrichment and ratios within the frame of similar major element variation. The largest melt fractions are the highest in MgO, Ni and Cr and lowest in the dispersed elements. Crystal fractionation of these rocks follows the trends outlined in Fig. 7. The sample pair SNS 1 and SNS 7 (No. 16 and 17, Table I) shown in the upper half of the figure indicates only 10-15% crystal fractionation and the sample pair SAL 55 and VMG 9 (samples 20 and 21, Table I) indicates about 50% fractionation. On Fig. 4 the former pair is shown to belong to the early fractionation in the Snaefellsnes trend and the later stems from extensive fractionation in the lower reach of the trend, well below the knee towards hawaiites, which also is shown in Fig. 8 in a trend marked Heimaey. The MgO rich members of both pairs are among the least evolved samples from both volcanic centers   seemingly different degree of melting in the same mineral matrix.

It might seem confusing at first that the present model postulates the regional formation of alkaline basalts at the mantle crust boundary below the rifts while alkaline lavas are found in the off rift volcanism. The model, however, suggests where to look for the alkaline magma. Example supporting the validity of the model is a late production of alkaline basalt in a now extinct volcanic center in the MIL (Fig. 5). The center (Miklafell) probably became decoupled from its mantle source while in the wide rift and subsequently recycled its material until extinct.

Rhyolites and dacites   the silicic end member

The alkali-silica relations of the subalkaline silicic to inter-
mediate rocks (samples 12-15, Table I) are shown in Fig. 8 by the lower
hatched area enclosed between the trends for Kerlingarfjöll (Grönvold,
1972) and Askja (Sigvaldason, 1979) silic volcanic centers. The alkaline
silicic rocks (samples 25-31, Table I) are represented by the upper
hatched area between the trends for Snaefellsjökull (samples 26-27)
and Torfajökull (samples 30-31). The silicic melts formed in Heltz´s
(1973, 1975) experiments are also shown in Fig. 8. Composition No. 1
is a minimum melt from ol-tholeiite. No. 2 is from qz-tholeiite and
point 3 represents a melt from an alkali olivine basalt with tholeiitic
affinities. Natural silicic glasses from Iceland (Carmichael & McDonald,
1961; Sigurdsson, 1968) cover the whole compositional range of the most
silicic rocks and their overall composition closely resembles the
experimentally formed melts. Silicic pitch-stones resembling rhyolites
in composition are common along the entire rift system and blebs of
intermediate to silicic glasses   are   found in basaltic lavas ranging
from primitive ol-tholeiites to qz-tholeiites (see Table Ia).

In a volcanic center evolving through a state transitional between
the tholeiitic and alkaline (case IIb, Fig. 3), two magma sources are
active in response to local subsidence, i.e. anatexis of tholeiites to
generate subalkaline silicic magmas and melting of amphibolite to form
ne-normative basalts. The first sign of homogenization in a digressing
volcanic center is the abridging of the "Daly gap",and that the silicic
magmas become successively more alkaline.

This state of transition is shown by the discontinuous alkali
silica trend for the Öræfajökull center (Fig. 8) on the EDV (Prestvik,
1979). The "Daly gap" is shortened by intermediate hybrid rocks and
the alkali enrichment is fairly high (sample 25, Table I).

The trend for Eyjafjallajökull (Arney, 1976) conforms to that
for Öræfajökull but at higher levels of alkali, and samples from Hekla
(samples 28-29, Table I) are also well above the subalkaline field.

The growing knowledge on crystal liquid relations in silicic
magmas during anatexis and crystallization was reviewed by Luth (1976).
The Icelandic silicic rock seem to belong exclusively to the low
pressure series, where plagioclase and amphibole are liquidus minerals
about 2 kb, with or without biotite, at the lowest temperatures of
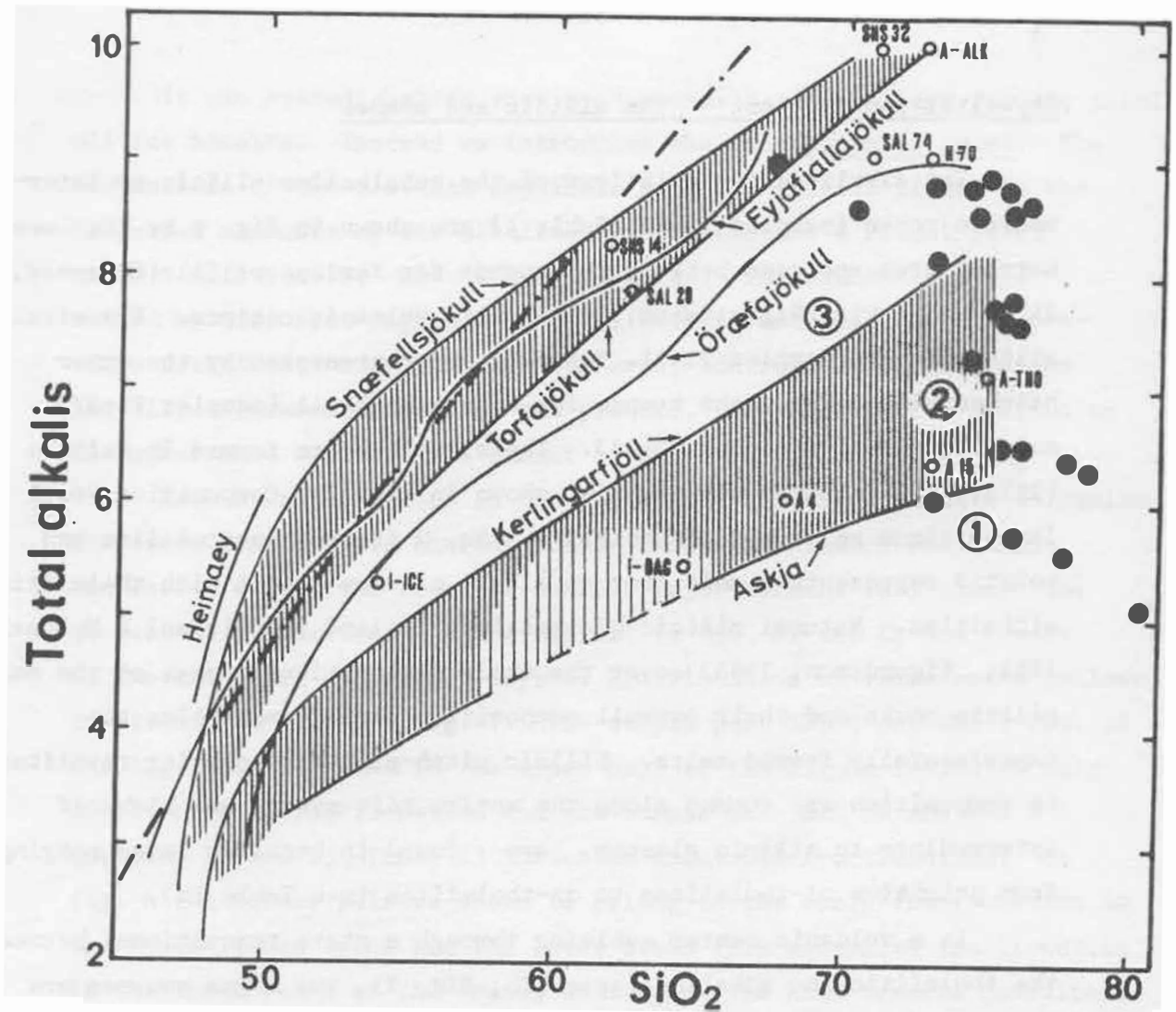formation. Alkali feldspar and quartz seem to be totally dissolved in

Fig. 8. The lower hatched area in the figure shows the range in alkalinity for the subalkaline rocks, silicic to intermediate rocks of the rift zone. The trends for Askja and Kerlingarfjöll define the minimum and maximum alkalinity respectively. The "Daly gap" is indicated in the figure. The upper hatched area between the trends for Snæfellsjökull and Torfajökull volcanic centers indicates the range in alkalinity for the alkaline silicic and intermediate rocks. The trend for Heimaey in the Vestmannaeyjar volcanic center represents a suite of sodic silica undersaturated rocks. The Hawaiian division line is shown dashed across the alkaline field. The filled circles are pitch stones and open circles represent samples listed in Table I. The points 1, 2 and 3 show the compositions of minimum melts from Heltz's (1973, 1975) experiments. The figure is redrawn from Fig. 1 in Imsland (1978).

the liquid. Heltz (1973) outlined the phase relations in different
hydrated basalts at 5 kb. It is evident that the bulk composition of
the basalt controls the alkalinity of the minimum melts and the amount
of liquid formed, but the fact that plagioclase and amphibole are
stable during melting between 680-950°C supports the present interpre-
tation that there are two separate suites of crustal derived magmas,
silicic and basaltic. The trace element chemistry of the silicic rocks re-
flects the persistence of plagioclase and hornblende during their
formation as outlined in a previous section. Here the elements fre-
quently referred to as "dispersed" in the basalt system obey mineral
control. The generally low strontium and a strong negative Eu anomaly
reflects the persistence of plagioclase, low K/Rb ratio is controlled
by the residual amphibole.

That these rocks are not formed by fractional crystallization
from a basaltic magma is supported by multiple evidence. In addition
to data on their halogen chemistry and K/Rb ratios reported in a later
section of this paper the following notes are illustrating:

(1) Oxygen isotope studies on silicic rocks from Iceland (Muehlenbachs,
1973) show that they are not derived from any existing basalt by
fractional crystallization.

(2) The Ce/Yb ratios of the silicic rocks (above 2) rule out frac-
tional crystallization as their genetic process since the majority
of basalts regarded as parental liquids are with Ce/Yb ratios far
lower. A brave attempt by Wood et al. (1979) to explain this by a
dynamic partial melting in the mantle (Wood, 1979) raises the
question why basalts with Ce/Yb below 2 do not fractionate.
Unless nature abuses rhyolites with Ce/Yb below 2 the answer is
troublesome.

(3) Strontium isotope evidence from the STZ (O´Nions & Grönvold, 1974)
suggests a case where rhyolite forms by remelting of a preexisting
sialic material.

(4) The common absence of intermediate magmas in silicic volcanic
centers speaks against crystal fractionation (Grönvold, 1972;
Jóhannesson, 1975).

(5) Tholeiitic silicic rocks produced in centers where the simultane-
ously produced basalts are alkaline (Eyjafjallajökull) rule out
fractional crystallization between the two magmas (alkali silica

diagram, Fig. 8).

(6)   In the only volcanic center outside the rift where intermediate
      rocks dominate (Hekla) all the above criteria for fractional
      crystallization are fulfilled.

We therefore conclude that fractional crystallization is a minor process
in the formation of silicic magmas of the Icelandic rift system but
might occur in the late evolution of silicic volcanic centers where
intermediate rocks appear.

Hybrid magmas

In a volcanic center in the rift zone we expect to see three
dominating types of hybrid magmas (see Fig. 3):

   (a) ol-tholeiite/ne-basanite

   (b) ol-tholeiite/silicic magmas

   (c) hybrid a/hybrid b or ol-tholeiite/hybrid b or c.

Here we seek the endless variety of magma compositions referred to as
the "primary magmas" of volcanic centers. The dispersed element abun-
dancies and ratios of these "primary magmas" cannot be asigned to
fractional crystallization of a common parental magma of the primitive
ol-tholeiite composition. The ol-tholeiite end member simply does not
evolve that way since the evolved basalts of the volcanic centers never
show its high K/Rb ratios and depleted REE pattern and always display
entirely different halogen chemistry. The basalt suite of each center,
however, can easily be assigned to fractional crystallization (Jakobsson
et al., 1978; Wood et al., 1979).

The first effect of magma mixing is therefore the induced crystal
fractionation (discussed in the next section) resulting from the inevit-
able disequilibrium between phases of the ascending magma and the liquid.
The hybrids outlined above can be anticipated by inspection of Fig. 4.
The rocks of the rift zone that fractionate are derived from parents of
different TiO_2 levels (also P_2O_5, Zr, Sr and F). Typical compositions
of such parental magmas are the samples NAL 27, RSG 19, MIL 15 and NAL 18
(Table I), the two latter being case a above and the first being case b,
where K and the dispersed elements are enriched. Here it is also to be

noted, that these rocks can evolve by crystallization towards qz-normative tholeiites (samples SAL 8 and A´61, Table I, Fig. 7) or alkaline ol-tholeiites of a transitional type. It is therefore concluded, that all qz-tholeiites contain a fraction of silicic magma and all the transitional basalts contain a fraction of ne-basanite. A repeated filling of a crustal magma domain is therefore, as outlined above, a mixing between an end member and a hybrid or between two hybrids.

Mixing of ne-basanite with silicic liquid in the transgressive and disgressive volcanism is by analogy with qz-tholeiites resulting in a further crystallization of the mixture towards Fe-Ti basalts (Fig. 4). These rocks are commonly slightly qz-normative (samples B-ALK and SAL 73, Table I). On Fig. 7 (right) the extensive crystallization range of the transitional alkaline basalts is shown (samples NSG 12, Table I).

The above discussion is summarized in the following: Hybrid rocks are found as single lavas or rock suites formed by fractional crystallization. Their petrochemical distinctions can be related to magma mixing between end members existing in their surroundings. The hybrid magmas are not derived by crystal fractionation or partial melting of a common parent.

MINERALOGICAL EVOLUTION OF BASALTS AND EXPERIMENTAL SIMULATION OF THEIR PETROGENESIS

Basalt evolution in terms of synthetic systems

The evolutionary processes to be considered are fractional crystallization, magma mixing and combinations of the two. The mixing considered here is silicic liquid + ol-tholeiite. To illustrate the principles in question a synthetic system approaching basalt in mineralogy is considered, the system forsterite-diopside-anorthite (Osborn & Tait, 1952; Presnall et al., 1978). The system is ternary, without a solid solution, and with a single eutectic point (Fig. 9a). All melts will evolve by crystallization towards the eutectic and become invariant.

A melt ($\bar{M}$) of composition (wt.%) 17% Fo, 29.2% Di, 53.8% An, which
is on the Fo An cotectic curve, will crystallize out Fo and An in the
ratio 31:69, and evolve to the eutectic (7.3% Fo, 47.7% Di, 45% An)
at 41.9% crystallization (13% Fo & 28.9% An). Then diopside begins to
crystallize as well, whereupon the melt will stay invariant in terms
of the major elements until the system is fully crystallized. Table IIa
shows the change in the major element chemistry, effected by this
crystallization (surface equilibrium assumed for the trace element).
For comparison, assume for the initial melt M the trace element concen-
trations of sample MIL 14 (Table I) then at M, Ni = 250 ppm and
Rb = 0.2 ppm, at E_0 the values are 26 and 0.34, respectively, at E_1
(75%) 4.3 and 0.57, and at E_2 (90%) 0.63 and 1.79. Two tholeiites in
the table, SAL 8 and A 1961, have for Ni the values 10 and 35 ppm, and
for Rb 7 and 4 ppm. In terms of Ni, these latter values are similar to
those of E_0 or E_1; in terms of Rb, however, they are an order of
magnitude too low, a discrepancy that is not easily resolved by frac-
tional crystallization alone.

　　With increasing pressure the primary field of forsterite in the
system Fo-Di-An shrinks (Presnall et al., 1978); since liquids forming
by partial melting in the upper mantle are in equilibrium with olivine,
the ascending magmas have forsterite (olivine) on the liquidus and
evolve, as the primary field of olivine expands with decreasing pressure,
towards the cotectic univariant curve plagioclase/olivine. Therefore,
magmas entering the crust from below will have fractionated out various
amounts of olivine as further evidenced by the experimental results of
Kushiro & Thompson (1972) and Fisk (1978) that olivine disappears from
basaltic compositions at about 10 kb. At 20 kb pressure a melt in the
system Fo-Di-An and in equilibrium with a mantle containing forsterite,
would have the approximate composition (wt.%) 26% Fo, 26% Di and 48% An
(Table 8 in Presnall et al., 1978). As the melt ascended towards the
surface, it would crystallize out forsterite (together with spinel), if
the liquid was always maintained at a point on a cotectic curve - that
this is necessarily so is by no means evident, for olivine tholeiite
usually has olivine alone on the liquidus, i.e. the plagioclase/olivine
cotectic has not been reached at the time of the eruption. Assuming
only Fo crystallization, this melt would at one atmosphere reach the
univariant curve Fo/An at 17% Fo, 29.2% Di, 53.8% An. Then 10.84 wt.%
forsterite would have crystallized in the magma since its departure at

60 km depth, until the onset of anorthite-crystallization at one atmos-
phere pressure.

The chemical changes in the liquid, affected by this crystalliza-
tion, are summarized in Table IIc.

By this token the Ni concentration in the initial liquid required
to give that of sample MIL 14 (250 ppm) at the surface is 833 ppm.

The system Fo-Di-An is of more limited use in evaluating the
effects of magma mixing between ol-tholeiite and silicic liquid, since
the alkalies are not present in the system. The addition of the feld-
spar rich natural silicic liquid A-THO, Table I (61.1% fsp, 32.4% qz,
4.6% px in the cation norm) to the eutectic composition of the system
Fo-Di-An, however, brings the liquid composition into the An-field.

To illustrate the principles at hand we investigate the conse-
quences of adding small amounts (1.5 and 10%) of liquid orthoclase to
the melt E_0 of Table IIa. The results of such a calculation are shown
in Table IIIa. All three mixtures are within the primary field of
anorthite. To bring the 1% hybrid (99% E_0 + 1% Or) back to the eutectic
composition, about 1% crystallization of An would be required; the 5%
mixture would crystallize first 3.6% An, followed by 3.3% cotectic
crystallization of An and Fo in the ratio 69/31. Finally, the 10%
mixture would crystallize 3.8% An, and 7.8% An + Fo in the same ratio.
Table IIIc shows the trace element compositions of the melts once they
have been restored to the eutectic, i.e. the major element chemistry is
that of E_0.

From this it is clear that in terms of the major element composi-
tion of the liquid a given composition is a "function of state", i.e.
that governed by invariant points in the silicate system. The trace
elements evolve independent of such invariants, according to laws first
exposed by Gast (1968). In these examples that are taken at random
from a continuous spectrum of possibilities, it is shown how it is
possible to have similar major element chemistry, and widely different
trace element chemistry, as particularly illustrated by the behaviour
of Rb, the true "dispersed element" in this assemblage.

Silicic anatectic melts added to the primary basaltic liquids will
have other effects than just changing the chemical composition: In the
first place they will be hydrous, and thus tend to alter the topology of
the physiochemical system - in the case of the system Fo-Di-An the
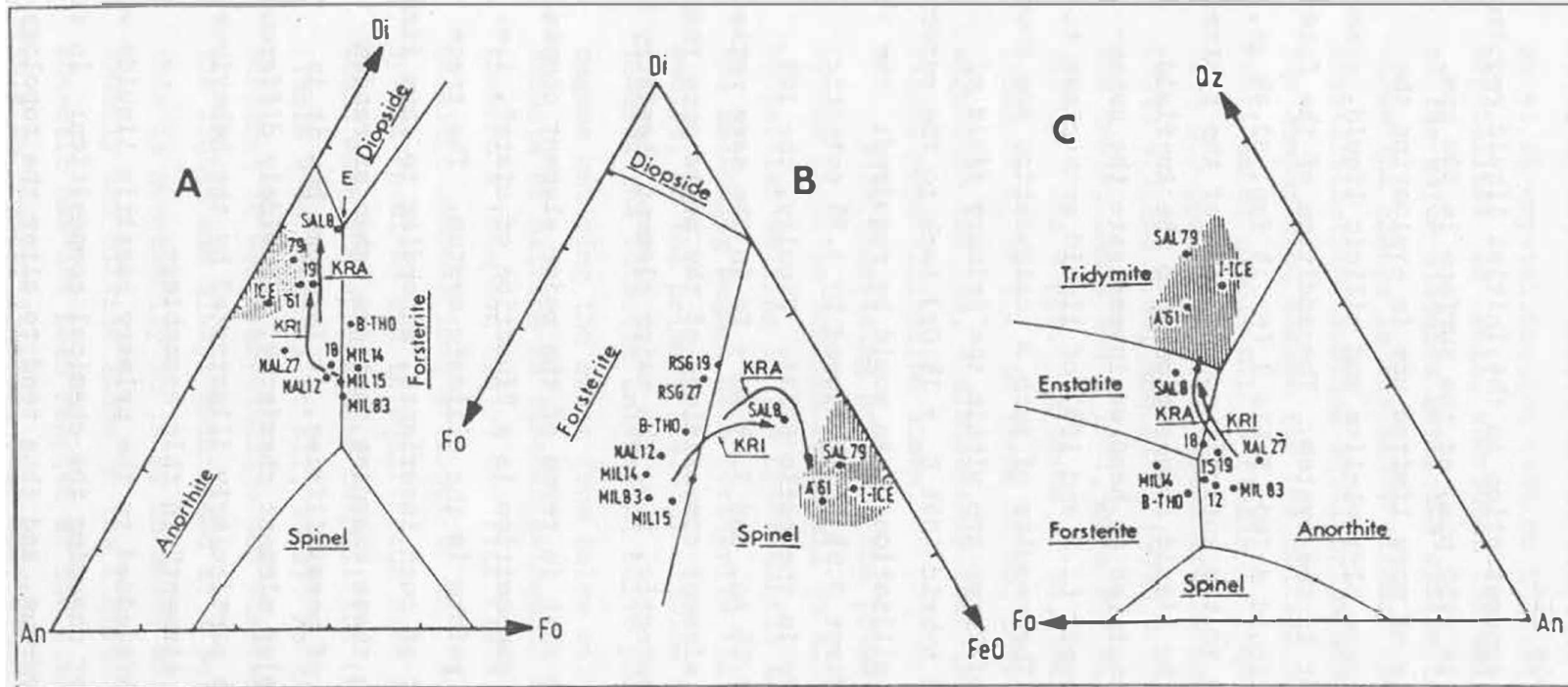addition of water to the subsystem An-Di (Yoder, 1965) will lower the

Fig. 9.

(A) The system An-Di-Fo (Osborn & Tait, 1952) illustrates the evolution of basalts during precipitation of its major phases. The phase compositions of rock samples are approximated as follows: An = mol Al_2O_3 - (mol Na_2O + mol K_2O); Di = mol CaO - mol An; Fo = 1/2 (mol MgO - Di). The arrows in the figure show the evolution path of basalts from the KRI and KRA volcanic centers (Fig. 5). The upper end of the arrows marks the coprecipitation of olivine, plagioclase and clino-pyroxene. The primitive ol-tholeiites plot in the olivine field relative to the arrows. The evolved basalts reach the coprecipitation ol-plag-cpx below the eutectic of the system (point E). Although not relevant to this system the posi-tion of the qz-normative basalts and icelandites is indicated by stippled area to the left.

(B) The system Fo-Di-FeO (Presnall, 1966) shows the iron enrichment relative to the proportion of ferromagnesian minerals. The Fo and Di content of the samples is estimated as in Fig. 6a. Decreasing Fo content of the basalts results in in-creased Fe content of the precipitating olivine. The arrows indicating ol-plag coprecipitation trend towards the field of qz-tholeiites (stippled area), where ore minerals are precipitated.

(C) The reaction relation of silica and forsterite is discussed within the system Fo-SiO₂-An (Andersen, 1915). The propor-tions of Fo and An are approximated as in Figs. 6a and 6b. The activity of silica is approximated as: SiO_2 = mol SiO_2 - (2An + Di + mol FeO + 1/2 mol MgO). The ol-tholeiites plot scattered around the Fo-An boundary. The arrows indicating evolution of volcanic centers towards qz-tholeiites cross the opx field, while the qz-normative rocks (stippled area)

temperature of the eutectic as well as shifting it drastically towards
the An end member. Secondly, the silicic melts have much lower
liquidus temperatures than do their basaltic counterparts - the energy
required to superheat them, as well as to bring about the anatectic
melting, would be provided by the latent heat of crystallization in
the basalt, helping to maintain the melt at a cotectic or invariant
composition.

Mineralogical evolution of the tholeiites

The crystallization of the ol-tholeiites starts with the precipi-
tation of olivine (Fo_{90-80}) followed by precipitation of plagioclase
(An_{90-80}). The early phases generally contain inclusions of chromian
spinel (Sigurdsson, 1976). Spinel is rarely found in the groundmass
but ore is abundant. The last major phase to precipitate, rarely obser-
ved as phenocryst, is clinopyroxene, commonly titaniferous diopsidic
augite (Sigvaldason, 1974; Mäkipää, 1978). Hypersthene is observed in
the groundmass of holocrystalline basalts (Wood, 1978). In the most
primitive lavas no further evolution is observed, the residual liquid
crystallized in ophitic to subophitic texture or finegrained groundmass.

The mineralogy of the ol-tholeiites clearly points towards the
existence of a mineralogical invariant stage in their evolution. All
compositions seem to reach this stage mineralogically and the most
primitive lavas show no further evolution. Studies on natural glasses
(Mäkipää, 1978; Fisk, 1978; Steinthórsson, 1979) reveal the composi-
tional restrictions most clearly.

In the hybrid basalts the early olivine is iron rich (Fo_{75}) and
the plagioclase is alkaline (An_{70}) compared to the primitive basalts
(Grönvold & Mäkipää, 1978; Mäkipää, 1978). The liquid remaining
when all three major phases appear, is iron rich and siliceous as com-
pared to that of the primitive lavas. The composition and quantity of
this residual liquid is the principal difference between evolved and
primitive lavas. Among the tholeiites a continued evolution is some-
times observed by disappearance of olivine and appearance of qz in the
norm. In few cases, observed within the silicic volcanic centers, the
massive precipitation of ore produces rocks of ferrobasalts or icelan-
dite composition (Carmichael, 1967), whereupon the evolution of the

basalt system reaches an end. This latter evolution regime points
towards a second invariant mineralogical stage for the qz-tholeiites,
commonly reached but never passed. The second stage is known to pre-
cipitate zoned plagioclase and a range of olivine compositions (Fisk,
1978).

The largest compositional deviation of the tholeiites from the
idealized basalt system (Yoder & Tilley, 1962), which results from
their higher content of iron and alkali, is amplified by crustal magma
mixing.

In Fig. 9a the evolution paths of the oceanic basalts are shown
in the system Di-An-Fo (Osborne & Tait, 1952; Presnall, 1978), which
is close to the plane of silica undersaturation in the tetrahedron
Di-An-Fo-SiO$_2$. Olivine is the first phase to precipitate. This is the
case for most ol-tholeiites here represented by their relevant oxides
(text to Fig. 9a) (B-THO, MIL 14, MIL 83, NAL 18, MIL 15 in Table I).
Composition of samples precipitating plagioclase as a primary phase are
represented by the samples NAL 12 and NAL 27 (Table I). The crossing
of the thermal valley at the Fo-An phase boundary is here explained by
addition of an aluminous silicic liquid (rhyolite) to the equilibrium
liquid composition at the Fo-An join (hybrid of type b in the last
section). This changes the crystallization order and results in a
massive precipitation of plagioclase, since the topology of the system
demands a long An path towards the eutectic of the system (point E,
Fig. 9a) and a shorter An-Fo cotectic path respectively. This group
of tholeiites is represented in the rift zone by plagioclase porphyritic
large fissure and shield eruptions, which, as a supporting evidence for
the above, contain significantly more alkalies than the lavas preci-
pitating olivine as a first phase.

The simplest model of further evolution of a silica contaminated
ol-tholeiite after reaching the An-Fo cotectic from the anorthite field
is fractional crystallization removing olivine and plagioclase. In
this case the length of the crystallization path towards E depends on
the amount of silicic magma added. Basalts crystallizing in the ol-tholeiite
system and reaching the point E, can thus have extremely different dis-
persed element contents depending on the evolution path taken. We illustrate
this in Fig. 9a by the samples SAL 8 and A´61 (Table I). We underline,
that the samples near the point E in Fig. 9a plot away from the plane
Di-An-Fo towards the silica corner in the tetrahedron Di-An-Fo-SiO$_2$.

The petrological evolution within a volcanic center proceeds
along similar paths as in the above example. Iron enrichment in the
deep crust within the higher grade amphibolite leads, however, to
lower liquidus temperatures of these magmas (Tilley et al., 1964).
In response to addition of volatiles and supposedly iron to the system
Di-An-Fo the position of phase boundaries will shift towards lower Fo
content of the liquid at the plagioclase-olivine boundary. In Fig. 9a
we illustrate the evolution path followed by the slightly evolved
volcanic center Krísuvík in the WRZ (Fig. 5) (Gunnlaugsson, 1977) and
the highly evolved Krafla silicic volcanic center on the ERZ (Fig. 5),
where in both cases pyroxene appears at the composition shown by the
arrow point (Grönvold & Mäkipää, 1978).

The large chemical spectrum within the tholeiites is demonstrated
by the samples RSG 19 (ol-tholeiite) and A´61 (qz-tholeiite) (Table I).
The sample RSG 19 is the most primitive of the Hengill volcanic center
(Fig. 5) (Sæmundsson, 1967), but the sample A´61 is the end stage of
the basalt suite of the Askja silicic volcanic center (Sigvaldason, 1979)
(Fig. 5).

On Fig. 9b the iron enrichment effect is shown on the phase dia-
gram Di-Fo-FeO (Presnall, 1966). The two fissure swarms illustrated in
Fig. 6a are shown along with the samples RSG 19 and A´61. The evolved
single fissure eruption represented by the sample SAL 8 is also shown in
relation to the primitive samples.

Rarely observed cases of extreme crystal fractionation appear in
volcanic centers, where intermediate rocks exist, represented by the
samples SAL 79, an highly alkaline qz-tholeiite, and the icelandite I-ICE
(Table I). The magnesium loss suffered by these highly qz-normative
samples, increase the probability of ore precipitation (Carmichael, 1967).

To overview the foregoing discussion the reaction relation of
silicic liquid and olivine in the tholeiites is illustrated in Fig. 9c,
showing the system SiO_2-Fo-An. The primitive tholeiites represented by
oxide ratios and approximated silica activity (text to Fig. 6c) again
plot dispersed about the three phase boundary. The two volcanic centers
shown in Fig. 6a and 6b occupy the enstatite field indicating the reac-
tion relations between silica and forsterite. The boundary position of
the sample SAL 8 is pointed out in contrast to the sample A´61, clearly
within the tridymite field indicating that silica activity is no longer
buffered by the reaction: $Fo + SiO_2 = 2 En$.

Mineralogical evolution of the alkaline basalts

The mineralogy of the Icelandic olivine basalts (Stein-thórsson, 1965; Sigurdsson, 1970) is characterized by the presence of three major phases, olivine, cpx and plagioclase, dispersed in an alkaline ne-normative groundmass. Titanomagnetite and ilmenite are abundant as microphenocrysts. It is therefore appropriate to discuss the genesis of these rocks qualitatively within the silica undersaturated tetrahedron Di-Fo-An-Ne (Yoder & Tilley, 1962) (Fig. 3).

Melting relation within the system Di-Ne-An (Shairer et al., 1968) are outlined in Fig. 10a. A natural constraint on melting behaviour in the system is that Ne is consumed during incipient melting and olivine is the last phase to disappear. The actual assemblage suffering melting, however, consists of amphibolite with ne-normative hornblende or kaer-sutite, giving the subsequent discussion validity only when a liquid in equilibrium with forsterite, diopside and anorthite has formed. The system Di-Ne-An has thermal minimum in the point A (1160°C) on the phase boundary Fo-Ne-An. Complete melting of Ne drives the liquid composition towards point B (1165°C) in equilibrium with Fo, An and Di. The plane Di-Ne-An as such gives no realistic picture of equilibration at tempera-tures higher than at B, since the liquid composition travels away from that plane towards a thermal minimum in the plane of silica undersatura-tion approximated by the plane Fo - Di - An. The natural constraints leave two liquid paths within the system. Firstly, when diopside is consumed before anorthite, the liquid composition leaves the three phase boundary along the Fo-An boundary, and secondly, when anorthite is consumed before diopside the liquid composition trends along the Fo-Di boundary. The projection of the three phase boundary on the plane Di-Ne-An stays in the An field below the Di-An boundary. Icelandic alkali basalts occupy this field on Fig. 10a indicating that diopside was consumed before anorthite. For comparison the trends for Galapagos (McBirney & Williams, 1968) and Mauna Kea/Kohala volcanic series of Hawaii (McDonald, 1968), are shown in the figure. In Table I the alkali basalt samples SNS 1, SNS 7 and SNS 10 represent rocks from the WDV, SAL 73, the EDV and SAL 55 represents the STZ (Fig. 10a). For compari-son the alkaline ne-normative differentiates of the hawaiite-mugearite type are represented by the samples VMG 9 from the STZ and SAL 76 from the EDV.
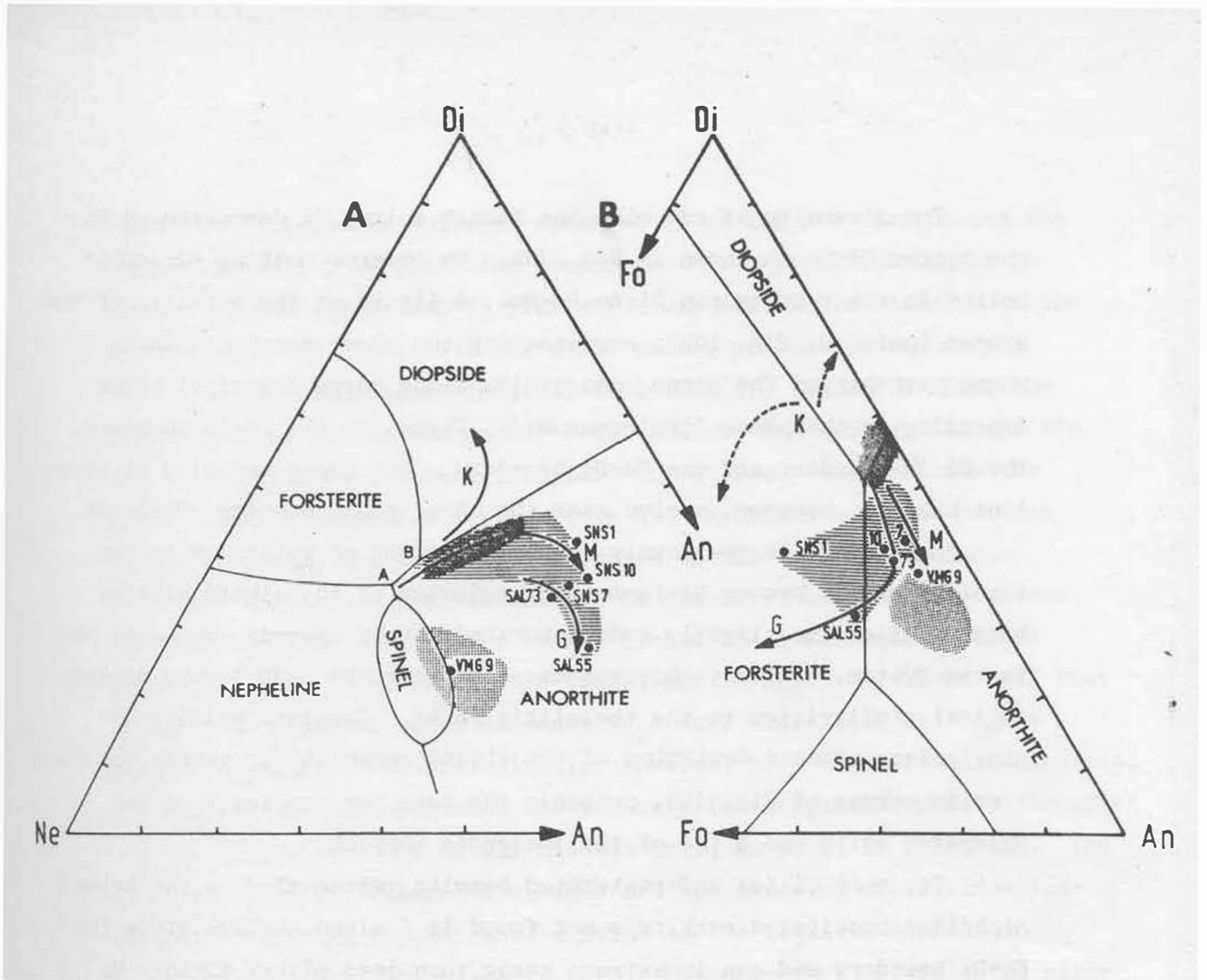
Fig. 10.

(A) A hypothetical mineralogical evolution of alkali olivine basalt
    during its formation by partial melting in silica depleted amphi-
    bolite. At point A in the system Ne-Di-An (Schairer et al., 1968) a
    liquid is formed at a thermal minimum. Consumption of the Ne-com-
    ponent results in change of the liquid composition towards the
    point B, where equilibrium with the major phases of alkali olivine
    basalt is established. The arrows in the figure indicate the evo-
    lution paths of different rock suites (K = Koloa, Hawaii; M =
    Mauna Kea and Kohala volcanoes, Hawaii; and G = Galapagos). The
    shaded area in the figure covers the compositions of the Icelandic
    alkali olivine basalts (Table I). The cross hatched area shows
    compositions of the most alkaline basalts. The dotted area in the
    figure is the field of undersaturated differentiates (sample VMG 9).

(B) The system Fo-Di-An viewed towards the Ne corner in the tetrahedron
    Fo-Di-An-Ne. The arrows point towards the plane Fo-Di-An (Fig. 3a).
    The alkali olivine basalt field is indicated by shaded field and
    the most alkaline members by a cross hatched field. The silica
    undersaturated differentiates are indicated by dotted area (sample
    VMG 9). The alkaline basalts in general trend from the inside of
    the tetrahedron Fo-Di-Ne-An towards the plane of silica undersatu-
    ration here approximated by the plane Fo-Di-An. During that evolu-
    tion, believed to reflect increased degree of partial melting, the
    alkalinity of the rocks decreases.

    The components Fo, Di and An are computed as in Fig. 6, but Ne is
    approximated by Ne = 2 mol Na_2O.

The diversity of the alkaline basalt suites is demonstrated in
the system Di-Fo-An shown in Fig. 10b. We observe melting of amphi-
bolite in the tetrahedron Di-An-Fo-Ne. A liquid at the eutectic of the
system (point E, Fig. 10b), representing the above mentioned three
phase path behind the plane, can evolve along three principal paths
depending on the phase first consumed. These are the Fo-An boundary,
the Di-An boundary and the Fo-Di boundary. The great majority of alka-
line basalts, however, evolve near the three phase boundary Di-Fo-An.

Regarding the previously mentioned effect of volatiles on the
topology of the system Di-Fo-An, the majority of the alkali olivine
basalts, i.e. the slightly undersaturated, trend towards the Fo-An path
in the system. In many observed cases these rocks bear strong minera-
logical similarities to the tholeiitic rocks. Complete melting of
plagioclase effects deviation of the liquid composition towards the for-
sterite corner of Fig. 10b, probably the case for samples from the
Galapagos suite and a few of the Icelandic samples.

The more silica undersaturated basalts represented by the Koloa
nepheline basalts, a rock type not found in Iceland, evolve along the
Fo-Di boundary and can in extreme cases turn into either field. We
are, however, aware that these rocks are only to be described in the
system Di-Fo-An in a qualitative sense.

Compositions on the Di-An are more alkaline than the first type
noted and contain very low Ni and Cr, comparatively. This indicates
their generation by olivine fractionation from early melt fractions, as
also indicated in Fig. 10a.

Experimental simulation of basalt petrogenesis

The crystallization of hybrid tholeiitic magmas were studied by
melting experiments at one atm. under oxygen fugacity controlled on the
FMQ buffer. Since the experiments were run in AgPd capsules experimen-
tal glasses are somewhat iron depleted. To compensate this problem par-
tially the iron loss is estimated at 10% (Fisk, 1978) and the microprobe
analysis behind the compositional trends discussed below are corrected
by this amount. Two synthetic hybrid series were studied: (1) Ol-tho-
leiite (B-THO) with 1%, 5%, 10% and 20% subalkaline rhyolite (A-THO)
and (2) Ol-tholeiite with 5%, 10% and 20% ne-rich basalts (sample SAL 4,

Table V). The former suite is referred to as the B-A series and the latter as the B-S series. For comparison the crystallization of a natural ol-tholeiite, NAL 13 (Table V), was studied in addition to the end member B-THO. Table IVa lists the phases present in the sample NAL 13 in the temperature interval 1270-1160°C. Table IVb lists the phases present in the end member B-THO and the B-A hybrids 90A and 80A in the temperature interval 1218-1156°C. At lower temperatures the glass fraction decreases very rapidly and experiments are as yet not complete towards the low temperature end of the crystallization.

The evolution of qz-tholeiites is simulated in the B-A mixtures. Considering first the trace elements (Table IIIc) Rb rises 68 times from $B_{100}A$ to $B_{80}A_{20}$, and K_2O 19 times, and in $B_{90}A_{10}$ by about half that amount. In terms of major elements $B_{90}A$ is a tholeiite, and $B_{80}A$ a basaltic andesite. Mineralogically, however, both are olivine tholeiites, and olivine and clinopyroxene are the sole ferromagnesian phases through-out the crystallization of all the mixtures, as shown in Table IVb. The chief observed mineralogical changes are the lowering of liquidus tem-peratures, and the replacing of olivine as the liquidus mineral in $B_{100}A$ and $B_{90}A$ by plagioclase in $B_{80}A$. Clinopyroxene is the third sili-cate mineral to crystallize in all instances.

The "cotectic curves" referred to above are in fact projections of cotectic planes, as the "eutectic" in the system Fo-Di-An is a piercing point of the ternary cotectic curve. Thus, olivine tholeiites evolve by crystallization towards the ternary cotectic curve ol/cpx/pl, and then along that curve towards the ol-tholeiite invariant point. In the quaternary system Fo-Di-An-SiO$_2$ that invariant point is maintained by the reaction Fo + SiO$_2$ = 2En, which fixes the silica activity in the melt. That this point is often reached in natural ol-tholeiites is evidenced by the formation of pigeonite in the groundmass of lavas or, more rarely, the formation of pigeonite phenocrysts (e.g. Wood, 1978). In our experiments we have, so far, only been able to recognize pigeonite crystals once - in sample NAL 18 (Table I) at 1143°C. In the quenched sample euhedral pigeonite crystals coexist with rounded olivines and laths of plagioclase.

In Fig. 11a the crystallization paths of B-THO (100A) and the hybrid 95A are shown along the Fo-An cotectic in the system Fo-Di-An and in Fig. 11b the paths of the hybrids 99A, 95A, 90A and 80A are shown

in the system $Fo-SiO_2-An$. It is evident that about 10% mixing is needed
to reach significantly into the tridymite field.

The evolution of transitional basalts is simulated in the B-S
mixtures. Table IVc shows the phases present, and the estimated amounts
of glass remaining at the four temperatures so far analyzed. All three
mixtures are within the plagioclase primary field of the synthetic
systems. In $B_{90}S$ and $B_{80}S$ olivine is replaced by clinopyroxene as the
second phase to crystallize. All three mixtures are on the tholeiite
side of the thermal divide separating the field of tholeiites from that
of the nepheline-normative rocks, as shown by their evolution by frac-
tional crystallization towards higher silica content.

The chemical components that are chiefly affected by the incorpo-
ration of SAL 4 are dispersed elements such as Rb (up ten times in $B_{80}S$
as compared to B-THO), K_2O (5 x), P_2O_5 (2.5 x), TiO_2 (2 x) and Sr (1.6 x).
Further 50% fractional crystallization brings the composition of this
sample ($B_{80}S$) to one similar to that of NSG 12 (Table I).

In Figs. 11a and b the trends for 90S and 80S are almost similar
to those for the volcanic centers KRI and KRA, which were shown in
Fig. 9(a-c). Here the three major phases, however, appear early in the
experiments, whereas the KRI and KRA trends end where cpx appears.

The following conclusion may be drawn: A relatively weak inter-
action of primitive ol-tholeiite melt with silica undersaturated liquids
together with subsequent crystallization, is capable of causing the
shift from pure tholeiitic trends to transitional ones. Another conclu-
sion regarding the topology of the system Fo-Di-An is that the left
shift in the plag/ol cotectic line results not only from volatiles (not
present here) but also from the addition of iron and alkali.

The formation of alkali olivine basalt was simulated experimentally
by the partial melting of three mixtures containing kaersutite (AI-III),
olivine, augite and anorthite in different proportions (Table V). The
preliminary results are shown in Table IVd and in Figs. 11c and d.

In order to appreciate fully the paths in the figures, one must
bear in mind the tetrahedron Ne-Di-An-Fo (Schairer et al., 1968, Fig. 76),
of which Fig. 11c forms one side and Fig. 11d another. In the tetra-
hedron the cotectic plane An/Fo lies within the tetrahedron at angles
with the plane Ne-Di-An and accordingly the path of the alkali basalt
VMG 4 (Table Vc) is first within the An volume, and then along the plane
An/Fo towards the Ne-Di-An face, in which the three phase cotectic curve
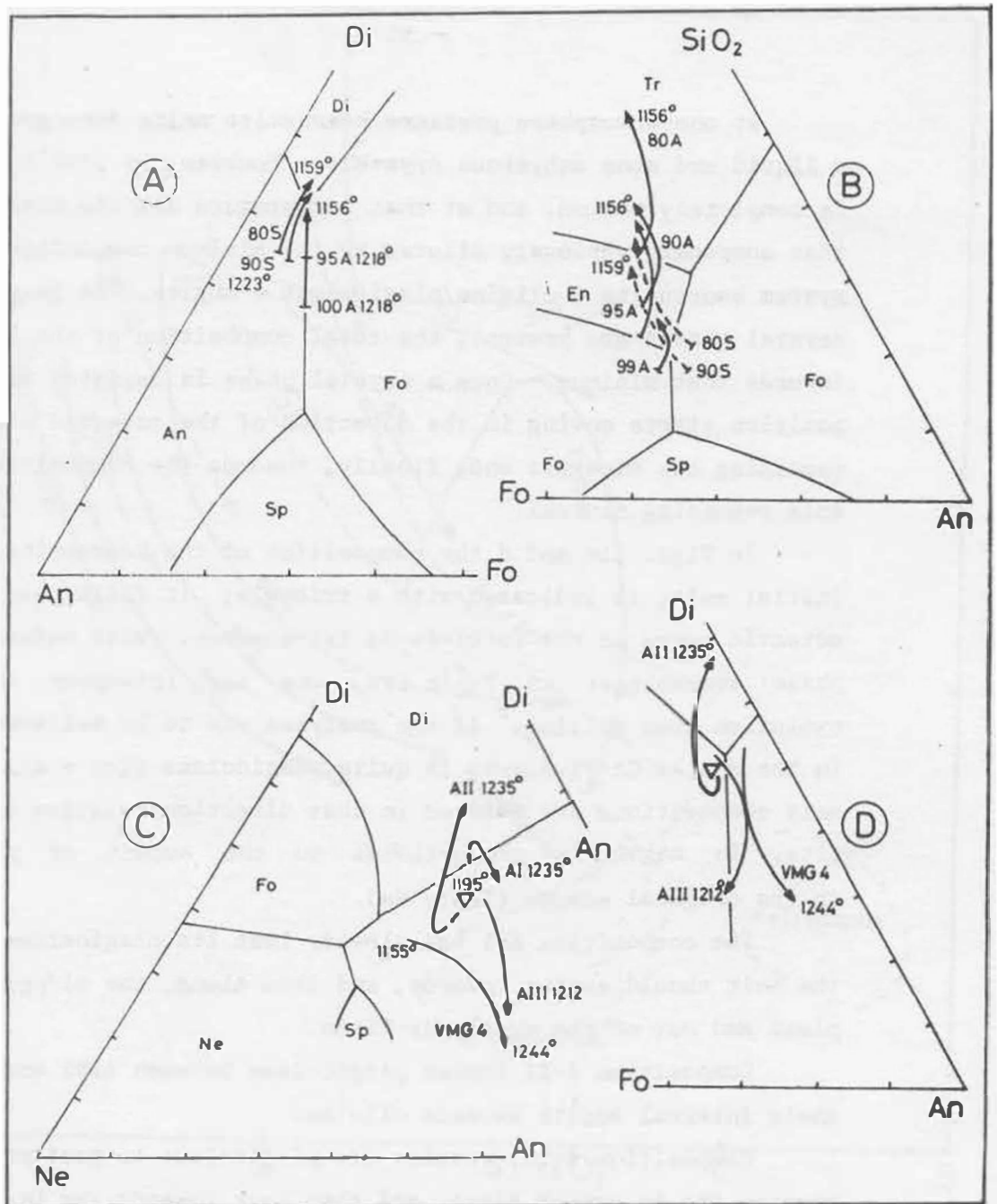Fo/Di/An forms a piercing point.

Fig. 11.

(A) The system Fo-Di-An. The component calculation is given in the text to Fig. 9a.

(B) The system Fo-SiO$_2$-An. The component calculation is given in the text to Fig. 9c.

(C) The system Ne-Di-An. The component calculation is tiven in the text to Fig. 10a.

(D) The system Fo-Di-An. The component calculation is given in Fig. 9a.

At one-atmosphere pressure kaersutite melts incongruently to form
a liquid and some anhydrous crystals. However, by 1195°C the kaersutite
is completely molten, and at that temperature all the mixtures contain
that component variously diluted by the minimum composition in the
system kaersutite + olivine/plagioclase + augite. As long as all three
crystal phases are present, the total composition of the liquid moves
towards that minimum. Once a crystal phase is depleted the liquid com-
position starts moving in the direction of the cotectic plane of the
remaining two minerals and, finally, towards the composition of the
sole remaining mineral.

In Figs. 11c and d the composition of the kaersutite, i.e. the
initial melt, is indicated with a triangle; it falls near the Fo-Di-An
cotectic curve in the Fo-Di-An-Ne tetrahedron. With reference to the
phase assemblages in Table IVd, one may interpret the paths of
evolution upon melting. If the analyses are to be believed, the minimum
in the system Ol-Pl-Aug-Ne is quite plagioclase rich - all the initial
melt compositions are shifted in that direction relative to the kaersu-
tite, in magnitude proportional to the amount of plagioclase
in the original sample (Table Va).

The composition A-I has already lost its plagioclase by 1195°C;
the melt should evolve towards, and then along, the ol/cpx cotectic
plane and out of the system Ne-Di-An.

Composition A-II looses plagioclase between 1195 and 1212°C. In
their interval augite exceeds olivine.

Composition A-III retains its plagioclase longest and evolves
towards the An corner first, and then back towards the Di/Fo boundary
as the An is depleted.

These compositions compare, both in terms of major
and incompatible elements, rather well with natural alkali olivine
basalts (SNS 1, SNS 10, SNS 7, SAL 73, SAL 55), especially A-I and III
in which olivine is the dominant mineral. All would with relatively
limited crystallization become triphyric, i.e. plagioclase would appear
on the liquidus together with olivine and augite, a situation that is
commonly encountered in the WDV and STZ basalts (WDV).

The somewhat complex crystallization paths of the hybrid magmas
as displayed in nature and here simulated by experiments are summarized
in Fig. 12, which is a simplified reproduction of Fig. 4, showing the
Mg/Mg+Fe ratio for the oceanic rock suites. The B-A hybrids and the
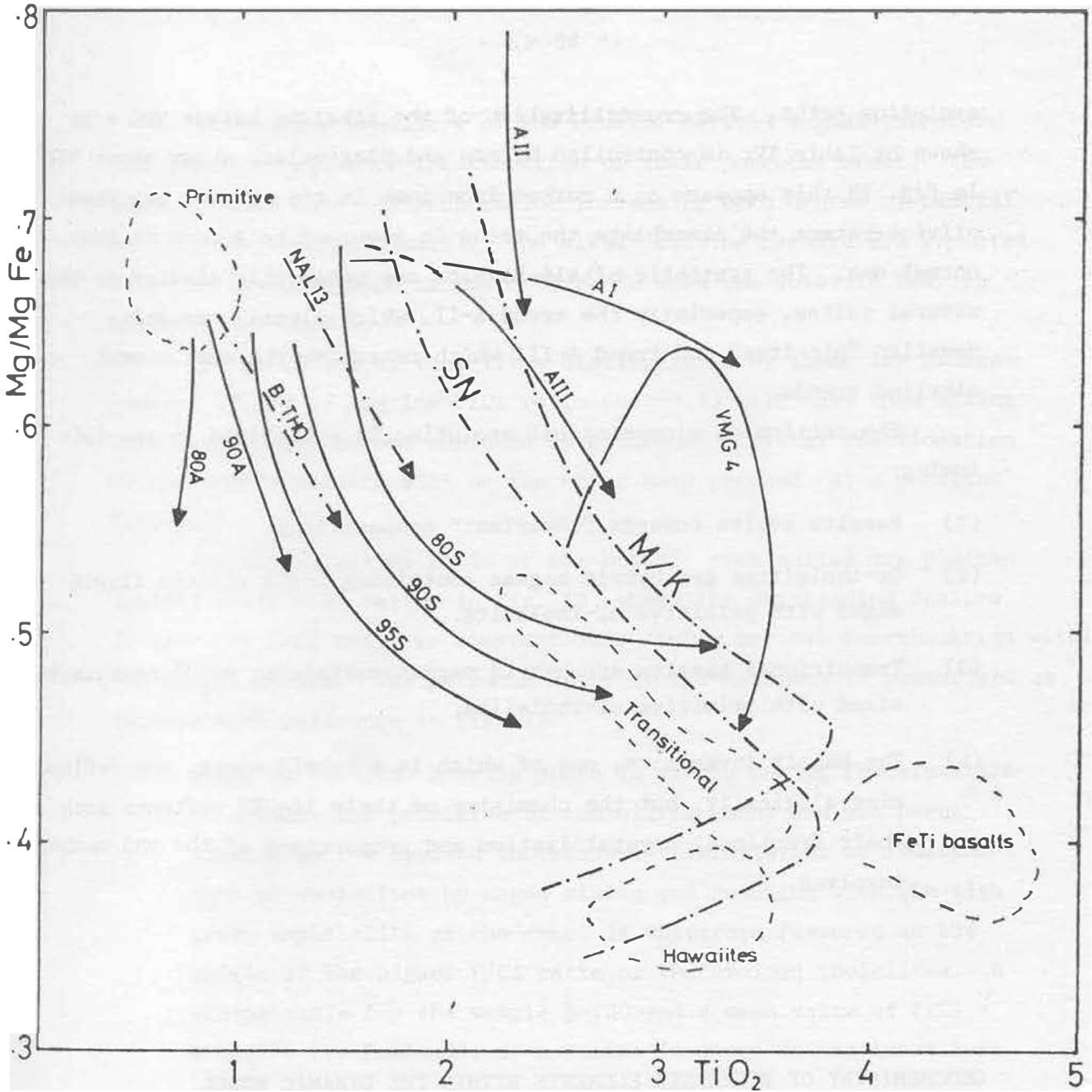B-S hybrids are indicated by arrows showing their entirely different

Fig. 12. The Mg/Mg+Fe (atomic ratio) vs. TiO₂ for experimental glasses in relation to natural rock suites (see also text to Fig. 4).

evolution paths. The crystallization of the alkaline basalt VMG 4 as
shown by Table IVc is controlled by ore and plagioclase above about 1180°C.
In Fig. 12 this appears as a marked iron loss in the liquid, but when
olivine enters the assemblage the trend is reversed to a more or less
normal one. The synthetic alkali basalts are remarkably similar to the
natural suites, especially the trend A-II, which closely resembles
Hawaiian "picrites" and trend A-III which resembles the most common
alkaline trends.

The section on mineralogical evolution is summarized in the fol-
lowing:

(1)   Basalts evolve towards "invariant" compositions.

(2)   Qz-tholeiites are hybrid magmas containing 0-15% silicic liquid
       mixed with primitive ol-tholeiite.

(3)   Transitional basalts are hybrid magmas containing 0-10% ne-basanite
       mixed with primitive ol-tholeiite.

(4)   The basalt invariants, one of which is a hybrid magma, are defined
       mineralogically, but the chemistry of their liquid reflects both
       their fractional crystallization and proportions of the end members
       involved.

GEOCHEMISTRY OF DISPERSED ELEMENTS WITHIN THE DYNAMIC MODEL

The halogens

The linear covariation of potassium and chlorine within the oceanic
basalts (Sigvaldason & Óskarsson, 1976), reveals the dispersed nature of
both elements in the basalt evolution. The geochemistry of fluorine in
the oceanic rocks reflects its more complex behaviour during fractiona-
tion of the rift zone crust. During subsidence through the low grade
amphibolite fluorine is preferred over chlorine in the lattice of horn-
blende, anatexis therefore produces alkaline silicic melts enriched in
chlorine. In the high grade amphibolite the volatile bearing phases
become successively more enriched in fluorine with depht (Carmichael et
al., 1974).

The halogen chemistry of the crustal derived magmas therefore indicate the degree of fractionation of their parental crust. The silicic rocks have low F/Cl ratios increasing with degree of partial melting (decreasing alkali). The alkali olivine basalts are expected to reach maximum value of the F/Cl ratio when the volatile bearing minerals are used up.

The primitive ol-tholeiites distinguished by their low halogen content (Table I) and low F/Cl ratio (0.3-0.7) will thus upon mixing with ne-basanite become enriched in fluorine. Crystal fractionation of the hybrid basalts will on the other hand proceed at a constant F/Cl ratio.

The alkali/silica ratio of the oceanic rock suites are plotted against their F/Cl ratios in Fig. 13, where the outstanding feature is that the F/Cl ratio is constant only during crystal fractionation within the basalt system. The petrochemistry of the halogens is summarized as follows with reference to Fig. 13.

(1)   Since no halogen bearing phase is stable during fractionation of basalts the primitive ol-tholeiites alone are not parental liquids to the evolved tholeiites. Assimilation of fluorine into ol-tholeiites by magma mixing and reaction with the high grade amphibolite of the crust is therefore favoured as the origin of the higher F/Cl ratio of the evolved tholeiites. A mixing scale for the sample B-THO and a mean value of F/Cl = 1560/278 for Icelandic ne-basanite is shown in the lower left of the figure.

(2)   Increase in the alkali/silica ratio of the hybrid tholeiites at almost constant value of F/Cl indicates fractional crystalli-zation from ol-tholeiite towards qz-tholeiites.

(3)   The subalkaline silicic rocks of the rift zone show large range in the F/Cl at a constant (mineral buffered) alkali/silica ratio. The increasing F/Cl ratio is believed to reflect in-creasing degree of partial melting. The minimum values (sample A-15, Table I) are for pitch-stones, but the maximum values are for dacites (sample I-DAC, Table I). The fact that the dacite shows higher F/Cl ratios than any other rift zone rock rules out its genesis by crystal fractionation of a tholeiitic basalt. A high degree of partial melting, where the liquid con-tains the bulk of available volatiles is thus favoured as a genetic process.
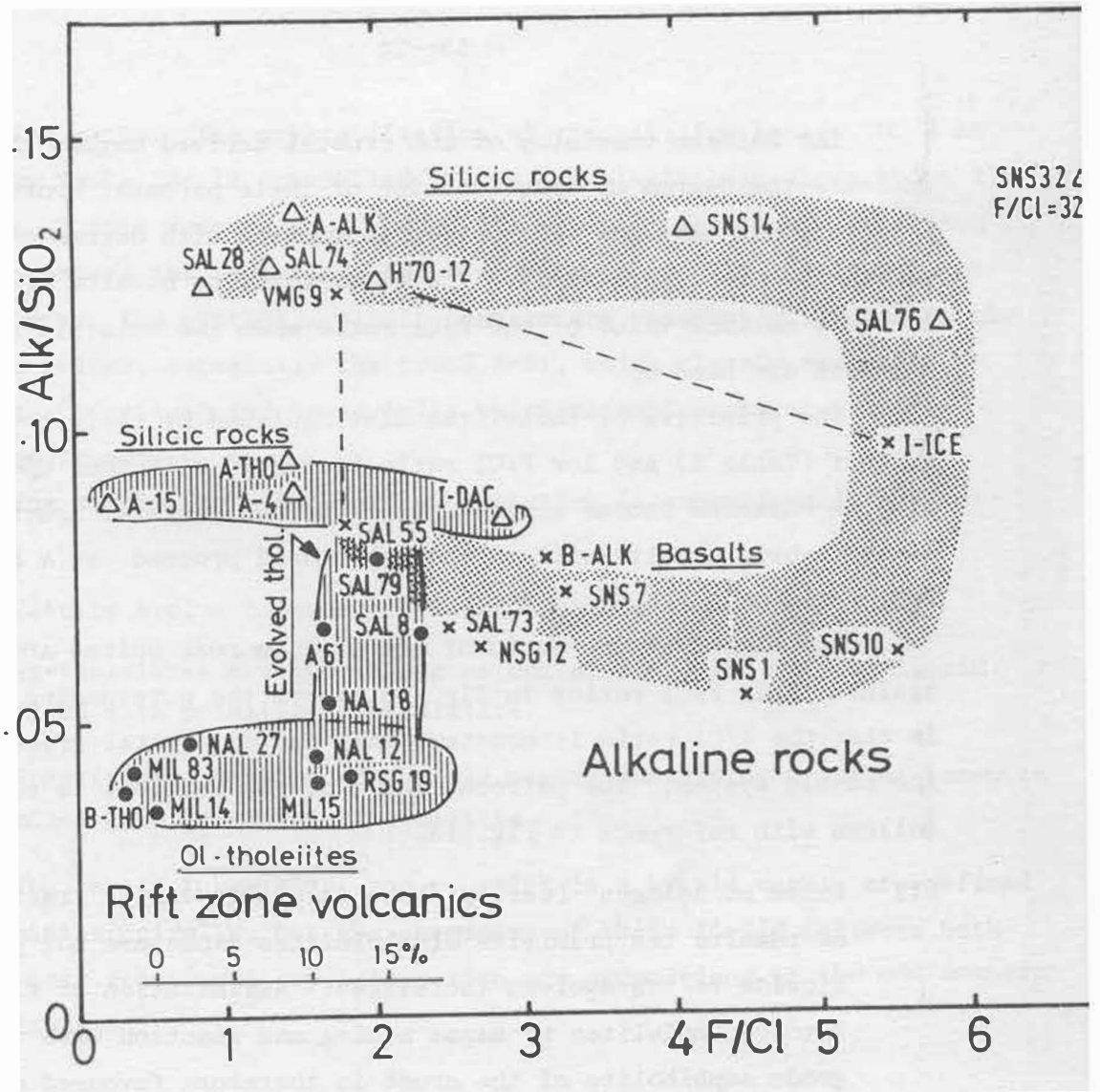
Fig. 13. The rift zone volcanics show increase in alkalinity in the group of evolved tholeiites, where also the F/Cl ratio remains within narrow limits. The alkaline rocks show similar pattern, but at a more silica undersaturated level. The figure indicates that fluorine behaves as a dispersed element only during crystal fractionation of the basalts. The effect of magma mixing of primitive ol-tholeiites and ne-basanite (lower left) is shown by the samples MIL 15 and RSG 19. The effect of crystal fractionation is shown by the sample SAL 79 (evolved qz-tholeiite) and the pair SAL 55 and VMG 9 from the Vestmannaeyjar volcanic center on the STZ. The effect of low degree of partial melting is indicated by the sample pair H´70-12 and I-ICE, the former being a silicic pitch-stone from the Hekla 1970 eruption, while the sample I-ICE represents the lava erupted.

(4)   The very variable F/Cl range of the alkaline transitional basalts
        (B-ALK and NSG 12) and the alkaline basalts (SAL 55 to SNS 10)
        indicate (a) different degree of magma mixing in transgressive
        volcanism (case 2) or (b) different degree of fractionation of
        the parental crust. The rocks highest in fluorine are those from
        highly evolved volcanic centers of the WDV and EDV.

(5)   Intermediate differentiated rocks of the alkaline suite show
        alkali increase at almost constant F/Cl (samples SAL 55 and
        VMG 9, Table I), while the alkaline silicic rocks have a pattern
        similar to the subalkaline suite in relation to their parental
        basalt. Inspection of Table I shows that the chlorine content
        of the alkaline silicic rocks (samples 25-31) is on average
        higher than chlorine in the alkaline basalts by a factor of about
        3. This degree of enrichment, if resulting from fractional cry-
        stallization, is much too low to allow for simultaneous removal of
        amphibole (Bailey, 1977). Further the silicic rocks with the
        highest F/Cl ratios are the lowest in chlorine. This is strongly
        speaking against fractional crystallization as a genetic process
        for rhyolites in general. A more favourable explanation is to
        assign the F/Cl ratio of the alkaline silicic magmas to this
        ratio for a volatile bearing phase during anatexis. In the
        Icelandic silicic rocks this phase would in most instances be
        amphibole except in the most potassic volcanic centers, where
        phlogopite might be stable. The F/Cl ratio of the potassic
        silicic rock represented by sample 26 (Table I, SNS 32 in Fig. 13)
        indeed supports this hypothesis.

The K/Rb ratio of the oceanic rocks

        The development of ideas regarding the K/Rb ratios of oceanic
rocks is briefly reviewed in the following. The negative covariation
of K/Rb and K for the oceanic ol-tholeiites, as contrasted to all other
terrestial rocks, is well established (Engel et al., 1965; Gast, 1965,
1968; Key et al., 1970).
        Gast (1960) suggested retention of K and Rb in the mantle. Oxburgh
(1964) suggested a K-bearing minor phase in the mantle. Hart & Aldrich
(1967) pointed out the straight forward resemblance of K/Rb ratios of

amphiboles and the oceanic ol-tholeîites, and suggested the breakdown
of amphibole as the source of the elements.

Gast (1968) concluded, on the basis of the low distribution
coefficients for the elements between accepted residual phases of the
mantle and a silicate melt, that Hart & Aldrich´s (1967) model con-
stituted disequilibrium melting, and therefore suggested the depletion
in the mantle of the elements as a result of an early melting event.
Of importance is Gast´s (1968) statement that the oceanic ol-tholeiites
and the oceanic alkali olivine basalts are not derived from the same
source, since the K/Rb ratio of a melt fraction would closely resemble
that of the source at early melting stages. Referring to Green &
Ringwood (1967) and Kushiro (1968), Gast (1968) assumed that the two
magma types are derived at various depths by varying degree of partial
melting in a heterogenous mantle, the alkali olivine basalts represen-
ting a smaller melt fraction from a deeper undepleted source. Carmichael
et al. (1974) pointed out the inconsistent volume relations of the two
magma types, with the depleted source, active over millions of years,
giving rise to 99 per cent of the ocean floors.

Beswick (1976) substituted Gast´s (1968) early depletion event
by partial melting of a chondritic mantle containing phlogopite as a
residual phase. In the resulting model the ol-tholeiites represent
large initial melts and the alkali ol basalts represent later melt frac-
tions consuming the residual phlogopite. The author was aware of his
optimism writing: "The necessary survival of phlogopite in residues
which have previously lost a melt fraction is difficult to understand".
Further, the very low K-contents of the ol-tholeiites are inconsistent
with phlogopite control, where K is not a dispersed element (Menzies,
1978).

To complicate matters further, various ultramafic rocks have been
suggested as mantle residues or even pieces of the mantle itself. The
alkali olivine basalts show strong evidence for genesis by partial
melting of ultramafic rocks of their associated xenoliths. Randomly
observed disequilibrium between K minerals and their matrix in the ultra-
mafic assemblages (Steuber & Ikramuddin, 1974), however, complicates
modelling of the partial melting process (Basu & Murthy, 1977).

The discussion on chondritic versus achondritic earth (Edwards &
Urey, 1955; Engel, 1965; Gast, 1965) and theoretical estimation of
the earth´s K/Rb ratio based on argon degassing and alkali differentia-

tion (Hurley, 1969; Russel & Ozima, 1971), also influence the inter-
pretation of the K/Rb ratio of the oceanic rocks.

 The dynamic model of oceanic petrogenesis greatly reduces the
moments of confusion appearing in the above review by assuming one single
source material for all oceanic magmas. Inconsistent usage of the
equilibrium concept is therefore eliminated from the discussion, since
the invariant composition of the primitive ol-tholeiites represents
equilibrium with major phases and their narrow chemical range indicates
that if there is a K component in the mantle it is contained in the
liquid. Alternatively the view of Yoder (1976, p. 38), that clino-
pyroxene is the host of the alkalis seems realistic. The K/Rb ratio
of the primitive rocks thus reflects the ratio for the oceanic mantle.
Assumed mantle xenoliths associated with alkali basalt magmas and
ultramafic rocks in general, are residues of crustal melting. Their
K/Rb ratio is inherited from their parental crust (below 500).

 Our interpretation of the K/Rb ratio of the oceanic rocks is
outlined in Fig. 14, showing K/Rb vs K. The primitive ol-tholeiites
show some scatter arising from (1) different proportions of mixing
(contamination) with crustal derived magmas and (2) crystal differen-
tiation during ascent to the crust. Combination of the two alternatives
is, however, likely since crystal controlled elements like Ni and Cr
show some scatter within the primitive rocks (samples MIL 14, NAL 12,
B-THO, Table I). The establishment of a volcanic center is indicated
by lines A and B in the figure. The crustal equilibration is simulated
by mixing 1-4% of the subalkaline rhyolite A-THO with two hypothetical
primitive compositions covering the range of the primitive rocks.
The shape of the stippled field in Fig. 14 indicates that the rocks
lowest in K and Rb are the most sensitive to crustal contamination.
The most primitive rocks from the Azores Rift (White & Schilling, 1978)
occupy the domain enclosed within a dashed line in the upper left of
the figure. It is likely that this domain represents samples totally
uncontaminated by crustal material. The field enclosed between the
lines A and B covers the compositions of "parental magmas" of the
tholeiitic volcanic centers. A complete K/Rb evolution of a tholeiitic
volcanic center is shown by line C, representing the extinct Álftafjördur
central volcano E-Iceland (Ólafsson, 1976). The basalts reach the
K/Rb ratio of the silicic rocks during the evolution of the center,
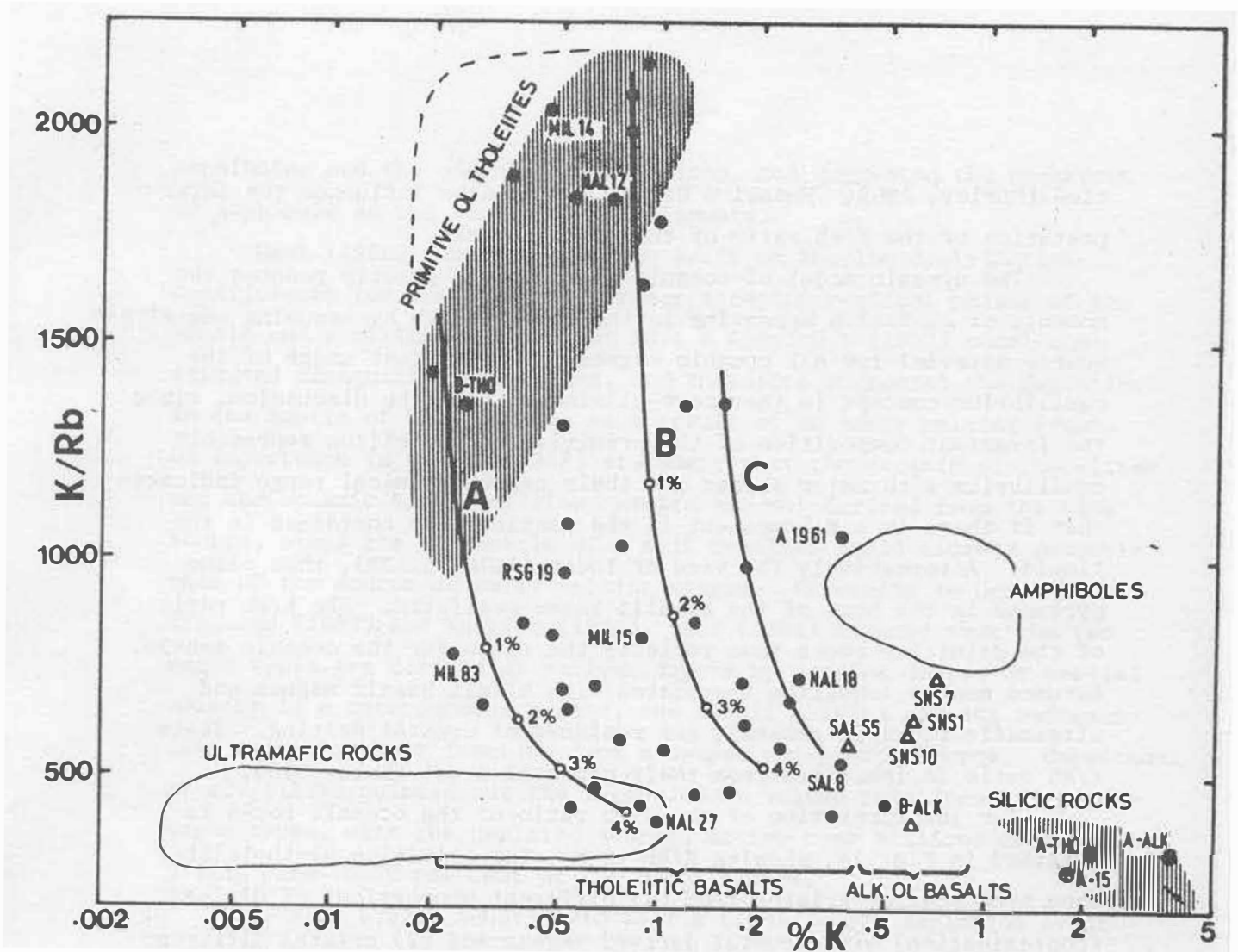indicating increased proportion of sialic material with increasing

Fig. 14. The field of the primitive ol-tholeiites (stippled area) is shown in the upper left of the figure. Few tholeiitic samples (filled circles are plotted to indicate the large spread of K and Rb in the rift zone rocks. The lines A and B are calculated trends for two mixtures of ol-tholeiite compositions and a subalkaline rhyolite (A-THO), shown in a stippled field in the lower right of the figure. The fraction of rhyolite is indicated by open circles (1-4%) on the lines. The evolved tholeiites in general have K/Rb ratios below 700. Extensive crystal fractionation of the basaltic parental magma of a volcanic center drives the potassium content of the liquid towards higher values of K at almost constant K/Rb. The line labelled C in the figure is the trend observed for a large eroded fissure swarm in Eastern Iceland. The alkaline basalts (triangles) show a narrow range of K/Rb and K as compared to the tholeiites. The parental amphibolite of the alkali olivine basalts is heterogeneous with respect to K/Rb. The high K/Rb ratio of the amphibole and the low K/Rb ratio of coexisting ultramafic phases is illustrated by K/Rb vs K ranges for amphiboles from mafic assemblages and ultramafic rocks. Alkali olivine basalts separated from amphibolite trend towards lower K/Rb ratios with decreasing K content indicating increasing degree of melting (samples SNS 7, SNS 1, SNS 10, Table I).

potassium. Sample A´61 (Table I) from the Askja volcano (Fig. 5) is
of comparable origin. Two samples in Table I, MIL 83 and SAL 8,
represent rarely observed cases. The former is among the smallest
primitive ol-tholeiitic lavas found in Iceland. In spite of its very low
alkali content the sample is considered to be slightly contaminated by
crustal material. The sample SAL 8 is a large homogeneous single
fissure eruption, in our interpretation contaminated and modified by
crystal differentiation as outlined in a previous section of this paper.

The K/Rb ratios of amphiboles (Hart & Aldrich, 1967) from amphi-
bolites is shown in the upper right of Fig. 10. Here the kinematic
model predicts the K/Rb source of the alkali olivine basalts. The
K/Rb trend for samples from the WDV (SNS 1, SNS 7, SNS 10) and the SEZ
(SAL 55) reflect the limited range possible for the K/Rb ratio during
partial melting of the amphibolite. Since only the earliest melts
reflect the K-host, most compositions trend towards the bulk composi-
tion. The range of K/Rb ratios for ultramafic rocks is shown in Fig. 10
(Wyllie, 1967, p. 378). The present discussion is based on the assump-
tion that these rocks are in general residues from crustal magma gene-
ration. This is supported by the identical K/Rb range for the ultra-
mafic rocks and the evolved basalts.

The K/Rb pattern of the Icelandic rocks matches what is
commonly found in oceanic area. Of striking similarity is the pattern
observed by White & Schilling (1978) for the Azores Rift, where the
width of the rift zone again plays the dominant role.

We summarize observations on the K/Rb ratio of oceanic rocks in
four notes:

(1)   The high K/Rb ratios of primitive ol-tholeiites reflect the ratio
       for their mantle sources.

(2)   In a wide rift zone the recycling of sialic material within vol-
       canic centers results in Rb enrichment of the products. These
       centers, however, constitute a small fraction of the oceanic
       plate.

(3)   The products of the enriched centers are heavily overrepresented
       at the plate surface outside the rifts.

(4)   Alkaline volcanism is exclusively derived from volcanic centers
       previously established in the rift zone and thus, reflect their
       low K/Rb ratio as do the ultramafic residues associated with alka-
       line volcanism.

Rb/Sr ratio of the oceanic rocks

The geochemical cycles of Rb and Sr during crystal fractionation
in a rift zone differ markedly due to the stability of plagioclase
during anatexis (Luth, 1976). The silicic magmas normally contain most
of the available Rb, while Sr is retained in the residue. The Sr
entering the high grade amphibolite from above is therefore derived
from an environment of high Rb/Sr ratio. The formation of hybrid magmas
in the crust thus results in Sr enrichment of the ol-tholeiites upon
mixing with ne-basanite at the mantle crust boundary and enrichment of
Rb in the amphibolite facies (Fig. 2).

Fig. 15 shows the variability of the Rb/Sr ratio of the Icelandic
rock suites. The stippled area in the lower left of the figure shows
the ol-tholeiites. Their Rb/Sr is very low (0.01) and stays constant
during olivine precipitation. The evolved tholeiites generally contain
more than 150 ppm strontium. It is evident from Fig. 15, that a hybrid
magma formed by mixing with ne-basanite can show a marked increase in
Sr without markedly changing the Rb/Sr ratio of the ol-tholeiitic end
member. The Rb/Sr ratio of the evolved tholeiites covers an order of
magnitude while the Sr increases by a factor less than 2. This is a
strong evidence for magma mixing since plagioclase factionation is un-
able to produce this variability. The Rb/Sr pattern of the silicic
magmas displays the different level of alkali in their associated basalts.
The lowest Rb/Sr reached by these magmas is about 0.25, but at different
concentration levels. A fundamental conclusion can be drawn from this
observation: The highest degree of partial melting (at the Daly gap) in
the amphibolite facies reflects the average Rb/Sr ratio of the silicic
magma systems of the crust. This material fraction of the crust con-
tains the elements involved in digressive or transgressive volcanism of
the oceanic plate. The minimum average Rb/Sr ratio for the silicic
magma system (0.75) is close to continental average. The variability
of the Rb/Sr ratio is however enormous within the volcanic centers.

The ranges of the Rb/Sr ratios for the various magma types appear
in Table I. The primitive ol-tholeiites generally contain less than
100 ppm Sr (Hart, 1976). Exceptionally high values (sample NAL 18)
are found in samples, which by the same time are well above average in
other elements characteristically high in the alkali olviine basalts
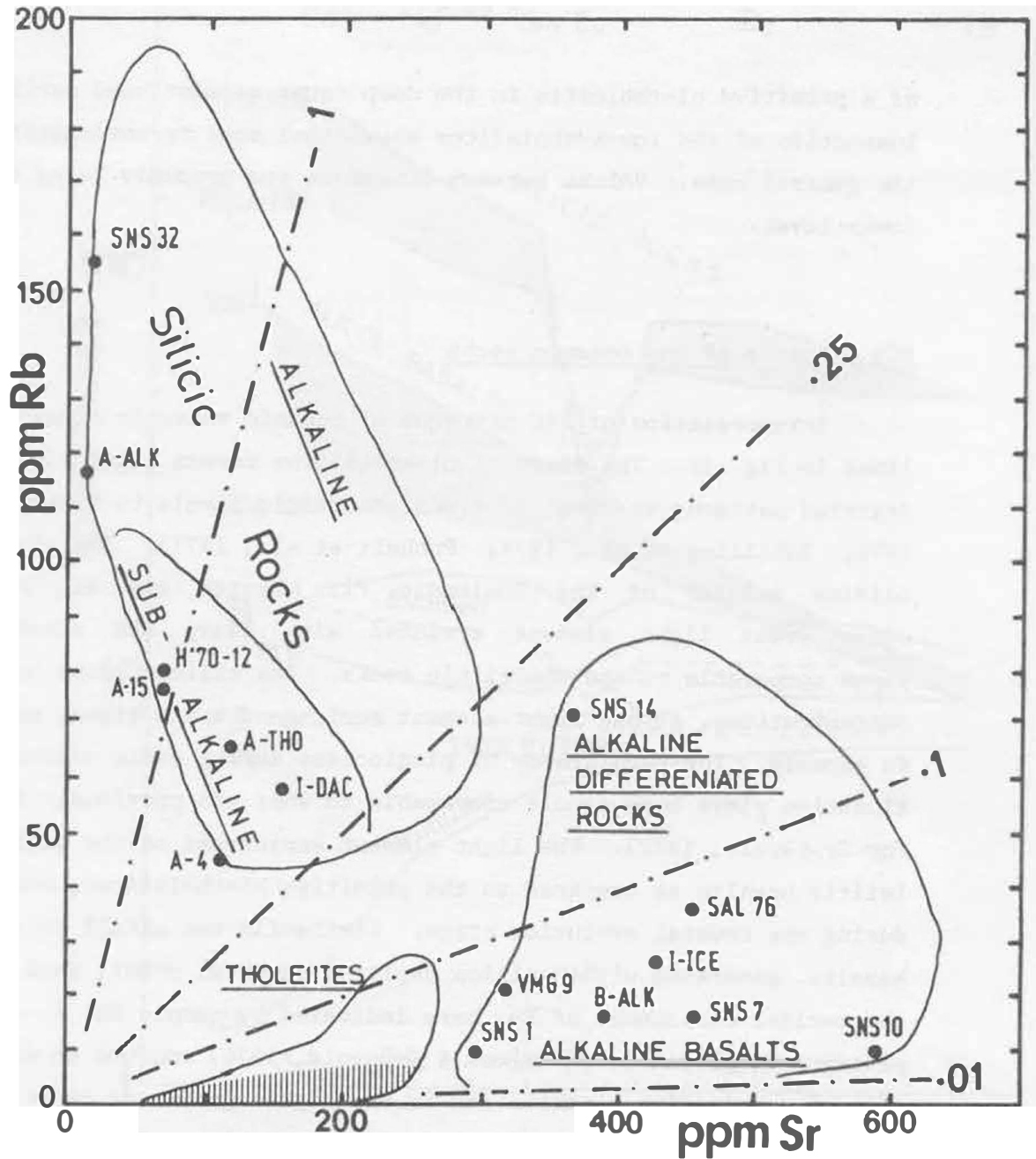(Ti, P, Zr, F). Therefore we explain this exception by equilibration

Fig. 15. The field in the upper left encloses the silicic to inter-
mediate rocks. The alkaline suite is Rb richer than the subalkaline
and shows more scatter due to the large variability in the alkalini-
ty of the volcanic centers outside the rift zone. The subalkaline
silicic rocks show considerably lower scatter than their alkaline
equivalents, roughly reflecting the restricted alkali range of their
tholeiitic parent. The stippled area within the tholeiitic field
shows the Rb/Sr ratio for the ol-tholeiites. The primitive ol-tho-
leiites show very narrow range in Rb at Sr below 100 ppm. The qz-
tholeiites on the other hand show a marked Rb increase during evolu-
tion. The alkaline basalts are distinguished by high level of Sr
and variable Rb/Sr ratio, in this respect comparable to the qz-tho-
leiites of the volcanic centers in the rift zone. The figure illu-
strates the different Rb/Sr ratio of the different magma systems.
The high (0.25) ratio for the crustal derived magmas is close to con-
tinental average.

of a primitive ol-tholeiite in the deep crust as mentioned earlier.
Inspection of the low K-tholeiites shows that some Sr-enrichment is
the general case. Values between 50 and 60 ppm probably being the
lower level.

REE patterns of the oceanic rocks

Interpretation of REE patterns of oceanic volcanic rocks is out-
lined in Fig. 16. The field of ol-tholeiites covers light element
depleted patterns to about 10 times chondritic levels (O´Nions & Grönvold,
1976; Schilling et al., 1978; Puchelt et al., 1977). The alkali
olivine basalts of the Icelandic rift system are as in
other areas light element enriched with heavy REE concentra-
tions comparable to the tholeiitic rocks. The silicic rocks have high
concentrations, strong light element enrichment and a strong negative
Eu anomaly. The persistence of plagioclase during early crustal frac-
tionation plays here a role comparable to what was previously described
for Sr (Drake, 1972). The light element enrichment of the evolved tho-
leiitic basalts as compared to the primitive ol-tholeiites, occurs
during the crustal evolution stage. Similarily the alkali olivine
basalts, generated within silica depleted parental crust, show signs of
the earlier enrichment of Eu, here indicated by sample SNS 7. The
patterns TH 16 and R 4 (O´Nions & Grönvold, 1976) conform to equilibra-
tion of a primitive ol-tholeiite in the higher grade and lower grade
amphibolite respectively. To be noted is the higher level and negative
Eu anomaly of the pattern for R 4 as compared to the lower level and
positive Eu anomaly for TH 16. Calculated REE patterns assuming 10%
mixing with crustal derived magmas is shown to illustrate this further.
The dynamic model here offers a interpretation of REE patterns
of the oceanic rocks, avoiding the laborous manipulations of crystal
differentiation (Wood, 1978) of plagioclase and mafic phases far
exceeding what can be expected from mineral equilibria close to inva-
riant mineralogical compositions. Other even more complicated models
requiring two mantle sources, both of variable major phase composition,
suffering partial melting between 8 and 50% and subsequent mixing and
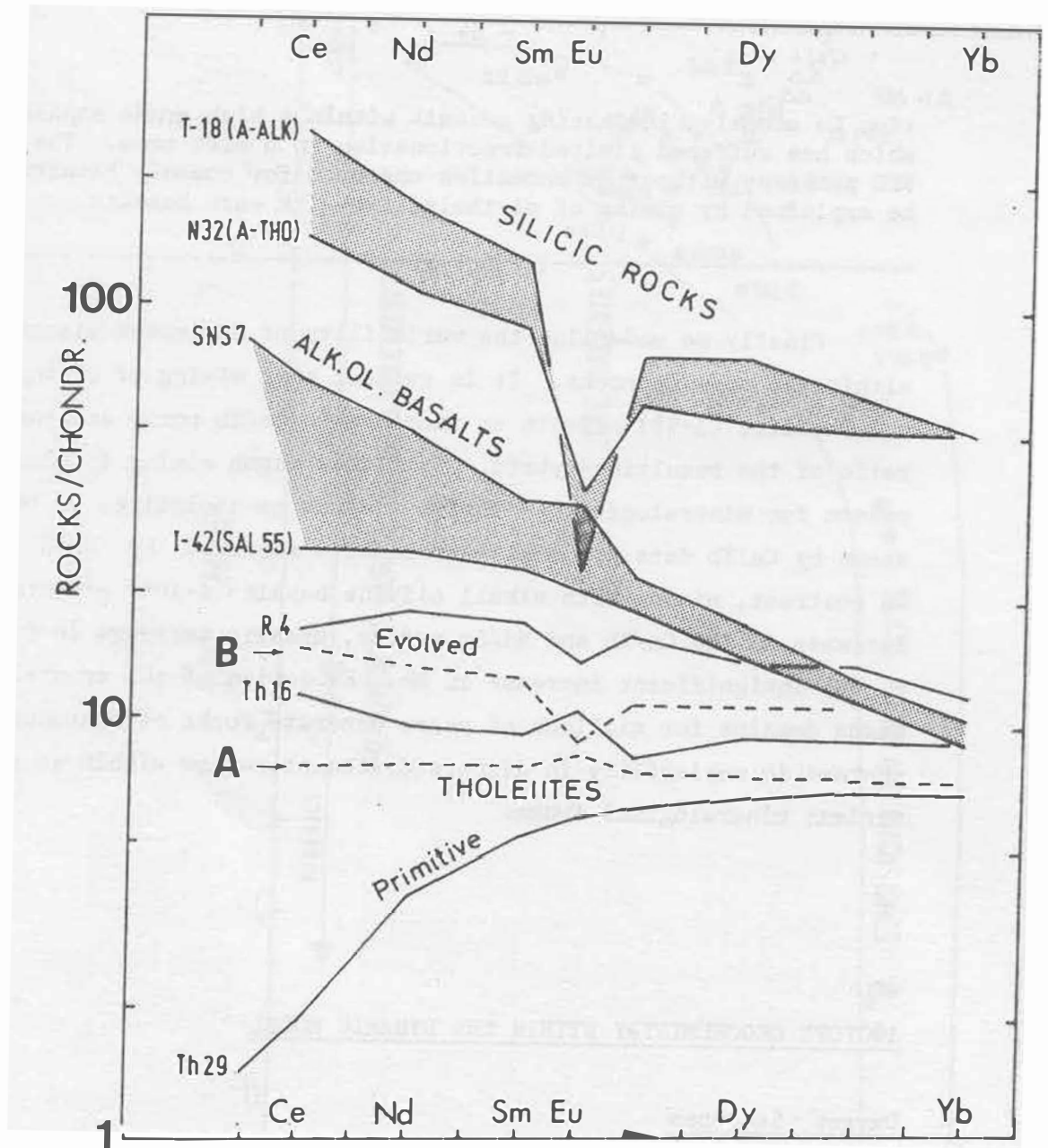fractional crystallization are also eliminated (Schilling et al., 1978).

Fig. 16. The data are taken from O´Nions & Grönvold (1973) and O´Nions et al. (1974). The primitive ol-tholeiites (sample Th 29) are in general strongly light REE depleted. The evolved tholeiites contain about ten times chondrite abundances of the REE (samples Th 16 and R 4). The alkaline basalts are moderately light REE enriched (samples SNS 7 and I-42), while the silicic rocks are strongly light REE enriched. The strong negative Eu anomaly of the silicic rocks is explained by the persistence of plagioclase during anatexis in amphibolite. A partial melting of strongly Eu enriched residual amphibolite as a genetic process for alkali olivine basalt therefore explains the positive Eu anomaly occasionally found in these rocks (sample SNS 7). This is also supported by the high Sr content of the alkali olivine basalts and the very low Sr content of the alkaline rhyolites (Fig. 12). The lines A and B simulate magma mixing. Line A represents the hybrid 90% Th 29, 10% SNS 7, and Line B represents 90% Th29, 10% A-THO. The Eu pattern of the samples R 4 and Th 16 is reproduced by the mixing model. The alkali olivine basalts with the strongest tholeiitic affinities show no signs of a posi-

tive Eu anomaly, indicating genesis within a high grade amphibolite, which has suffered limited fractionation in a rift zone. The V shaped REE patterns without Eu anomalies observed for oceanic basalts might be explained by mixing of ol-tholeiites with such basalts.

Finally we underline the variability of dispersed element ratios within the oceanic rocks. It is evident that mixing of ol-tholeiite and rhyolite (1-5%) effects an increase in Ce/Yb ratio and the Nd/Sm ratio of the resulting hybrid. That this magma mixing is also the reason for mineralogical evolution towards qz-tholeiites is beautifully shown by Ce/Yb data for Icelandic basalts reported by Wood (1978). In contrast, mixing with alkali olivine basalt (1-10%) effects moderate increase in the Ce/Yb and Nd/Sm ratios, drastic increase in Sr, Zr and P, but insignificant increase in Rb. Evolution of the crustal trapped magma domains for millions of years generate rocks of enormous but systematic variability in dispersed element ratios within an almost in-variant mineralogical frame.

ISOTOPE GEOCHEMISTRY WITHIN THE DYNAMIC MODEL

Oxygen   isotopes

Muehlenbachs et al. (1974) found the $^{18}O/^{16}O$ ratio for Icelandic rocks to range from about +5.5 o/oo for the ol-tholeiites to about -10 o/oo for silicic pitch-stones. The evolved basalts are enriched in the light isotope roughly proportional to their dispersed element en-richment and mineralogical evolution (Sigvaldason, 1974a). The most highly evolved samples reach values as low as +3 o/oo. In Fig. 17 the $^{18}O/^{16}O$ ratios of the Icelandic rocks are plotted against K_2O. The field of tholeiites is shown in the upper left of the figure. A typical ol-tholeiite is represented by sample NAL 16 and the ol-tholeiites re-ferred to as parental magmas of volcanic centers, are represented by samples NAL 12, MIL 15 and NAL 27 (Table I). More enriched in the light isotope are the qz-tholeiites A´61 and SAL 8. The range of $^{18}O/^{16}O$ ratios of rocks from a metamorphic aureole of an extinct central volcano
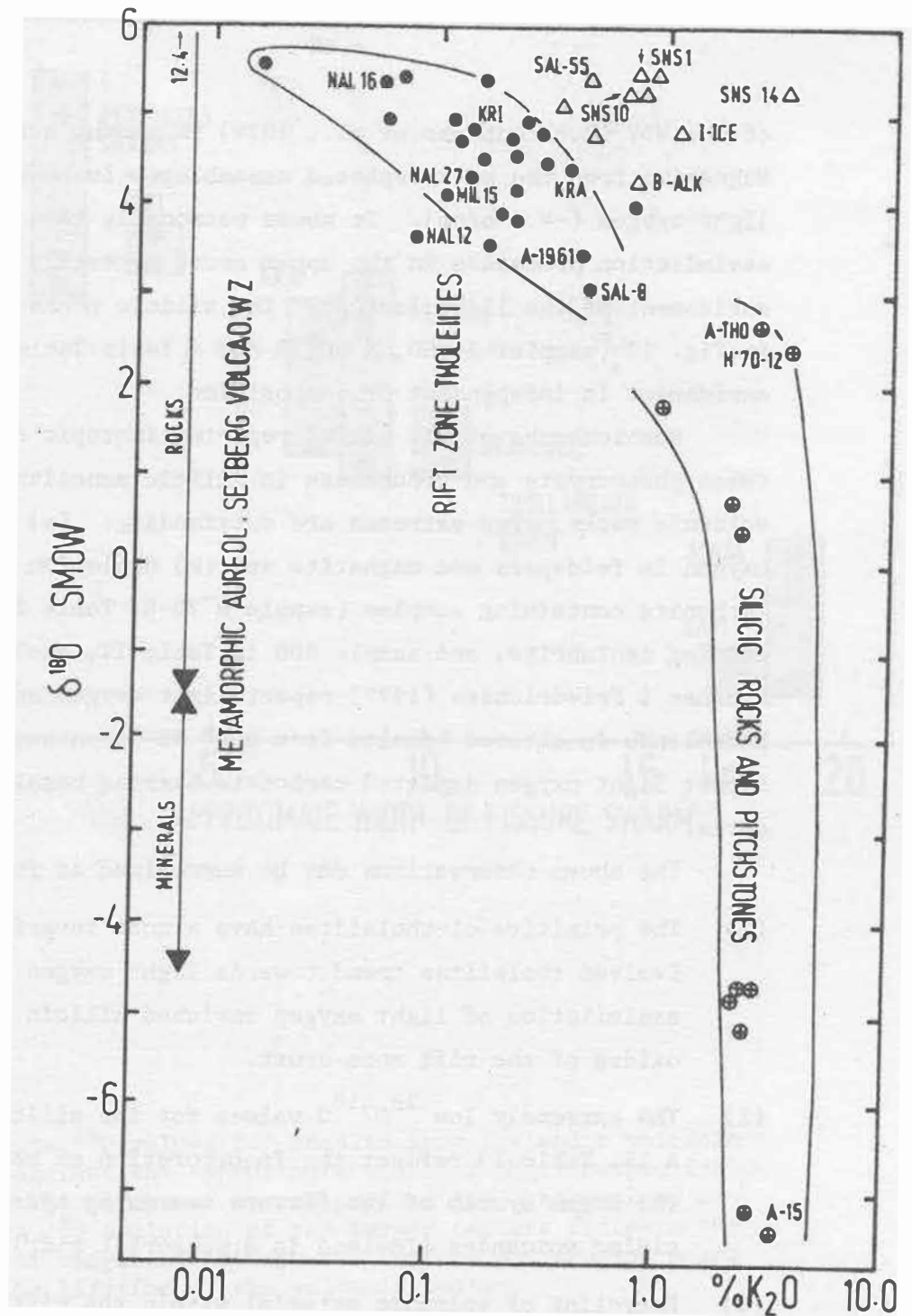
Fig. 17. Arrows at the left margin of the figure show the delta [18]O range of the metamorphic aureole of the Setberg volcano on the WDV. The elongated field ranging from +2 down the right margin of the figure shows the delta [18]O values for silicic rocks and pitch-stones. It is suggested that these rocks are derived from anatexis of meta-morphic mineral assemblages. The primitive ol-tholeiites define the upper margin of the field of rift zone tholeiites (filled circles). Mixing with [18]O depleted silicic magma effects the gradual lowering of delta [18]O values for the evolved tholeiites. The positions for the volcanic centers KRI and KRA are indicated in the figure along with few samples from Table I. The alkaline basalts and intermediate rocks (triangles) resemble the evolved tholeiites in delta [18]O indicating that the meteoric water incorporated in the superstructure of a volcanic center to a large extent enters the silicic magma formed by anatexis. The sample pair I-ICE and H´70-12 from the 1970 Hekla eruption is shown as a supporting evidence.

of the WDV (Muehlenbachs et al., 1974) is shown in the right of Fig. 17.
Magnetite from the metamorphosed assemblages is heavily enriched in
light oxygen (-4.5 o/oo). It seems reasonable that iron enrichment by
assimilation processes in the upper crust generally is associated with
enrichment of the light isotope. The silicic rocks plot to the right
in Fig. 17 (samples A-THO, H´70-12 and A 14 in Table I). Here the O_{16}
enrichment is independent of composition.

Muehlenbachs et al. (1974) reported isotopic disequilibrium be-
tween phenocrysts and groundmass in silicic xenoliths and metamorphic
volcanic rocks. Two extremes are outstanding: (a) Enrichment of light
oxygen in feldspars and magnetite and (b) depletion of light oxygen in
carbonate containing samples (sample H´70-8, Table III, a siderite con-
taining ignimbrite, and sample 009 in Table IV, Muehlenbachs op.cit.).
Hoernes & Friedrichsen (1977) report light oxygen enriched magnetite and
hornblende in altered basalts from DSDP 36 cores and Grey et al. (1977)
report light oxygen depleted carbonate bearing basalts from DSDP 37
cores.

The above observations can be summarized as follows:

(1)   The primitive ol-tholeiites have almost invariant $^{18}O/^{16}O$ ratios.
       Evolved tholeiites trend towards light oxygen enrichment due to
       assimilation of light oxygen enriched silicic liquid and iron
       oxides of the rift zone crust.

(2)   The extremely low $^{18}O/^{16}O$ values for the silicic rocks (sample
       A 15, Table I) reflect the incorporation of meteoric water into
       the magma system of the fissure swarms by hydration of the sub-
       siding volcanics (Iceland is a subaerial rift).

(3)   Recycling of volcanic material within the rift zone and conti-
       nuous outgassing of carbonate in geothermal areas of silicic
       volcanic centers effect formation of increasingly light oxygen
       enriched silicic magmas.

(4)   Disequilibrium with respect to oxygen of the deuteric minerals
       and the igneous silicates of hydrated basalts seems to persist
       through the greenschist facies well down into the amphibolite
       facies. Below the anatectic boundary (Fig. 2) the crust is
       homogeneous with respect to oxygen isotopes. The alkaline rocks
       forming outside the rift zone thus show only slightly enriched
       values as compared to the hybrid basalts of the rift zone (fis-
       sure swarms KRI and KRA marked in Fig. 17).
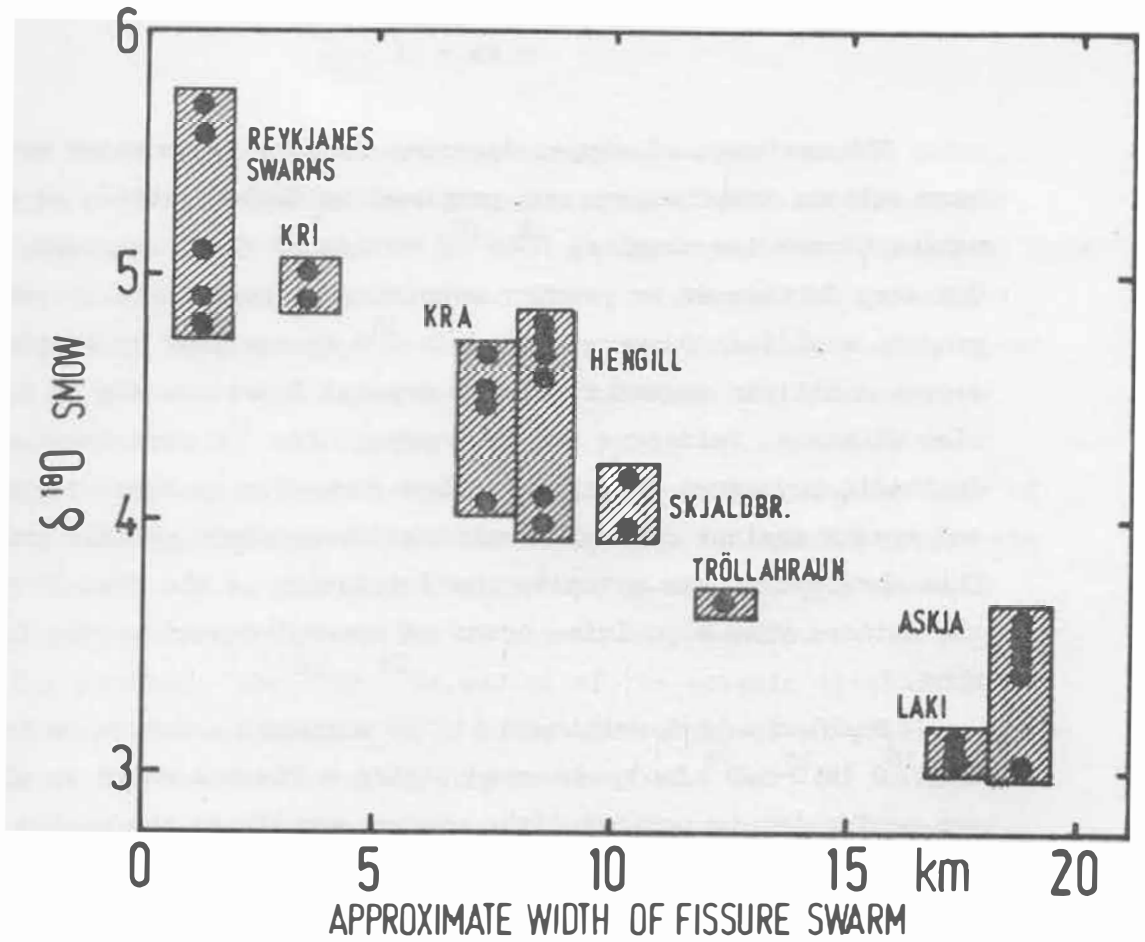
Fig. 18. The delta [18]O values for basalts from Icelandic volcanic centers plotted against the approximate width of their respective fissure swarms. The narrowest swarms produce the less evolved basalts. The delta [18]O depletion of the larger centers indicate the increasing role of recycling between the surface and crustal magma domains during the lifetime of the volcanic center.

The exchange of oxygen isotopes between groundwater and rocks near solidus temperatures was proposed by Taylor (1968), as an explanation of the low marginal $^{18}O/^{16}O$ ratios of the Skaergaard intrusion. One step further is to predict remelting of such rocks by anatexis to produce a silicic magma enriched in ^{16}O in contrast to slightly ^{16}O depleted silicic magmas formed by crystal fractionation of ferromagnesian minerals, feldspars and iron ores. The ^{16}O enrichment of the Icelandic rhyolites strongly favours formation by anatectic melting and speaks against crystal fractionation as their genetic process. This observation was actually the initiation of the present paper, in the authors view a positive proof of crustal fractionation in the rift zone.

Muehlenbachs & Jakobsson (1979) supposed a narrow range in the $^{18}O/^{16}O$ (4.9-5.6 o/oo), observed within a fissure swarm in the Reykjanes peninsula, to reflect light oxygen anomaly in the earths mantle. The dynamic model suggests that the probability of ^{16}O enrichment increases proportional to the width of a fissure swarm or a rift segment. Fig. 18 is a plot of $^{18}O/^{16}O$ for Icelandic basalts versus the approximate width of the fissure swarms. It turns out that the narrow range of $^{18}O/^{16}O$ observed at the Reykjanes peninsula merely reflects the initiation of the processes described above.

Our conclusion is that the range of the $^{18}O/^{16}O$ ratio of basalts within the Icelandic rift system can be explained within the dynamic framework, as a consequence of equilibration of ol-tholeiitic magma with a fractionated crust. The magnitude of crustal assimilation sets limits to the mineralogical evolution of the tholeiitic magma and controls its level of dispersed elements as outlined above. Therefore covariation of $^{18}O/^{16}O$ ratios and parameters such as K_2O, Mg/Fe, normative ol, and volume, i.e. chemistry and occurrence pattern, is to be expected among the rift zone basalts.

Strontium isotopes

Hart (1969) discussed the isotope geochemistry of crust-mantle processes and emphasized the difficulties of selecting a single $^{87}Sr/^{86}Sr$ evolution model for the earth, since the basic assumptions to be made concern processes far outside our frame of observation. The large scale

buted to the nature and development of the individual magma sources, i.e. the geochemical diversity of the oceanic rocks was considered to be a mirror image of a heterogeneous mantle. Wood et al. (1979) discuss Sr-isotope data from the North Atlantic region and follow the interpretation of O´Nions et al. (1976).

Hart (1976) pointed out the existence of oceanic tholeiites with $^{87}Sr/^{86}Sr$ ratios significantly lower than .7028, greatly extending the observed range of Sr-isotope ratios of the mineralogically primitive oceanic rocks. This was further confirmed by White & Schilling (1978).

For the purpose of the subsequent discussion we underline the following observations.

(1)   Covariation of the $^{87}Rb/^{86}Sr$ and $^{87}Sr/^{86}Sr$ ratios is not observed for the oceanic basalts in general.

(2)   Primitive ol-tholeiites have a large range of $^{87}Sr/^{86}Sr$ ratios (.7023-.7030) without a simple covariation between the isotope ratios and other geochemical parameters.

(3)   Primitive to slightly evolved ol-tholeiites within fissure swarms show covariation of $^{87}Sr/^{86}Sr$ with the dispersed elements and strontium, even within a single heterogeneous lava flow.

(4)   Evolved rocks of a rift segment have a well defined upper level of the $^{87}Sr/^{86}Sr$ ratio.

(5)   Digressive volcanic centers show time (distance) dependant evolution of the $^{87}Sr/^{86}Sr$ range of its parental ridge, roughly coinciding with the degree of petrochemical evolution of the center.

From point 1 above we conclude: The general lack of covariation between $^{87}Rb/^{86}Sr$ and $^{87}Sr/^{86}Sr$ strongly suggests that closed system evolution of magmas do not take place within the rift zone and that the high productivity of ^{87}Sr within the low grade amphibolite due to high Rb/Sr ratio (Fig. 15), dominates the evolved rocks. The persistent high Rb/Sr ratio of the upper crustal magma systems indicate that Rb is retained within the rift zone crust longer than Sr, which to some extent enters the deeper crustal layers. No significant change in $^{87}Sr/^{86}Sr$ ratios occurs during the lifetime of a single volcanic center, but a continuous equilibration of silicic and basic rocks by material recycling increases the overall $^{87}Sr/^{86}Sr$ ratio of a rift segment.

From point 2 above we conclude: The lowest part of the $^{87}Sr/^{86}Sr$ range reflects the equilibration of a primitive mantle derived magma (.7023) during ascent through the upper mantle containing gradually increasing proportion of supergene Sr previously equilibrated with the rift zone crust. This group is invariably of the primitive dispersed element depleted ol-tholeiite type representing chemical and isotopic equilibrium with the upper mantle between the dehydration line of amphibole and the unknown deeper site of formation of the tholeiitic magma. The ascent path is not the source region releasing the magmatic energy although it undoubtedly belongs to the upper mantle. Therefore the oceanic mantle is definately heterogeneous with respect to Sr-isotopes but the mantle source region of the oceanic tholeiites is assumed to be homogeneous on a quantity scale necessary to produce the large primitive lava flows.

From point 3 above we conclude: The primitive ol-tholeiites when mixing with ne-basanite become enriched in Sr which is isotopically equilibrated with the crust. Mixing with the silicic magmas increases the dispersed elements subsequently. This is the part of the petrochemical evolution which gave rise to two source mixing models (see also point 4).

From point 4 above we conclude: The assumption of the dynamic model that the productivity of a rift segment determines the kinematic parameters of the rift suggests that a specific time integrated high Rb/Sr ratio is developed within each rift segment due to chemical fractionation. This Rb/Sr ratio controls the level of the $^{87}Sr/^{86}Sr$ within the rift. Assuming steady state the $^{87}Sr/^{86}Sr$ range of rocks equilibrating within the rift zone crust reflects the duration (age) of the rift segment.

From point 5 above we conclude: Since only the volcanic centers trapped in the plate are supposed to sustain volcanism or to be reactivated, the $^{87}Sr/^{86}Sr$ ratio observed for off ridge volcanism show trends diverging with time (distance) from the Sr-isotope ratios of the parental rift margin. The growth rate of ^{87}Sr here depends on the Rb/Sr ratio of the plate trapped centers. Two extreme growth schemes are evident: (a) a rapid evolution of the silica enriched low grade amphibolite and (b) slow evolution of $^{87}Sr/^{86}Sr$ ratios of the high grade amphibolite. In a regenerated digressing center a scatter between the two extremes is to be expected, while the regeneration of volcanism in

a fractionated crust is expected to show bimodal $^{87}Sr/^{86}Sr$ distribution.
A support for these assumptions is given by the isotopic disequilibrium
observed for xenoliths associated with oceanic alkaline volcanism.
Here the time interval between metamorphic mineral equilibration and
magma regeneration within the crust permits differential growth of
radiogenic Sr within minerals. This is not observed in rift zones.
Another supporting evidence for this bimodal distribution is the
$^{87}Sr/^{86}Sr$ ratios for the rocks on the STZ (Fig. 6) where only the
southernmost volcanism produces rocks with low ratios.

The Sr-isotope evolution within the dynamic framework is based on
the steady recycling of Sr and Rb within the rift zone. To illustrate
this further the $^{87}Sr/^{86}Sr$ ratio for rift zone volcanics in general
is shown in relation to their Sr-content in Fig. 19. The open circles
representing the Icelandic rift system and the Reykjanes ridge are en-
closed within a dashed line (Hart et al., 1973; O'Nions et al., 1976;
Wood et al., 1979). The $^{87}Sr/^{86}Sr$ range is between .7028-.7033 at a
range of 10-220 ppm Sr, with basalts always containing more than
50 ppm Sr.

The shaded area covering Sr values between 50 and 150 ppm and the
entire $^{87}Sr/^{86}Sr$ range of rift zone rocks represent the field of minera-
logically primitive basalts with K/Rb higher than 800. Above $^{87}Sr/^{86}Sr$
.7030 the area also contains the dispersed element enriched basalts from
volcanic centers. The filled circles in the figure representing data
from the Azores rift (White & Schilling, 1978) reach still higher levels.
Data from Hart (1976), marked by crosses in the figure, confirm that
the overall pattern of $^{87}Sr/^{86}Sr$ for the oceanic rifts is shown in the
figure. Assuming that more detailed data on rift zone volcanics would
not alter the overall pattern shown in Fig. 19, we proceed by comparing
this pattern with predicted $^{87}Sr/^{86}Sr$ ratios within the kinematic frame-
work.

The establishment of a stable oceanic rift starts with production
of a primitive mantle derived magma of Sr $\sim$ 80 ppm and $^{87}Sr/^{86}Sr$ ratio
about .7023 (a maximum value), and plate accretion by this material.
During the lifetime of the earliest volcanic centers the widest, most
productive, segments of the rift effect fractionation of the upper crust
into rock suites covering a Sr-range between 10 and 220 ppm, but a
homogeneous $^{87}Sr/^{86}Sr$ ratio. This initial state of the productive seg-
ment is outlined in the lower part of Fig. 19. The productive rift
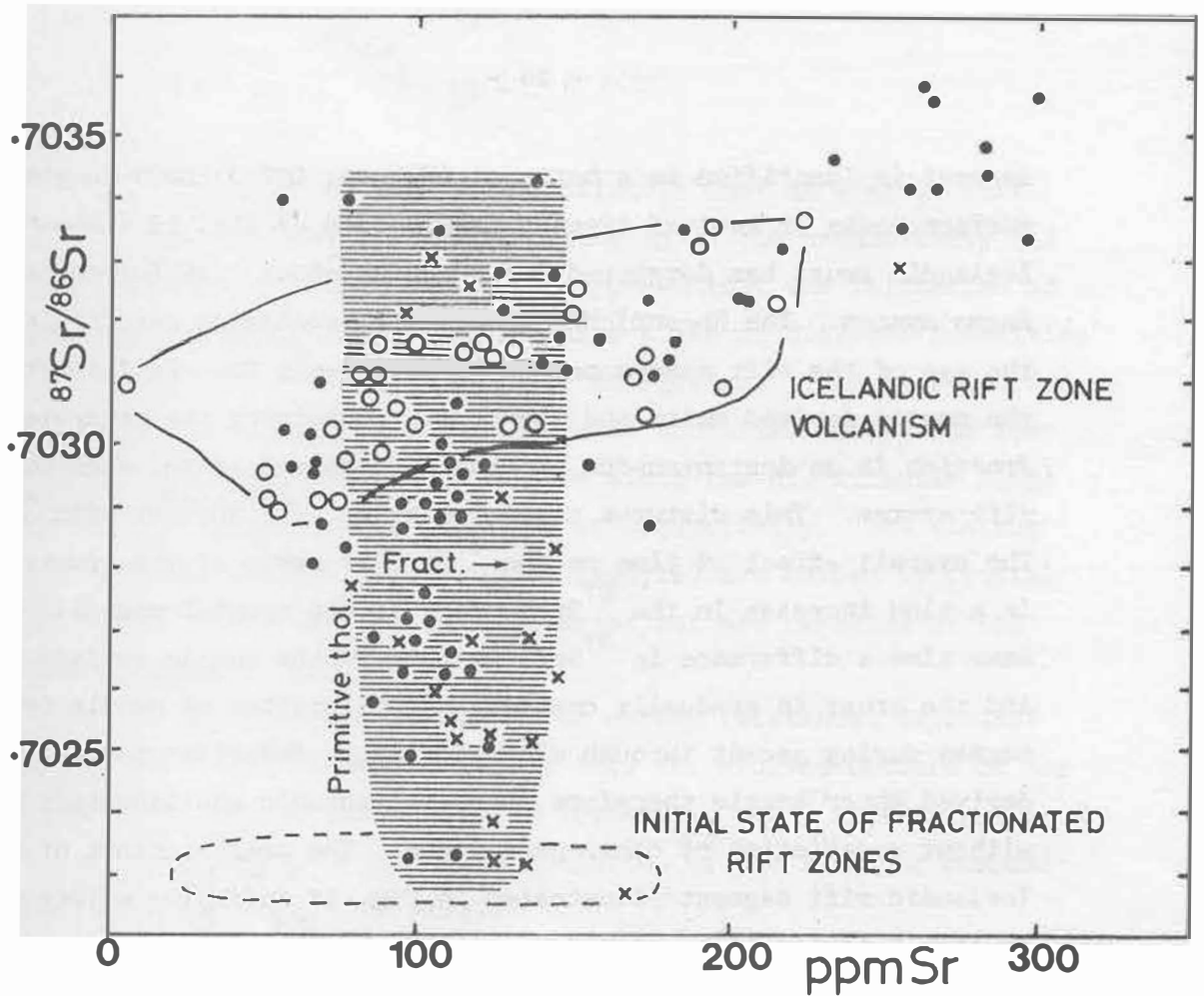
Fig. 19. The diagram $^{87}Sr/^{86}Sr$ vs Sr for oceanic rocks of the
tholeiitic series (rift zone volcanism) is based on data from
the Icelandic rift system (Hart & Schilling, 1977; O´Nions &
Grönvold, 1976; Wood et al., 1979) shown by open circles, the
Azores rift system (White & Schilling, 1978) shown by filled
circles and data from Hart (1976) crosses. The primitive mantle
derived ol-tholeiites (Sr below 100 ppm) are believed to equili-
brate with supergene Sr of the upper mantle during ascent. The
scatter in Sr for the ol-tholeiites is attributed to an early
fractionation taking place at successively higher $^{87}Sr/^{86}Sr$
levels (arrow in the figure).

segment is identified as a hot spot (Morgan, 1972) known to yield
surface rocks of evolved types. Examination of Fig. 15 shows that the
Icelandic crust has developed Rb/Sr ratios about .25 for the silicic
magma system. The Rb-enriched fraction of volcanics persists through
the age of the rift system producing radiogenic Sr. Equilibration of
the mantle derived melts and the crust, containing the separated sialic
fraction is an instantaneous process as compared to the duration of the
rift system. This disturbs the correlation of $^{87}Rb/^{86}Sr$ with $^{87}Sr/^{86}Sr$.
The overall effect of time on the $^{87}Sr/^{86}Sr$ ratio of the crustal rocks
is a slow increase in the ^{87}Sr content of the crustal magmas. By the
same time a difference in $^{87}Sr/^{86}Sr$ between the mantle derived magmas
and the crust is gradually created. Equilibration of mantle derived
magmas during ascent through mineralogically invariant partially crustal
derived upper mantle therefore involves isotopic equilibration of Sr
without covariation of other parameters. The present state of the
Icelandic rift segment illustrated in Fig. 19 indicates a long standing
crustal fractionation. A rough estimate of the past duration of a rift
segment can be made if the average Rb/Sr ratio of the crustal derived
magmas is known, and the average $^{87}Sr/^{86}Sr$ of rocks leaving the rift
zone. Sample NAL 12 (Table I) is a primitive ol-tholeiite which we
believe to represent the time averaged $^{87}Sr/^{86}Sr$ ratio of the ERZ margin.

The Rb/Sr ratio .25 as estimated from Fig. 15 gives $^{87}Rb/^{86}Sr$
of about .73. Rewriting the growth scheme of ^{87}Sr:

$$(^{87}Sr/^{86}Sr)_t = (^{87}Sr/^{86}Sr)_i + (^{87}Rb/^{86}Sr)_t \ (e^{\ t}-1), \quad \text{in the form:}$$

$$t = 1/2 \ \ln \frac{(^{87}Sr/^{86}Sr)_t - (^{87}Sr/^{86}Sr)_i}{(^{87}Rb/^{86}Sr)_t} + 1, \quad \text{and inserting the values}$$

.7022 for the mantle and .7033 (mean value for Askja vocanic center
(Wood et al., 1979)) as average for the rift margin, a rift duration
of about 110 m.y. is reached, if the ^{87}Sr growth of the mantle is neg-
lected. It is evident that if these lines of thought are valid, the
Azores hot spot (White & Schilling, 1978) is older than the Icelandic
one assuming equal or less production of the former. Another interesting
conclusion is that the activity of the Icelandic hot spot would have
started well before the establishment of the North Atlantic rift system
(about 55 m.y.) (Talwani et al., 1977).

A conclusion of the above discussion is that an oceanic rift develops marginal $^{87}Sr/^{86}Sr$ ratios depending on the productivity and duration of the rift. Further it is supposed that the initiation of magmatism and crustal fractionation takes place at discrete localities of high productivity (hot spots) prior to rifting. This is supported by the increased distance between magnetic anomalies across the Icelandic hot spot. The $^{87}Sr/^{86}Sr$ pattern along the Mid-Atlantic Ridge shows variable upper levels depending on productivity. The minimum values representing the source region (mantle) are masked by crustal contamination in the most productive areas but are revealed at the narrowest submerged rifts.

The plate trapped volcanism shows a time (distance) dependant growth of the $^{87}Sr/^{86}Sr$ ratio. Since only the evolved centers of the rift zone give rise to plate trapped volcanism, the $^{87}Sr/^{86}Sr$ ratio of the remnant centers is a continued evolution of the isotopic composition of their parental rift margin.

In Fig. 20a the $^{87}Sr/^{86}Sr$ ratios for rocks from the WDV and STZ are plotted against distance from active plate margins. The silicic rocks of the STZ (O´Nions & Grönvold, 1973) show the most rapid growth as expected from their high Rb/Sr ratios. The alkaline basalts of the WDV and STZ, scatter around a line conforming to the average Rb/Sr values of these volcanic centers. The lower value for the sample SAL 55 (Table I) is interpretated as deep seated magma generation at the south termination of the STZ in a Rb-depleted high grade amphibolite.

In Fig. 20b the growth of the $^{87}Sr/^{86}Sr$ ratio is illustrated on a larger scale. Values for the potassic alkaline islands Tristan da Cunha and Jan Mayen (O´Nions et al., 1974) show that the enormous variability of $^{87}Sr/^{86}Sr$ in the oceanic islands aside the ridges can be interpretated in terms of volcanotectonics. Jan Mayen represents deep seated crustal magma generation as stated by Imsland (1978) and Tristan represents reactivation of a volcanic center of high Rb/Sr.

Hedge (1978) interpretated the $^{87}Sr/^{86}Sr$ ratios for oceanic islands in the Pacific as magma regeneration in mantle domains enriched in Rb during Precambrian times. We point out that his data conform well to the present model. The alkaline islands of the Pacific show increasing $^{87}Sr/^{86}Sr$ values away from their parental ridges. Further the larger magma systems (Hawaii, Galapagos) show a range comparable to a productive rift margin.
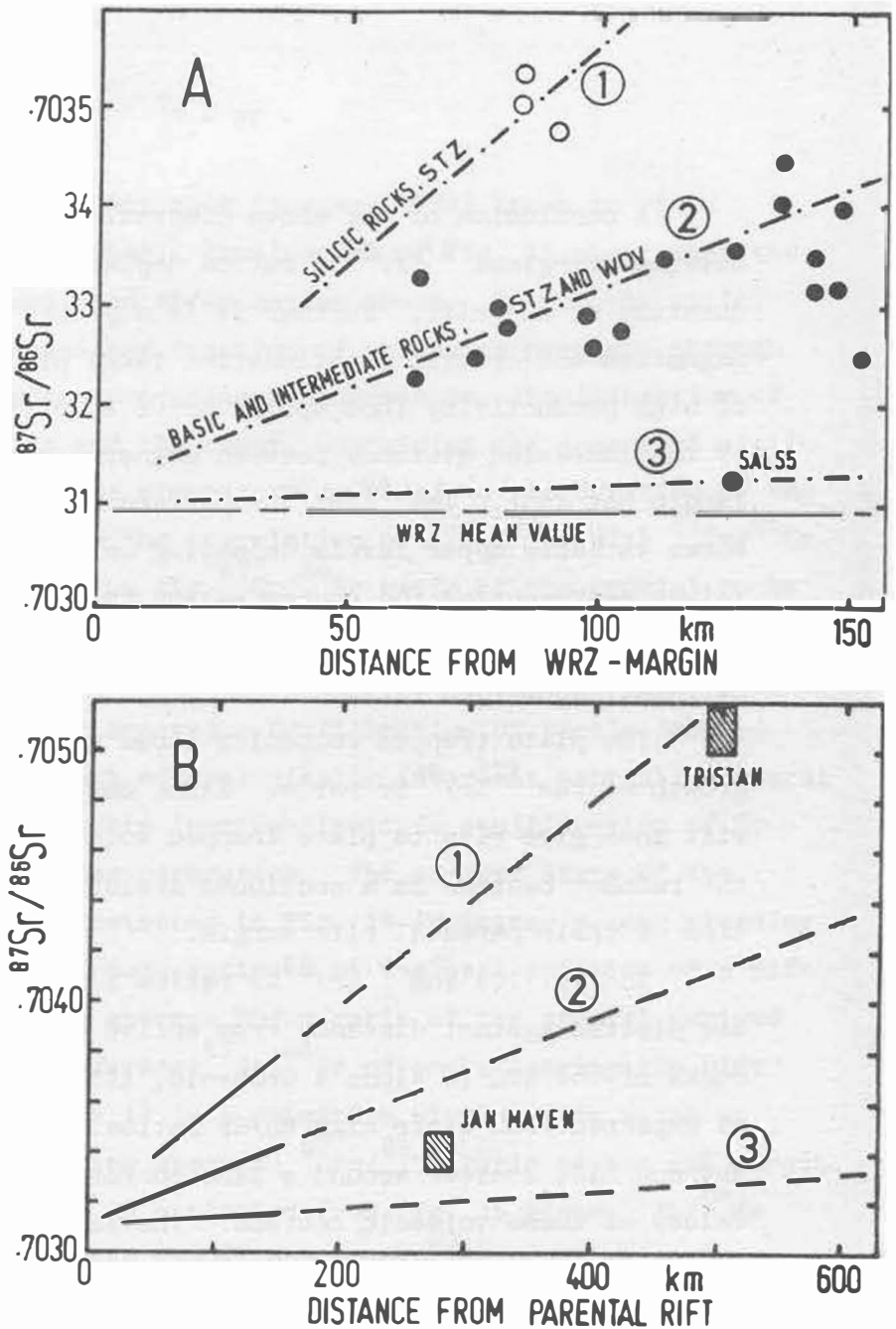
Fig. 20.

(A) $^{87}Sr/^{86}Sr$ plotted against distance form an active rift margin. The transgressive volcanism on the STZ, believed to result from regeneration of volcanic centers in a cooling plate, show bimodal $^{87}Sr/^{86}Sr$ distribution. The silicic rocks are represented by line 1 in the figure and the silica undersaturated rocks from Vestmannaeyjar by line 3. The data point for sample SAL 55 (out of cluster of others) is shown in relation to the WRZ mean value. Rocks from the digressing volcanic centers on the WDV and the basic and intermediate rocks from the northern part of the STZ are scattering around line 2 in the figure. The three lines are interpretated as time dependant evolution of volcanic centers with different average Rb/Sr ratios.

(B) The three lines in Fig. 20a are extended to longer distances than observable within the Icelandic rift system. The different evolution of the two alkaline islands is interpreted as different Rb/Sr ratios of their magma systems.

Following the $^{87}Sr/^{86}Sr$ pattern predicted within the kinematic framework to its ultimate end, the sialic fraction separated from an oceanic crust in an island arc is expected to show much larger scatter of Sr-isotope ratios than the productive ridge and further the averaged values would be expected to show higher levels of ^{87}Sr the older the plate suffering subduction.

Nd-isotopes

It was suggested earlier in this text, that REE ratios of the oceanic rocks changed systematically with the degree of mixing between silicic magma and ol-tholeiite. The significant light REE enrichment of the silicic magmas was suggested as a controlling factor in this evolution.

The alpha decay of ^{147}Sm to ^{143}Nd offers a possibility to trace long standing differences in REE enrichment of rocks by measuring their Nd-isotope ratios (Richard et al., 1976). O'Nions et al. (1977) reported $^{143}Nd/^{144}Nd$ ratios for a wide compositional range of oceanic rocks. A negative covariation between $^{143}Nd/^{144}Nd$ and $^{87}Sr/^{86}Sr$ was found for the Icelandic rift system while Hawaiian volcanics showed large scatter of $^{87}Sr/^{86}Sr$ within a narrow range in $^{143}Nd/^{144}Nd$

In the rift zone crust the highest Sm/Nd ratios are found among the REE depleted primitive ol-tholeiites. The highest $^{143}Nd/^{144}Nd$ ratios are found in samples with the lowest $^{87}Sr/^{86}Sr$ ratios (O'Nions et al., 1977). This suggests that these rocks represent the present ratios of the oceanic source region of the ol-tholeiites. Since the crustal evolution of the oceanic rocks decreases their Sm/Nd ratio by light REE enrichment, the growth of the $^{143}Nd/^{144}Nd$ ratio is retarded. The lowest $^{143}Nd/^{144}Nd$ ratios are thus to be expected in systems which were light REE enriched early in their evolution history. By the same time the $^{87}Sr/^{86}Sr$ growth rate is increased by increased Rb/Sr ratio.

The rift zone rocks thus show a range in $^{143}Nd/^{144}Nd$ from the present ratio of the mantle towards a minimum ratio in systems with the longest retention of dispersed elements. The plate trapped volcanism (Hawaii) shows an increase in $^{87}Sr/^{86}Sr$ ratio with time (distance from parental rift), while the $^{143}Nd/^{144}Nd$ ratio is only slightly modified. A general prediction of the dynamic model is therefore that the

^{143}Nd/^{144}Nd ratios for digressing or regenerated volcanics will be found to decrease away from the oceanic ridges.

Another prediction of the model is that the upper mantle receives very limited amounts of light REE from the subsiding rift zone crust in contrast to Sr. This leads to the conclusion that equilibration of crustal derived Sr with ascending mantle derived ol-tholeiite takes place earlier than mixing with crustal derived REE. A crustal residence of magma thus effects a significant change in ^{143}Nd/^{144}Nd ratios whereas the ^{87}Sr/^{86}Sr already have assumed crustal value during ascent through the mantle crust boundary. This idea is supported by data from Zindler et al. (1979), showing a marked change in the ^{143}Nd/^{144}Nd ratio in a small rock suite from the Reykjanes peninsula and the Reykjanes ridge, where the ^{87}Sr/^{86}Sr ratios remain around the WRZ mean value.

The isotope evolution of Sr and Nd within the dynamic framework is shown in Fig. 21. The growth rate of ^{87}Sr in the crust increases when crustal fractionation is initiated. The Nd isotope growth rate is at the same time reversed due to the decreasing Sm/Nd ratio.

The conclusions drawn from Fig. 21 are:

(1)   The range of Sr and Nd isotope ratios within a rift segment increase with time and a negative covariation between maximum ^{87}Sr/^{86}Sr and minimum ^{143}Nd/^{144}Nd of a rift segment is established.

(2)   The initiation of crustal fractionation of mantle derived rocks takes place long (tens of millions of years) before ocean floor spreading is established by that rift.

It is further evident that the uncertainies behind the isotope evolution represented in Fig. 21 are large. The Rb/Sr ratios are estimated from Fig. 15 and the crustal ratio for Sm/Nd is estimated from O'Nions & Grönvold (1973) (Fig. 14). The mantle source ratio for Sm/Nd is estimated at 0.8 with reference to this ratio for ultramafic phases (Richard et al., 1976) and the distribution of Sm and Nd between liquid and garnet bearing residue (Schilling, 1975). The most primitive ol-tholeiites assumed to be mantle derived reach Sm/Nd values as high as 0.44.

The mantle source value for ^{87}Sr/^{86}Sr (.7022) and the maximum value of a rift margin (.7033) are taken from Hart (1976) and Wood et
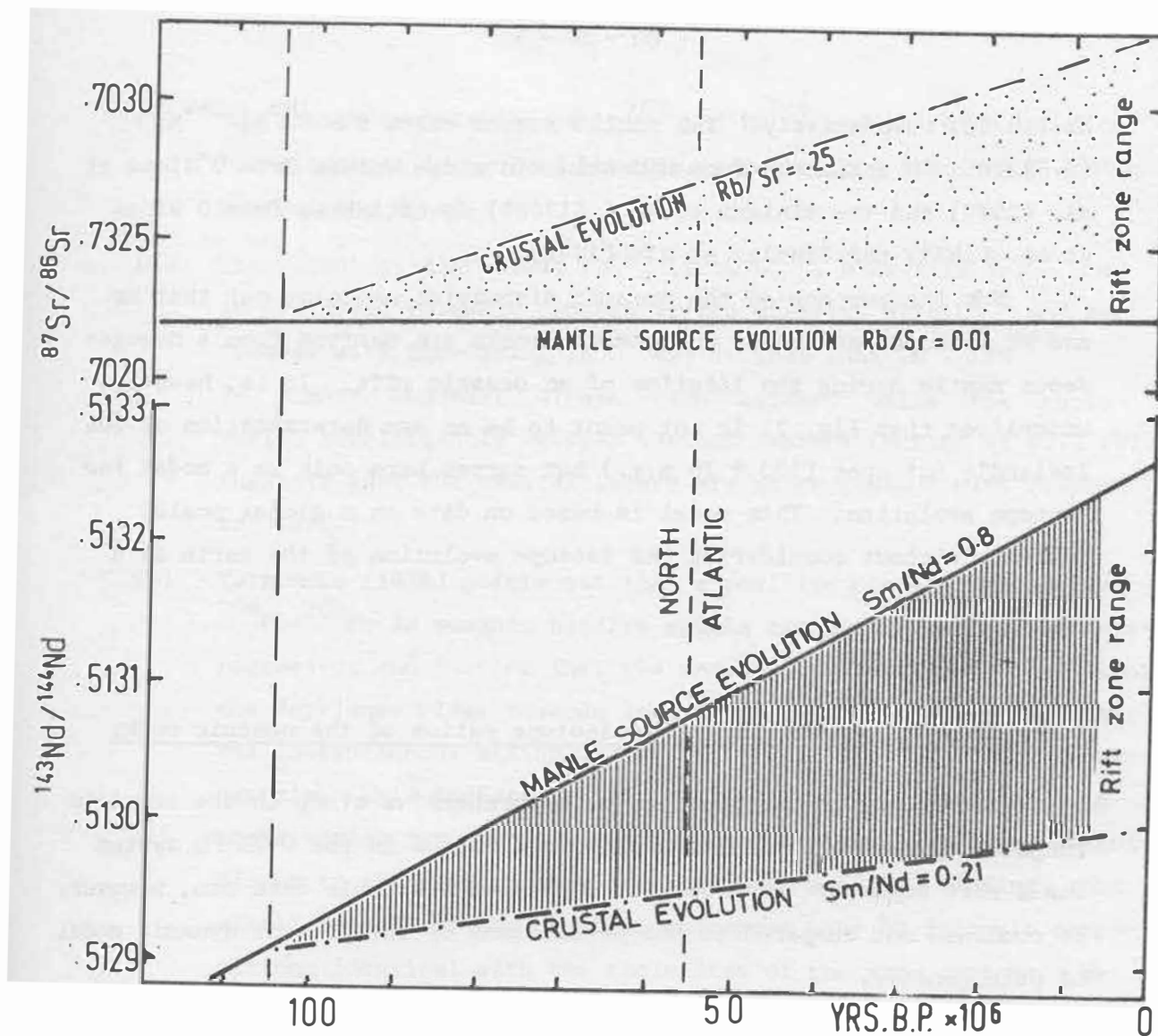
Fig. 21. The upper half of the figure shows a hypothetical evolution of Sr-isotopes within the Icelandic rift system. The ^{87}Sr/^{86}Sr range of a rift zone is thought to be within the limits of the assumed mantle source value (Rb/Sr = 0.01) and the value for the crustal magma systems (Rb/Sr = 0.25). The range increases with time. The lower part of the figure shows the hypothetical evolution of the ^{143}Nd/^{144}Nd ratio of a rift system. Here the upper line represents the mantle source evolution (Sm/Nd = 0.8), while the lower limit indicates the crustal evolution (Sm/ Nd = 0.21). The figure illustrates the possibility of explaining a negative covariation of Sr and Nd isotope ratios by assumung a steady state crustal fractionation of mother and daughter element. The duration of the crustal fractionation (volcanism) in the Icelandic hot spot is shown to have persisted about twice as long as the North Atlantic rifting.

al (1979), respectively. The mantle source value for $^{143}Nd/^{144}Nd$
(0.513295) is estimated from Mid-Atlantic ridge values from O´Nions et
al. (1977) and the minimum value (.513000) is estimated from O´Nions
et al. (1977) and Zindler et al. (1979).

For the purpose of the present discussion we point out that Sr
and Nd isotope ratios for the oceanic rocks are derived from a homoge-
neous mantle during the lifetime of an oceanic rift. It is, however,
underlined that Fig. 21 is not meant to be an age determination of the
Icelandic hot spot (100 ± 10 m.y.) but serves here only as a model for
isotope evolution. This model is based on data on a global scale,
however, without considering the isotope evolution of the earth as a
whole.

Notes on U-Th systematics and Pb isotope ratios of the oceanic rocks

Unfortunately there exists no comprehensive study on the complete
range of element abundancies and isotope ratios in the U-Th-Pb system
for a rift segment. The somewhat scattered available data can, however,
be combined and compared to the predictions of the present dynamic model
of petrogenesis.

(1)   The concept of crustal fractionation that the formation and sepa-
      ration of crustal derived magmas effects chemical separations on
      a regional scale, indicates that Th is to some extent retained in
      the silica depleted amphibolite of the lower crust. The minerals
      apatite and clinopyroxene are the Th-hosts of the high grade
      amphibolite (Seitz, 1973) and the high Th/U ratios of amphiboles
      (Murthy & Stueber, 1967) might even indicate that Th is retained by
      hornblende and kearsutite. The silicic magmas separated by vol-
      canism will therefore contain U and Pb in excess of Th. The Th/U
      ratios of oceanic rocks (Unruh & Tatsumoto, 1976; Tatsumoto,
      1978; Wood et al., 1979) are significantly higher in the alka-
      line basalts than in tholeiites and silicic rocks.

(2)   The significantly high Pb^{208}/Pb^{204} ratio for the alkaline basalts
      and to a lesser extent evolved tholeiites as compared to the ol-
      tholeiites (Sun et al., 1975; Sun & Jahn, 1975; Unruh & Tatsumoto,
      1976; Tatsumoto, 1978) suggests that the Pb^{208} (from Th^{232}) is
      produced in long standing Th enrichment of the lower crust.

(3)   The smooth covariation of Pb^{207} and Pb^{206} and the high level of
both isotopes in evolved basalts indicate long standing U enrich-
ment of the crust.

(4)   The recent evidence that Th^{230} (from U^{238}, half life $8 \cdot 10^4$ yrs)
in Icelandic volcanic centers varies directly with U^{238} and de-
creases with increasing Th^{232} and further that Th^{230}/Th^{232}
is almost constant within each center, while the ratio
varies significantly between various centers (Morand et al., 1979),
suggests that the crustal layers are heterogeneous with respect
to Th/U.

(5)   Tatsumoto (1978) points out that a positive correlation between
$^{208}Pb/^{204}Pb$ in oceanic basalts speaks against random mantle hete-
rogeneity, and further that the increase in radiogenic lead along
the Reykjanes ridge towards Iceland is unlikely to result from
the instantaneous mixing of the two mantle sources during basalt
genesis. This indicates that the Th/U ratio of the tholeiitic
rocks varies systematically with petrochemical evolution. Signi-
ficant to the present model is Tatsumoto´s (1978) finding, that
alkali basalts of the Hawaiian volcanoes have Pb isotopic compo-
sitions identical with the tholeiites of the same centers. We
point out that this is consistent with the hypothesis that the
alkaline suites are formed by partial melting of silica depleted
amphibolite of a subsiding volcano where material recycling is a
relatively short term event. Another point of interest is the
Pb isotope variation between the extinct volcanic centers of
Hawaii, not showing covariation with absolute age. In the dynamic
model this indicates the different degree of material fractiona-
tion within the centers where different Th/U ratios of the rock
suites control the Pb systematics rather than the age of last
equilibration.

SUMMARY

The present paper is an introduction to a model for the genesis
of the oceanic rocks, and the petrological consequences of that model
assuming a single mantle derived magma type (ol-tholeiite) as the ulti-

mate source of the oceanic rocks. The geology of the Icelandic rift
system is discussed and interpretated within the frame of the new model.
Important points in the discussion are:

(1)   The oceanic rift zone is fed from a single mantle source. The
       intruded and extruded material is brought outwards by ocean floor
       spreading and downwards by isostatic subsidence. The material of
       the crust is thereby transported through varying PT conditions
       before reaching a stable state in the accreting plate margin.

(2)   The equilibration of rocks near the rift zone surface results in
       hydration. The hydrated rocks assume metamorphic zonation from
       zeolite to amphibolite facies during subsidence. Upon crossing
       the locus of anatectic melting in the granite system the rift zone
       crust suffers a chemical fractionation by segregation and separa-
       tion of silicic magmas. A complete dehydration of the subsiding
       material results in fractionation by segregation of alkali olivine
       basalt liquid forming in the nepheline basanite system by incon-
       grous breakdown of amphibole. Below the dehydrating PT conditions
       the material assumes granulite facies of the upper mantle. The
       layering of the oceanic crust is therefore brought about by sepa-
       ration of two magma types from the subsiding crust. The crustal
       derived magmas become a part of the plate above their site of for-
       mation or equilibrate with the ascending ol-tholeiite in a counter-
       current fashion. Below the crust the mantle consists of material
       from below and a fraction of supergene material, which equilibra-
       ted isotopically with the rift zone crust. The amount of supergene
       material depends on productivity of the rift.

(3)   The olivine tholeiitic magma produced within the oceanic mantle is
       the ultimate source of all oceanic magmas. Three evolution possi-
       bilities and combination of these are discussed.

       (a) Solidification of the primitive magma in the ol-tholeiite
           system.
       (b) Mixing of ol-tholeiite with the crustal derived basalt and
           evolution within the ol-tholeiite system.
       (c) Mixing of ol-tholeiite and the silicic component of the
           upper crust giving way to petrogenesis within the tholeiitic
           system.

(4)   The processes 3b and 3c take place in crustal magma domains. These
       volcanic centers, when trapped in the accreting oceanic plate,
       occasionally continue their activity after their supply of ol-tho-
       leiite is terminated. In these centers the crustal derived magmas,
       formed upon subsidence, dominate the production (digressive vol-
       canism or off rift volcanism). A comparable petrogenesis results
       from reactivation of volcanic centers of a cooling plate, when ex-
       posed to the thermal gradient from a rift zone termination (trans-
       gressive volcanism).

(5)   The mineralogical evolution and major element chemistry of the
       oceanic rocks is described in terms of quaternary invariant points
       in the basalt system and assimilation of crustal derived magmas
       into ol-tholeiite.

       (a) The mantle derived basalts are crystallizing in the ol-tholeiite
           system (ol-plag-cpx-opx). Mixing with a subordinate amount of

crustal derived basalt formed at the ne-basanite invariant (ol-plag-cpx-ne) do not alter the mineralogical evolution, but leaves imprints of alkaline chemistry, - most prominent towards the end of crystallization.

(b) Mixing of ol-tholeiite with silicic crustal derived magmas extends its crystallization path beyond the ol-tholeiite invariant. Silica in excess of available forsterite at the appearance of cpx drives the crystallization towards the tholeiite invariant (plag, cpx, opx, tr).

(6) The chemical pattern of the oceanic tholeiites reflects

(a) the mineralogical control of major elements and trace elements incorporated into the major precipitating phases and

(b) the assimilation of dispersed element enriched crustal derived magmas into the mantle derived ol-tholeiites.

The combination of a and b gives a broad continuous nonlinear covariation of dispersed element pairs of the tholeiites. Each petrogenetic unit (volcanic center) shows, however, a linear covariation (point a). The different dispersed element ratios of the volcanic centers are assigned to different level of crustal contamination (point b).

(7) The isotope geochemistry of the oceanic rocks is interpretated as the result of mixing of mantle derived magma and crustal derived magmas. Three cases are discussed:

(a) Light oxygen enrichment of tholeiites during their evolution results from assimilation of silicic magmas, which are extensively equilibrated with meteoritic water.

(b) The ^{87}Sr enrichment of tholeiites during their evolution results from mixing with crustal derived material, which is enriched in ^{87}Sr due to long standing high Rb/Sr ratio rift zone crust. Similarily the ^{143}Nd depletion of the tholeiites during their evolution results from mixing with crustal material suffering long standing depletion in Sm relative to Nd. The radioisotope geochemistry of the oceanic rocks in general is controlled by long standing steady state of dispersed element enrichment and separation of mother and daughter elements in the rift zone crust.

(c) The Th/U systematics are compared to the scattered data available. The geochemistry of Th in crustal fractionation processes suggests that Pb^{208} is accumulating in alkaline magmas.

REFERENCES

Anderson, O., 1915. The system anorthite-forsterite-silica. Am. J. Sci. 39, 407-454.

Annels, R.N., 1968. A geological investigation of a tertiary intrusive center in the Víðidalur Vatnsdalur area, Northern Iceland. P.HD. dissertation of St. Andrews.

Bailey, J.D., 1977. Fluorine in granitic rocks and melts: A Review. Chemical Geology 19, 1-42.

Bayer, G., 1969. Thorium. In: Handbook of Geochemistry, (ed. K.H. Wede-pohl), Springer Verlag, Berlin.

Basu, A.R. & Murthy, R.V., 1977. Kaersutites, suboceanic low velocity zone, and the origin of mid oceanic ridge basalts. Geology 5, 365-368.

Beswick, A.E., 1976. K and Rb relations in basalts and other mantle de-rived materials. Is phlogopite the key? Geochim, Cosmochim. Acta 40, 1167-1183.

Beswick, A.E. & Carmichael, I.S.E., 1978. Constraints on mantle source compositions imposed by phosphorus and the rare earth elements. Contr. Miner. Petrol. 67, 317-330.

Björnsson A. et al., 1977. Current rifting episode in North Iceland. Nature 266, 318-323.

Burnham, C.W., 1967. Hydrothermal fluids in the magmatic stage. In: Geochemistry of Hydrothermal Ore Deposits Melt, (ed. H.L. Barnes), New York.

Carmichael, I.S.E., 1967. The mineralogy of Thingmuli, a tertiary vol-cano in Eastern Iceland. Am. Min. 52, 1815-1841.

Carmichael, I.S.E. & McDonald, A., 1961. The geochemistry of some natural acid glasses from the North Atlantic Tertiary volcanic province. Geochim. Cosmochim. Acta 25, 189-222.

Carmichael, I.S.E. et al., 1974. Igneous Petrology. McGraw Hill, New York.

Dungan, M.A. & Rhodes, J.M., 1978. Residual glasses and melt inclusions in basalts from DSDP Legs 45 and 46: Evidence from magma mixing. Contr. Miner. Petrol. 67, 417-431.

Drake, J.M., 1972. The distribution of major and trace elements between plagioclase feldspars and a magmatic silicate liquid: An experi-mental study. Ph.D. Thesis at the Dept. of Geology at the Univer-sity of Oregon, U.S.A.

Engel, A.E.J. & Engel, C.G., 1964. Composition of basalts from the
      Mid-Atlantic Ridge. Science 144, 1330-1333.

Engel, A.E.J. et al., 1965. Chemical characteristics of oceanic basalts
      and upper mantle. Bull. Geol. Soc. Am. 76, 719-734.

Fisk, R.M., 1978. Melting relations and mineral chemistry of Iceland
      and Reykjanes Ridge basalts. Ph.D. thesis at the University of
      Rhode Island.

Gass, G. & Smewing J.D.m 1973. Intrusion, extrusion and metamorphism
      at constructive margins: evidence from the Troodos massif, Cyprus.
      Nature 242, 26-29.

Gast, P.W., 1960. Limitations on the composition of the upper mantle.
      J. Geophys. Res. 65, 1287-1297.

Gast, P.W., 1965. Terrestrial ratio of potassium to rubidium and the
      composition of the Earth´s mantle. Science 147, 858-860.

Gast, P.W., 1968. Trace element fractionation and the origin of tholeiitic
      and alkaline magma types. Geochim. Cosmochim. Acta 32, 1057-1086.

Gray, J. et al., 1977. Oxygen and strontium isotopic compositions and
      thorium and uranium contents of basalts from DSDP 39 cores. In:
      Initial Reports of the Deep Sea Drilling Project, (eds. F. Aumento,
      W.G. Melson et al.), Vol. 37, U.S. Government Printing Office,
      Washington.

Green, D.H. & Ringwood, A.E., 1967. The genesis of basaltic magmas.
      Contr. Miner. Petrol. 15, 103-190.

Gunnlaugsson, E., 1976. Chemistry of the postglacial lavas in the Krísu-
      vík area S.W.-Iceland. Soc. Sci. Islandica, Greinar V, 160-166.

Grönvold, K., 1972. Structural and petrochemical studies in the Kerlingar-
      fjöll region, Central Iceland. Ph.D. thesis, Oxford University.

Grönvold, K. & Mäkipää, H., 1978. Chemical composition of Krafla lavas
      1975-1977. Nord. Volc. Inst. Research Report 7816.

Hart, S.R., 1969. Isotope geochemistry of crust mantle processes. In:
      The earths crust and upper mantle, Geophys. Monograph 13, (ed.
      P.J. Hart), Am. Geophys. Union.

Hart, S.R., 1976. LIL-element geochemistry, Leg 34 basalt. In: Initial
      Reports of the Deep Sea Drilling Project, (eds. R.S. Yeats & S.R.
      Hart et al.), Vol. 34, U.S. Government Printing Office, Washington.

Hart, S.R. & Aldrich, L.T., 1967. Fractionation of K/Rb by amphiboles:
      Implications regarding mantle composition. Science 155, 325-327.

Hart, S.R. et al., 1973. Basalts from Iceland and along the Reykjanes
      Ridge: Sr isotope geochemistry. Nature 246, 104-107.

Hart, S.R. & Brooks, C., 1974. Clinopyroxene-matrix partitioning of K,
      Rb, Cs, Sr and Ba. Geochim. Cosmochim. Acta 38, 1799-1806.

Hedge, C.E., 1978. Strontium isotopes in basalts from the Pacific Ocean
      Basin. Earth Planet. Sci. Lett. 38, 88-94.

Hedge, C.E. & Peterman, Z.E., 1970. The strontium isotopic composition
      of basalts from the Gordo and Juan de Fuca Rises, Northeastern
      Pacific Ocean. Contr. Miner. Petrol. 27, 114-120.

Helz, R.T., 1973. Phase relations of basalts in their melting range at
      P_{H_2O} = 5 kb as a function of oxygen fugacity. Part I: Mafic phases.
      J. Petrol. 14, 299-302.

Helz, R.T., 1976. Phase relations of basalts in their melting ranges at
      P_{H_2O} = 5 kb. Part II: Melt compositions. J. Petrol. 17, 139-193.

Hermance, J.F. & Grillot, L.R., 1974. Constrains on temperatures beneath
      Iceland from magnetotelluric data. Phys. Earth Planet. Inter. 8,
      1-12.

Hoernes, S. & Friedrichsen, H., 1977. Oxygen isotope investigation of
      rocks of Leg 37. In: Initial Reports of the Deep Sea Drilling
      Project, (eds. F. Aumento, W.G. Melson et al.), Vol. 37, U.S.
      Government Printing Office, Washington, 603-605.

Holloway, J.R. & Burnham, C.W., 1972. Melting relations of basalts with
      equilibrium water pressure less than total pressure. J. Petrol. 13,
      1-29.

Imsland, P., 1978. The petrology of Iceland. Some general remarks.
      Nord. Volc. Inst. Research Report 7809.

Imsland, P., 1978. The geology of Jan Mayen volcanic island, Arctic
      Ocean. Nord. Volc. Inst. Research Report 7813.

Jakobsson, S.P. et al., 1973. Petrology of mugearite-hawaiite: Early
      extrusives in the 1973 Heimaey eruption, Iceland. Lithos 6, 203-214.

Jakobsson, S.P. et al., 1978. Petrology of the Western Reykjanes Peninsula,
      Iceland. J. Petrol. 19, 669-705.

Jóhannesson, H., 1975. Structure and petrology of the Reykjadalur central
      volcano and the surrounding areas, Midwest Iceland. Ph.D. thesis,
      University of Durham.

Kay, R.W. et al., 1970. Chemical characteristics and origin of oceanic
      ridge volcanic rocks. J. Geophys. Res. 75, 1585.

Kesson, S. & Price, R.C., 1972. The major and trace element chemistry of kaersutite and its bearing on the petrogenesis of alkaline rocks. Contr. Miner. Petrol. 35, 119-124.

Kushiro, I. & Thompson, R.N., 1972. Origin of some abyssal tholeiites from the Mid-Atlantic Ridge. Carnegie Inst. Wash. Yearbook 71, 403-406.

Larsen, G., 1979. The Vatnaöldur eruption. Nord. Volc. Inst.

Luth, W.C., 1976. Granitic rocks. In: The evolution of the crystalline rocks, (eds. D.K. Bailey & R. McDonald), Academic Press, New York, 335-412.

MacDonald, G.A., 1968. Composition and origin of Hawaiian lavas. Geol. Soc. Am. Mem. 116, 477-522.

Mäkipää, H., 1978. Petrological relations in some Icelandic basaltic hyaloclastites. Bull. geol. Soc. Finland 50, 81-112.

Mäkipää, H., 1978: Mineral equilibria, geothermometers and geobarometers in some Icelandic hyaloclastites. Bull. geol. Soc. Finland 50, 113-134.

Mason, B. & Allen, R.O., 1973. Minor and trace elements in augite, hornblende and pyrope megacrysts from Kakanui, New Zealand. N.Z. Journ. Geology and Geophysics 16, 935-947.

McBirney, A.R. & Gass, I.G., 1967. Relations of oceanic volcanic rocks to mid-oceanic rises and heat flor. Earth Planet. Sci. Lett. 2, 265-276.

McBirney, A.R. & Williams, H., 1969. Geology and petrology of the Galapagos Islands. Geol. Soc. Am. Memoir 118.

Menzies, M., 1978. Comment on "Is phlogopite the key?" by A.E. Beswick. Geochim. Cosmochim. Acta 42, 146-150.

Mevel, C. et al., 1978. Amphibolite facies conditions in the oceanic crust: Example of amphibolitized flaser gabbro and amphibolites from the Chenaillet ophiolite massif (Hautes Alpes, France). Earth Planet. Sci. Lett. 39, 98-108.

Moores, E.M. & Vine, F.J., 1971. Troodos Massif, Cyprus and other ophiolites as oceanic crust: Evaluation and implications. Roy. Soc. London Philos. Trans. A 268, 443-466.

Morand, P., Condomines, M. & Allegre, C.J., 1979. Desequilibri Th^{230}-U^{238} dans les laves historiques de l´Islande. Implications sur la nature du mantean sous-jacent. Laboratorie de Geoch. Cosmoch. Univ. de Paris VI et VII (mimeographed).

Morgan, W.J., 1972. Deep mantle convection plumes and plate motions.
    Bull. Am. Assn. Petrol. Geol. 56, 203-213

Muehlenbachs, K., 1973. The oxygen isotope geochemistry of siliceous
    volcanic rocks from Iceland. Geophys. Lab. Yearbook 72, 593-597.

Muehlenbachs, K. et al., 1974. Low O^{18} basalts from Iceland. Geochim.
    Cosmochim. Acta 38, 577-588.

Muehlenbachs, K. & Jakobsson, S.P., 1979. The ^{18}O anomaly in Icelandic
    basalts related to their field occurrence and composition (abstract).
    Am. Geophys. Union 1979, Spring Meeting.

Murthy, R.V. & Stueber, A.M., 1967. Potassium-rubidium in mantle derived
    rocks. In: Ultramafic and related rocks, (ed. P.J. Wyllie),
    John Wiley & Sons Inc., New York, 376-380.

O´Hara, M.J., 1977. Geochemical evolution during fractional crystalliza-
    tion of a periodically refilled magma chamber. Nature 266, 503-507.

Olafsson, M., 1977. Dikes in Berufjördur, Eastern Iceland. Field rela-
    tions and petrochemistry. (In Icelandic). B.Sc. Hon. thesis at
    the University of Iceland.

O´Nions, R.K. & Grönvold, K., 1973. Petrogenetic relationship of acid
    and basic rocks in Iceland and rare earth elements in late post-
    glacial volcanics. Earth Planet. Sci. Lett. 19, 397-409.

O´Nions, R.K. et al., 1973. Strontium isotopes and rare-earth elements
    in basalts from the Heimaey and Surtsey volcanic eruptions. Nature
    243, 213-214.

O´Nions, R.K. & Pankhurst, R.M., 1974. Petrogenetic significance of
    isotope and trace element variations in volcanic rocks from the
    Mid Atlantic. J. Petrol. 15, 603-634.

O´Nions, R.K. et al., 1976. Nature and development of basalt magma
    sources beneath Iceland and the Reykjanes Ridge. J. Petrol. 17,
    315-338.

O´Nions, R.K. et al., 1977. Variations in $^{143}Nd/^{144}Nd$ and $^{87}Sr/^{86}Sr$
    ratios in oceanic basalts. Earth Planet. Sci. Lett. 34, 13-22.

Osborn, E.F. & Tait, D.B., 1952. The system diopside-forsterite-anorthite.
    Am. J. Sci. Bowen Vol., 413-433.

Oxburgh, E.R., 1964. Petrological evidence for the presence of amphibole
    in the upper mantle and its petrogenetic and geophysical implica-
    tions. Geol. Mag. 101, 1-19.

Oxburgh, E.R. & Turcotte, D.L., 1968. Mid-ocean ridges and geotherm
    distribution during mantle connection. J. Geophys. Res. 73,
    2643-2661.

Pálmason, G., 1971. Crustal structure of Iceland from explosion seis-
    mology. Soc. Sci. Islandica XL, 9-187.

Pálmason, G., 1973. Kinematics and heat flow in a volcanic rift zone,
    with application to Iceland. Geophys. J. R. astr. Soc. 33, 451-481.

Pálmason, G. et al., 1979. The Iceland crust: Evidence form drillhole
    data on structure and processes. In: Ocean crust: Maurice Ewing
    Series 2, Deep drilling results in the Atlantic Ocean, (eds. M. Tal-
    wani, C.G. Harrison & D. Hayes), A.G.U.

Peterman, Z.E. & Hedge, C.E., 1971. Related strontium isotopic and
    chemical variations in oceanic basalts. Bull. Geol. Soc. Am. 82,
    493-499.

Philpotts, J.A. & Schnetzler, C.C., 1970. Phenocryst-matrix partition
    coefficients for K, Rb, Sr and Ba with applications to anorthosite
    and basalt genesis. Geochim. Cosmochim. Acta 34, 307-322.

Powers, H.A., 1955. Composition and origin of basaltic magma of the
    Hawaiian Islands. Geochim. Cosmochim. Acta 7, 77-107.

Presnall, D.C., 1966. The join forsterite-diopside-iron oxide and its
    bearing on the crystallization of basaltic and ultramafic magmas.
    Am. J. Sci. 264, 753-809.

Presnall, D.C. et al., 1978. Liquidus phase relations on the join
    diopside-forsterite-anorthite from 1 atm to 20 kbar: Their bearing
    on the generation and crystallization of basaltic magma. Contr.
    Miner. Petrol. 66, 203-220.

Prestvik, T., 1979. Geology of the Öræfi district, Southeast Iceland.
    Nord. Volc. Inst. Research Report 7901.

Richard P. et al., 1976. $^{143}Nd/^{146}Nd$, a natural tracer: An application
    to oceanic basalts. Earth Planet Sci. Lett. 31, 269-278.

Russel, R.D. & Ozima, M., 1971. The potassium/rubidium ratio of the
    earth. Geochim. Cosmochim. Acta 35, 679-685.

Saemundsson, K., 1967. Vulkanismus und Tektonik des Hengill Gebietes in
    Südwest-Island. Acta Nat. Isl. II, 1-105.

Saemundsson, K., 1978. Fissure swarms and central volcanoes of the
    neovolcanic zones of Iceland. Geol. Journal, Spec. Issue 10,
    415-432.

Schairer, J.F. & Yoder, H.S., 1964. Crystal and liquid trends in simpli-
    fied alkali basalts. Carnegie Inst. Wash. Yearbook 63, 65-73.

Schairer, J.F. et al., 1968. The join nepheline-diopside-anorthite and
    its relation to alkali basalt fractionation. Carnegie Inst. Wash.
    Yearbook 66, 467-471.

Schilling, J.-G., 1973. Iceland mantle plume: Geochemical study of
     Reykjanes Ridge. Nature 242, 565-571.

Schilling, J.-G., 1975. Rare-earth variations across "normal segments"
     of the Reykjanes Ridge, 60°-53°N, Mid Atlantic Ridge, 29°S, and
     East Pacific Rise, 2°-19°S, and evidence on the composition of the
     underlying low-velocity layer. J. Geophys. Res. 80, 1459-1473.

Schilling, J.-G., 1975. Azores mantle blob: Rare earth evidence. Earth
     Planet. Scil Lett. 25, 103-115.

Schilling, J.-G. et al., 1978. Skagi and western neovolcanic zones in
     Iceland: 2. Geochemical variations. J. Geophys. Res. 83. 3983-4002.

Seitz, M.G., 1973. Uranium and thorium diffusion in diopside and fluor-
     apatite. Carnegie Inst. Wash. Yearbook 72, 586-588.

Seitz, M.G., 1973. Uranium and thorium partitioning in diopside-melt
     and whitlockite-melt systems. Carnegie Inst. Wash. Yearbook 72,
     581-586.

Shibata, T., Thompson, T. & Frey, F.A., 1979. Tholeiitic and alkali
     basalts from the Mid-Atlantic Ridge at 43°N. Contr. Miner. Petrol.
     70, 127-141.

Sigurdsson, H., 1968. Petrology of acid xenoliths from Surtsey. Geol.
     Mag. 105, 440-453.

Sigurdsson, H., 1970. The petrology and chemistry of the Setberg vol-
     canic region and the intermediate and acid rocks of Iceland.
     Ph.D. thesis, University of Durham.

Sigurdsson, H., 1976. Spinels in Mid-Atlantic Ridge basalts: Chemistry
     and occurrence. Earth Planet. Sci. Lett. 29, 7-20.

Sigurdsson, H. et al., 1978. Skagi and Langjökull volcanic zones in
     Iceland: 1. Petrology and structure. J. Geophys. Res. 83,
     3971-3982.

Sigvaldason, G.E., 1974a. Basalts from the centre of the assumed Icelandic
     mantle plume. J. Petrol. 15, 497-523.

Sigvaldason, G.E., 1974b. The petrology of Hekla and origin of silicic
     rocks in Iceland. Soc. Sci. Islandica V, 1-44.

Sigvaldason, G.E., 1979. Rifting, magmatic activity and interaction
     between acid and basic liquids. The 1975 Askja eruption in Iceland.
     Nord. Volc. Inst. Research Report 7903.

Sigvaldason, G.E. et al., 1974. Compositional variation in recent Ice-
     landic tholeiites and the Kverkfjöll hot spot. Nature 251, 579-582.

Sigvaldason, G.E. et al., 1974. The simultaneous production of basalts enriched and depleted in large lithophile trace ions (LIL) within the same fissure swarms in Iceland. Bull. Soc. Géol. France XVIII, 863-867.

Sigvaldason, G.E. & Óskarsson, N., 1976. Chlorine in basalts from Iceland. Geochim. Cosmochim. Acta 40, 777-789.

Steinthorsson, S., 1964. The ankaramites of Hvammsmúli, Eyjafjöll, South Iceland. Acta Nat. Isl. II, 1-32.

Steinthorsson, S., 1965. Petrology and Chemistry. Surtsey Research Progress Report I, 77-86.

Steinthorsson, S., 1978. Tephra layers in drill core from the Vatnajökull ice cap. Jökull 27, 2-27.

Stormer, J.C. & Carmichael, I.S.E., 1971. Fluorine-hydroxyl exchange in apatite and biotite: A potential igneous geothermometer. Contr. Miner. Petrol. 31, 121-131.

Sun, S.S. et al., 1975. Mantle plume mixing along Reykjanes ridge axis: Lead isotope evidence. Science 190, 143-147.

Sun, S.S. & Jahn, B., 1975. Lead and strontium isotopes in post-glacial basalts from Iceland. Nature 255, 527-530.

Talwani, M. & Edholm, O., 1977. Evolution of the Norwegian-Greenland Sea. Bull. Geol. Soc. Am. 88, 969-999.

Tatsumoto, M., 1978. Isotopic composition of lead in oceanic basalts and its implication to mantle evolution. Earth Planet. Sci. Lett. 38, 63-87.

Tatsumoto, M. et al., 1965. Potassium, rubidium, strontium, thorium, uranium, and the ratio strontium-87 to strontium-86 in oceanic tholeiitic basalts. Science 153, 1094-1101.

Taylor, H.P., 1968. The oxygen isotope geochemistry of igneous rocks. Contr. Miner. Petrol. 19, 1-71.

Thorarinsson, S., 1969. The Lakagígar eruption of 1783. Bull. Volc. 33, 910-929.

Thorarinsson, S. et al., 1973. The eruption on Heimaey, Iceland. Nature 241, 372-375.

Tryggvason, E., 1973. Seismicity, earthquake swarms and plate boundaries in the Iceland region. Bull. Seism. Soc. Am. 63, 1327-1348.

Tryggvason, T., 1943. Das Skjaldbreid-Gebiet auf Island. Bull. Geol. Inst. Uppsala 30, 273-320.

Unruh, D.M. & Tatsumoto, M., 1976. Lead isotopic composition and uranium, thorium, and lead concentrations in sediments and basalts from the Nazca plate. In: Initial Reports of the Deep Sea Drilling Project, (eds. R.S. Yeats, S.R. Harts et al.), Vol. 34, U.S. Government Printing Office, Washington, 341-347.

White, W.M. & Schilling, J.-G., 1978. The nature and origin of geo-
    chemical variation in Mid Atlantic Ridge basalts from the Central
    North Atlantic. Geochim. Cosmochim. Acta 42, 1501-1516.

Wood, D.A., 1978. Major and trace element variations in the tertiary
    lavas of Eastern Iceland and their significance with respect to
    the Iceland geochemical anomaly. J. Petrol. 19, 394-436.

Wood, D.A., 1979. Dynamic partial melting: Its application to the
    petrogenesis of basalts erupted in Iceland, the Faeroe Islands,
    the Isle of Skye (Scotland) and the Troodos Massif (Cyprus).
    Geochim. Cosmochim. Acta 43, 1031-1046.

Wood, D.A. et al., 1979. Elemental and Sr isotope variations in basic
    lavas from Iceland and the surrounding ocean floor. Contr. Miner.
    Petrol. 70, 319-339.

Yoder, H.S., Jr. 1965. Diopside-anorthite-water at five and ten kilobars
    and its bearing on explosive volcanism. Carnegie Inst. Wash. Year-
    book 64, 82-89.

Yoder, H.S., Jr. 1976. Generation of basaltic magma. National Academy of
    Science, Washington D.C.

Yoder, H.S., Jr. & Tilley, C.E., 1962. Origin of basaltic magmas: An
    experimental study of natural and synthetic rock systems. J. Petrol.
    3, 392-532.

Zindler, A. et al., 1979. Nd and Sr isotope ratios and rare earth element
    abundances in Reykjanes peninsula basalts: Evidence for mantle
    heterogeneity beneath Iceland. Earth Planet. Sci. Lett. 45, 249-262.

TEXT TO TABLE I

Petrochemical range of Icelandic rocks

Samples 1-11 are tholeiitic basalts from the rift zones and rift margins. Samples 1-3 are primitive ol-tholeiites. Samples 4-8 are ol-tholeiites covering the compositional range of parental magmas of volcanic centers of the rift zones. Samples 9-11 are evolved tholeiites resembling the range of basalt compositions found within volcanic centers. Samples 12-15 are the subalkaline silicic and intermediate rocks of the volcanic centers of the rift zones. Samples 16-24 are alkaline basalts occurring outside the rift zones. Samples 25-31 are silicic and intermediate rocks from volcanic centers outside the rift zones.

List of samples

a) Tholeiites_from_the_rift_zones_and_rift_margins

Sample 1, B-THO (Reykjavik). Ol-tholeiite from the middle of the WRZ. Large composite intraglacial shield structure. (Ref.: O´Nions et al., 1974; samples of the R-series.)

Sample 2, MIL 14 (Þórisjökull). Ol-tholeiite from the northwest termination of the WRZ. Large interglacial volcanic structure.

Sample 3, MIL 83 (Dvergar). Ol-tholeiite from near the east margin of the ERZ adjoining the MIL area. Small postglacial lava flow.

Sample 4, NAL 12 (Urdarháls). Ol-tholeiite from near the east margin of the ERZ. Large composite shield structure. (Ref.: Sigvaldason, 1974a.)

Sample 5, MIL 15 (Skjaldbreidur). Ol-tholeiite from the middle north of the WRZ. Postglacial shield structure. (Ref.: Tryggvason, 1943.)

Sample 6, RSG 19 (Selvogsheidi). Ol-tholeiite from the south termination of the Hengill fussure swarm (No. 2, Fig. 5) on the WRZ. Postglacial shield structure.

Sample 7, NAL 18 (Upptyppingar). Ol-tholeiite from the ERZ margin east of Askja volcanic center (No. 4, Fig. 5). Interglacial volcanic structure (pillows, tuffs and breccias). (Ref.: Sigvaldason, 1974a.)

Sample 8, NAL 27 (Leifhafnarfjall). Ol-tholeiite from interglacial volcanic structure at the north termination of the ERZ. (Ref.: Sigvaldason, 1974a.)

Sample 9, SAL 8 (Skaftáreldahraun, Laki 1783). A boundary case between ol-tholeiite and qz-tholeiite (1% ol in the norm) from the south termination of the ERZ. A large postglacial fissure eruption. (Ref.: Thorarinsson, 1969.)

Sample 10, A´61 (Askja 1961 eruption). A qz-normative tholeiite produced within the Askja center (No. 4, Fig. 5). A small fissure eruption. (Ref.: Thorarinsson & Sigvaldason, 1962.)

Sample 11, SAL 79 (Kverkfjöll, KFA). Qz-tholeiite from the KFA center east of the ERZ (No. 7, Fig. 5). The sample is alkaline basalt with strong tholeiitic mineralogical affinities. A small glacial fissure eruption. (Ref.: Sigvaldason et al., 1974; Wood et al., 1979.)

b) Silicic_and_intermediate_rocks_of_the_rift_zones

Sample 12, A-THO (Hrafntinnuhryggur). An obsidian from the KRA center (No. 5, Fig. 5). A subglacial ridge. (Ref.: O´Nions & Grönvold, 1973, sample N32.)

Sample 13, I-DAC (Hraunbunga). Dacite from the south termination of the KRA center. A small postglacial dome.

Sample 14, A-15 (Askja 1875 eruption). A rhyolitic pitch-stone from the pyroclastic deposits of a large explosive eruption. (Ref.: Sigvaldason, 1979.)

Sample 15, A-4 (Askja 1875 eruption). Dacite from the last event of the 1875 eruption. A small fissure lava. (Ref.: Sigvaldason, 1979.)

c) Alkaline_basaltic_rocks_of_the_digressive_and_transgressive_volcanic zone

Sample 16, SNS 1 (Ytri-Raudamelskúla). Alkaline small postglacial fissure eruption on the WDV.

Sample 17, SNS 7 (Hraunsmúli). A small postglacial fissure eruption on the WDV.

Sample 18, SNS 10 (Prestahraun). Postglacial alkaline basalt from the Snæfellsjökull center (No. 6, Fig. 5).

Sample 19, SAL 73 (Esjufjöll). Alkaline basalt. Interglacial palagonite formation on the EDV east of Öræfajökull center (No. 8, Fig. 5).

Sample 20, SAL 55 (Surtsey, 1963-67 eruption). Alkali olivine basalt from the Vestmannaeyjar center of the south termination of STZ (No. 9, Fig. 5). (Ref.: Steinthórsson, 1965; O´Nions et al., 1973, sample I-42.)

Sample 21, VMG 9 (Heimaey 1973 eruption). Mugearite lava from the Vestmannaeyjar center STZ (No. 9, Fig. 5). (Ref.: Thorarinsson et al., 1973.)

Sample 22, SAL 76 (Kálfafellsdalur). Alkaline interglacial basalt from the EDV.

Sample 23, B-ALK (Eldgjá). Fe-Ti basalt from postglacial fissure eruption at the north termination of the STZ. (Ref.: Larsen, 1979; Wood, 1979a.)

Sample 24, NSG 12 (Hraun á Skaga). Alkaline basalt with strong tholeiitic affinities. Postglacial fissure eruption from the north termination of the NTZ. (Ref.: Sigurdsson & Schilling, 1978.)

d) Silicic_and_intermediate_rocks_of_the_alkaline_volcanic_centers

Sample 25, SAL 74 (Öræfajökull). Obsidian from the Öræfajökull center (No. 8, Fig. 5). (Ref.: Prestvik, 1979.)

Sample 26, SNS 32 (Mælifell). Interglacial rhyolite dome from the WDV.

Sample 27, SNS 14 (Háahraun). Postglacial andesitic lava from the Snæfellsjökull center (No. 6, Fig. 5).

Sample 28, H´70-12 (Hekla 1970 eruption). Glassy pitch-stone, earliest product of the eruption (No. 12, Fig. 5). (Ref.: Sigvaldason, 1974b.)

Sample 29, I-ICE (Hekla 1970 eruption). Icelandite lava (No. 12, Fig. 5). (Ref.: Sigvaldason, 1974b.)

Sample 30, A-ALK (Hrafntinnusker). Postglacial obsidian from the Torfajökull center at the north termination of the STZ (No. 13, Fig. 5). (Ref.: O´Nions & Grönvold, 1973, Sample T18.)

Sample 31, SAL 28 (Námshraun). Postglacial andesitic lava from the Torfajökull center (No. 13, Fig. 5). (Ref.: O´Nions & Grönvold, 1973, sample T14.)

TABLE I

	1	2	3	4	5	6	7	8
	B-THO	MIL 14	MIL 83	NAL 12	MIL 15	RSG 19	NAL 18	NAL 27
SiO_2	48.04	47.20	48.45	47.90	47.55	48.60	47.85	48.60
Al_2O_3	15.14	15.50	16.80	17.15	15.50	15.45	15.35	17.80
TiO_2	.88	.83	.58	1.03	1.40	1.14	1.68	1.02
Fe_2O_3	2.62	1.58	.96	2.07	3.27	2.47	2.27	1.38
FeO	7.81	8.93	8.40	7.47	8.48	7.93	9.27	7.54
MnO	.17	.19	.14	.13	.19	.18	.17	.13
MgO	9.95	10.75	10.40	9.25	9.40	7.66	8.15	7.03
CaO	13.45	12.95	12.65	13.12	12.05	13.90	11.48	13.89
Na_2O	1.80	1.59	2.01	2.03	1.78	1.96	2.20	2.15
K_2O	.03	.05	.02	.08	.11	.05	.36	.14
P_2O_5	.06	.09	.04	.09	.11	.06	.12	.04
H_2O	.03	.08	.09	.32	.14	.13	.36	.31
Sum	99.98	99.74	100.54	100.64	99.98	99.53	99.26	100.03
F	30	47	43	112	128	90	290	105
Cl	90	90	120	70	80	50	175	140
V	290			198			250	275
Cr	447	441	148	305	471	360	502	245
Ni	155	250	191	189	226	121	224	85
Cu	107	99	197	108	148	152	113	165
Zn	54	64	105	67	90	83	96	114
Rb	0.2	0.2	0.3	0.4	1.1	0.6	4	3
Sr	89	100	89	151	144	111	243	133
Y	17	17	20	20	23	21	21	35
Zr	14	26	27	54	60	31	94	67
Ba	2			8				
87/86 Sr	.70301	.70304	.70311	.70321				.70304
^{18}O				3.6	4.1			4.3

TABLE I (continued)

	9	10	11	12	13	14	15	16
	SAL 8	A-1961	SAL 79	A-THO	I-DAC	A-15	A-4	SNS 1
SiO_2	49.75	50.30	51.25	74.48	64.68	73.00	68.00	47.80
Al_2O_3	13.85	13.10	13.50	12.07	15.26	13.70	12.90	12.70
TiO_2	2.73	2.98	3.10	.27	.88	.18	.91	1.65
Fe_2O_3	2.57	1.93	2.34	.88	1.33	1.97	3.14	4.12
FeO	10.85	13.68	12.17	2.55	4.82	.00	1.53	6.59
MnO	.23	.23	.23	.10	.12	.03	.11	.15
MgO	5.90	4.88	4.05	.10	1.46	.02	.89	12.48
CaO	10.37	8.87	8.54	1.75	4.83	1.18	3.14	11.06
Na_2O	2.75	2.86	3.26	4.31	4.12	4.65	3.90	1.83
K_2O	.47	.53	.74	2.72	1.37	3.33	2.21	.77
P_2O_5	.29	.27	.39	.04	.21	.03	.16	.26
H_2O	.13	.34	.30	.15	.45	.67	.82	.22
Sum	99.89	99.97	99.87	99.42	99.53	98.77	97.71	99.63
F	350	397	640	770	350	38	520	310
Cl	150	245	320	530	130	240	350	70
V				29		4		155
Cr	40	65		4	tr	3	9	1560
Ni	10	35		7	tr	13	8	427
Cu	27	156		13	17	22	34	87
Zn	60	216		140	50	102	93	74
Rb	7.1	4.2	13	67	28	78	45	10
Sr	119	161	236	105	158	61	111	299
Y	21	42	33	213	54	345	71	19
Zr	100	178	245	916	339	630	377	115
Ba				740	283	407	237	132
87/86 Sr	.70314		.70327					.70327
^{18}O	3.1	3.5		2.8		-7.4	0.4	5.6

TABLE I (continued)

	17	18	19	20	21	22	23	24
	SNS 7	SNS 10	SAL 73	SAL 55	VMG 9	SAL 76	B-ALK	NSG 12
SiO_2	47.10	47.45	48.76	46.65	48.40	49.93	48.25	49.40
Al_2O_3	15.05	14.95	13.51	16.25	16.55	16.36	12.38	12.50
TiO_2	3.22	2.63	4.00	2.00	3.08	2.56	4.22	3.33
Fe_2O_3	5.15	4.34	3.27	.73	2.34	1.73	4.12	2.69
FeO	8.60	7.87	11.61	10.48	10.67	9.89	10.81	11.84
MnO	.20	.17	.22	.21	.23	.22	.22	.25
MgO	5.48	7.20	5.40	8.56	4.06	4.15	5.35	6.00
CaO	10.95	11.80	9.23	10.28	7.60	7.00	10.00	10.40
Na_2O	2.55	2.16	2.63	3.38	4.92	4.33	2.97	2.58
K_2O	.92	.74	.64	.48	1.04	1.58	.77	.48
P_2O_5	.36	.41	.52	.24	.49	.84	.56	.42
H_2O	.16	.24	.24	.30	.25	.48	.25	.38
Sum	99.74	99.96	100.03	99.56	99.63	99.07	99.90	100.27
F	550	1160	507	370	813	752	443	380
Cl	170	210	210	205	460	130	140	140
V	420	148					467	
Cr	180	420		160	18		49	
Ni	72	146		67	16		30	
Cu	91	69		44	55		34	
Zn	118	96		69	148		130	
Rb	17	10	11	6.9	21	32	16	6
Sr	454	588		167	320	455	390	200
Y	24	39		16	50	40	35	31
Zr	167	250		81	294	430	240	221
Ba	393	521			264		180	
87/86 Sr	.70341	.70324	.70334	.70316	.70313		.70333	.70309
^{18}O		5.4		5.5	5.6		4.3	

TABLE I (continued)

	25	26	27	28	29	30	31
	SAL 74	SNS 32	SNS 14	H´70-12	I-ICE	A-ALK	SAL 28
SiO_2	70.44	71.45	62.45	72.22	54.55	72.87	62.69
Al_2O_3	14.10	14.42	16.15	13.23	14.50	12.26	15.37
TiO_2	.19	.13	.90	.30	2.02	.30	.72
Fe_2O_3	3.14	.87	1.63	.63	4.83	1.49	1.65
FeO	.10	2.27	5.49	1.51	7.34	1.83	4.86
MnO	.08	.16	.18	.09	.27	.07	.14
MgO	.10	.10	.70	.35	2.95	.07	2.10
CaO	1.14	.40	3.28	.33	6.96	.47	4.29
Na_2O	5.30	5.35	4.75	5.20	3.95	5.48	4.80
K_2O	3.74	4.70	3.35	3.89	1.28	4.59	2.96
P_2O_5	.01	.05	.20	.09	1.02	.01	.11
H_2O	.84	.13	.18	.54	.29	.51	.15
Sum	99.18	100.03	99.26	98.38	99.96	99.90	99.84

	25	26	27	28	29	30	31
F	1080	9600	1260	1640	1230	2320	520
Cl	840	300	310	810	225	1550	640
V					8	20	
Cr		1	4	tr	13	tr	
Ni		7	8	9	5	tr	
Cu		6	15	9	7	tr	
Zn		158	138		155	119	
Rb	83	155	71	80	26	116	
Sr		17	362	66	430	6	
Y		115	71	120	95	108	
Zr		819	649	840	540	870	
Ba		3	1240		410	160	
87/86 Sr			.70335		.70322	.70351	.70342
^{18}O			5.3		4.8		4.0

The analytical procedure for major elements is described in Sigvaldason (1974a). Analysis of the elements V, Cr, Ni, Cu, Zn, Sr, Y, Zr and Ba are made by XRF on pressed pellets of rock powder. Rubidium is analysed by XRF after preconcentration and collection on a filter paper (Óskarsson, 1978). The analytical procedure for chlorine is described in Sigvaldason & Óskarsson (1976). Fluorine is analysed by electrochemical method (Ingram, 1970). Data on Sr-isotope ratios are from Hart & Schilling (1973), O´Nions & Grönvold (1973), O´Nions et al. (1974) and Wood et al. (1979a). Oxygen isotope data are from Muehlenbachs et al. (1974) and Muehlenbachs (1974).

TABLE II

a Chemical changes in the system Fo-Di-An as a result of 41.9% cotectic
   crystallization of anorthite and forsterite in the ratio 69:31, and
   and subsequent crystallization of all phases in the eutectic.   Trace
   elements calculated by $c/c_O = F^{(D-1)}$; distribution coefficients as
   in Table IIb.

Point	M	$K^{x/1}$	E_0 [x]	$K^{x/1}$	E_1	E_2
% crystallization	0		41.9		75	90
Ni	1	5.17	.104	3.125	.017	.0025
Rb	1	.043	1.68	.051	3.74	8.93
Sr	1	1.152	.921	.99	.929	.937
K	1	1.159	.917	.125	1.92	4.28
SiO_2	46.60		48.51			
Al_2O_3	18.56		15.87			
CaO	17.46		22.40			
MgO	17.38		13.34			

[x] Major element composition of the eutectic from Pressnall et al. (1978,
   Table 2).

b Distribution constants used for calculations in Tables II (a,c,d)

$K^{1/x}$	Ni	Rb	K	Sr
Fo	0.06[x]	38	57	180
Di	0.25[x]	18	20	2
An		20	4.5	0.6

From Griffin & Rama Murthy (1969, p. 1404), except
[x] from Häkli & Wright (1967).

c Chemical changes in the system Fo-Di-An as a result of 10.84% crystal-
   lization of Fo. Distribution coefficients as in Table IIb.   Surface
   equilibrium assumed.

Ni	1	0.3
Rb	1	1
SiO_2	46.05	46.60
Al_2O_3	16.06	18.56
CaO	15.04	17.46
MgO	22.86	17.38

TABLE III

a Compositions of three "hybrid melts" resulting from mixtures of the
   eutectic composition in the system Fo-Di-An and orthoclase liquid.
   Trace element compositions for the "silicic liquid" are those of
   A-THO (Table I).

Composition	SiO_2	Al_2O_3	MgO	CaO	K_2O	Ni	Rb	Sr
E_0 [x)	48.51	15.87	13.34	22.40	1.10	26.00	0.34	92.00
Or	64.86	18.20			16.94	7.00	67.00	105.00
99% E_0+1% Or	48.67	15.89	13.21	22.18	1.26	25.80	1.01	92.13
95% E_0+5% Or	49.33	15.99	12.67	21.28	1.89	25.05	3.67	92.65
90% E_0+10% Or	50.15	16.10	12.01	20.16	2.68	24.10	7.01	93.30

[x)]Values for trace elements assuming MIL 14 composition at M (Table IIa).

b Cation norm of the compositions in Table IIIa, omitting K_2O.

Composition	An	Di	Fo	SiO_2
E_0	41.98	52.76	7.21	−1.95
99% E_0	42.13	51.98	7.30	−1.41
95% E_0	42.77	48.73	7.65	0.84
90% E_0	43.56	44.63	8.12	3.69

c Trace element compositions at E_0, after 1, 5 and 10% mixing with a
   silicic melt (A-THO, Table I), and the subsequent restoration of
   the system to the eutectic by fractional crystallization. Distri-
   bution coefficients as in Table IIb, initial compositions as   in
   Table IIIa.

Composition	Ni	Rb	Sr	K
E_0	26	0.34	92	0.91
1% mixture	26	1.02	91.5	1.05
5% mixture	22.6	3.92	89.9	1.65
10% mixture	17.86	7.86	89.8	2.45

TABLE IV

a Phases present in sample NAL 13, formed by fractional crystallization
   over a 110°C temperature range (to approx. 66% crystallization from
   relative increase in P_2O_5 in probe analysis of glasses).

T°C	phases
1270	gl
1263	gl + ol
1258	gl + ol + pl
1244	gl + ol + pl
1202	gl + ol + pl
1182	gl + ol + pl + cpx
1160	gl + ol + pl + cpx

b Phases present in some of the B-A runs. Volume estimates of glass from
   increase in TiO_2. x = phase present, as determined optically. - = phase
   not detected. Compositions determined with the microprobe.

B_{100}	gl	ol	pl	px
1218°	78%	x	x	
1184°	63%	$Fo_{85}(5)$	x	$En_{46}Wo_{44}Fs_{09}(6)$
1179°	51%	x	$An_{89}(1)$	x
1156°	46%	$Fo_{85}(2)$	$An_{88}(1)$	$En_{51}Wo_{41}Fs_{08}(1)$

$B_{90}A$	gl	ol	pl	px
1218°	97%	x		
1216°	87%	x	x	
1198°	76%	$Fo_{93}(1)$	$An_{90}(2)$	
1179°	66%	x	x	
1156°	55%	$Fo_{80}(2)$	$An_{88}(2)$	$En_{44}Wo_{46}Fs_{10}(1)$

$B_{80}A$	gl	ol	pl	px
1218°	x			
1216°	99%[x)]		x	
1198°	88%	x	x	
1179°	75%[x)]	x	$An_{87}(1)$	x
1156°	53%	$Fo_{85}(3)$	$An_{83}(2)$	x

[x)]Estimated optically in polished section.

TABLE IV cont.

c Phases present in the B-S runs. Volume estimates of glass from
   relative increase in TiO_2. Symbols as in Table IVb.

$B_{95}S$	gl	ol	pl	cpx
1223°	90%[x)	Fo_{95}	x	x
1206°	82%	x	x	x
1180°	59%		x	x
1159°	43%	x	x	x
$B_{90}S$				
1223°	100%[x)			
1206°	85%		x	x
1180°	67%		x	x
1159°	48%	x	x	x
$B_{80}S$				
1223°	99%[x)		tr.	
1206°	83%		x	x
1180°	61%		x	x
1159°	45%	x	x	x

[x) viazual estimate.

d Phases present, as determined optically, in the runs A-I to A-III
   at four temperatures. Mineral compositions by electron microprobe.
   Symbols as in Table IVb.

T°C	gl	ol	pl	cpx
A-I				
1195°	x	$Fo_{88}(4)$	tr.	x
1212°	x	x		x
1235°	x	$Fo_{88}(1)$		x
1252°	x	x		x
A-II				
1195°	x	$Fo_{88}(5)$	$An_{84}(1)$	x
1212°	x	$Fo_{86}(2)$		$En_{52}Wo_{40}Fs_{08}(2)$
1235°	x	$Fo_{86}(1)$		$En_{45}Wo_{47}Fs_{08}(4)$
1252°	x	x		x
A-III				
1195°	x	$Fo_{84}(1)$	x	$En_{49}Wo_{43}Fs_{08}(2)$
1212°	x	$Fo_{86}(1)$	x	x
1235°		x		x
1252°	x	x		x

TABLE IV cont.

e   Phases present in VMG 4 (VE-67) formed by fractional crystalliza-
    tion over a 100°C temperature range (about 50% crystallization
    from relative increase in P_2O_5).

T°C	phases
1244	gl + op
1228	gl + pl + op
1207	gl + pl + op
1198	gl + pl + op
1174	gl + pl + op + ol
1158	gl + pl + op + ol
1155	gl + pl + ol
1136	gl + pl + ol
1135	gl + pl + ol

TABLE V

a Phase proportions in synthetic amphibolite used in experimental
   runs. Kaersutite - Juan Carlos, olivine - Búðasandur (separa-
   ted phenocrysts), labradorite - Surtsey (megacrysts, separa-
   ted), pyroxene - Sólheimajökull (separated from ankaramite tuff).

amphibolite	I	II	III	
	60%	60%	60%	olivine
	15	5	5	plagioclase
	15	25	25	pyroxene
	10	10	10	kaersutite

b Chemical composition of phases in Table Va

	kaersutite	pyroxene	plagioclase	olivine
SiO_2	40.80	51.80	52.95	39.60
Al_2O_3	12.35	3.80	29.40	.83
TiO_2	4.70	.90	.10	.33
FeO^t	15.30	4.67	.18	16.70
MnO	.24	.11	.01	.26
MgO	8.75	15.45	.15	38.95
CaO	11.10	21.60	11.95	2.24
Na_2O	2.90	.40	3.86	.10
K_2O	1.18	.05	.21	
P_2O_5	.79	.06	.04	
Sum	98.11	98.84	98.85	99.01

c

	SAL 4	VMG 4	NAL 13
SiO_2	46.95	47.69	47.60
Al_2O_3	12.20	17.36	16.66
TiO_2	4.30	2.30	1.09
Fe_2O_3	3.45	5.83	1.79
FeO	11.56	6.25	7.94
MnO	0.23	0.22	0.14
MgO	5.92	5.32	9.56
CaO	10.43	9.75	12.76
Na_2O	2.74	3.33	2.14
K_2O	0.56	0.71	0.11
P_2O_5	0.49	0.32	0.09
H_2O	0.50	0.31	0.21
Sum	99.33	99.39	100.09